UNIVERSIDADE DE LISBOA
FACULDADE DE CIÊNCIAS

S100 proteins as novel modifiers of proteostasis in pathophysiological states

"Documento Definitivo"

Doutoramento em Biologia
Especialidade de Biologia de Sistemas

Mariana Amoroso das Neves Romão

Tese orientada por:
Cláudio Emanuel Moreira Gomes
Frederic Rousseau

Documento especialmente elaborado para a obtenção do grau de doutor

2022

UNIVERSIDADE DE LISBOA

FACULDADE DE CIÊNCIAS

S100 proteins as novel modifiers of proteostasis in pathophysiological states

Doutoramento em Biologia

Especialidade de Biologia de Sistemas

Mariana Amoroso das Neves Romão

Tese orientada por:

Cláudio Emanuel Moreira Gomes

Frederic Rousseau

Júri:

Presidente:

- Doutor Rui Malhó, na qualidade de Presidente do DBV da Faculdade de Ciências da Universidade de Lisboa.

Vogais:

- Doutor Stefano Ricagno, Full Professor do Dipartimento di Bioscienze da Università Degli Studi di Milano,Itália;
- Doutora Sandra de Macedo Ribeiro, Investigadora Principal do i3S-Instituto de investigação e Inovação em Saúde da Universidade do Porto;
- Doutora Célia Maria Valente Romão, Investigadora DL57 do Instituto de Tecnologia Química e Biológica da Universidade Nova de Lisboa;
- Doutor Cláudio Emanuel Moreira Gomes, Professor Associado com Agregação da Faculdade de Ciências da Universidade de Lisboa, Orientador.

Documento especialmente elaborado para a obtenção do grau de doutor

Bolsa de Doutoramento financiada pela Fundação para a Ciência e Tecnologia (FCT)

com a referência SFRH/BD/114390/2016

2022

Acknowledgments

The completion of this thesis could not have been possible without the support of the amazing and inspirational people that surround me. Here, I want to leave my sincere gratitude to all people who have contributed, directly and indirectly, for the completion of this work, to whom I am very grateful.

First, to my thesis supervisor, Prof. Cláudio M. Gomes, for always giving me the necessary motivation and suggestions to improve the quality of my work, for giving me all the support I needed to reach my goals, for fostering my critical sense and for teaching me “how to do science”. Thanks for the patience, mainly in the last stages of the thesis.

To Prof. Frederic Rousseau, my co-supervisor, and Prof. Joost Schymkowitz from VIB-KU Leuven Center for Brain & Disease Research, for welcoming me in their lab, and for giving me the opportunity to gain knowledge in peptide design and synthesis. I am also grateful to Rodrigo Gallardo for assisting me in the experiments and for all the great discussions we had.

To Prof. Andreas Grabrucker and Dr. Simone Hagmeyer, from Ulm University, for the warm reception and for teaching me how to run experiments working with cells and mice brains. The experience and the knowledge that I have gained have been very useful for my scientific growth.

To Dr. Isabel Cardoso for the TEM assays, and to Dr. Ana Carapeto, Msc. Tiago Robalo, Dr. Mário Rodrigues, BioISI AFM Magnano laboratory, for AFM analysis.

To the BioSys PhD Programme for choosing me and welcoming me to be part of the programme which made me grow scientifically and personally.

To “Fundação para a Ciência e Tecnologia” I am thankful for the financial support, otherwise it would be very difficult to have this opportunity to value my scientific career.

To Cost Action TD1304 through networking support a Short-Term Scientific Mission (STSM) Grant 2015 to work in Ulm University, Ulm, Germany, and to Cost Action TD1304 to support STSM Grant 2017 to work VIB-KU Leuven Center, which allowed me to go further with the experiments.

To “Colégio Mente Cérebro ULisboa” for networking support and several transdisciplinary activities.

To the current and past members of the Protein Folding and Misfolding Laboratory, especially Joana Cristóvão, Guilherme Moreira, Joana Ribeiro, Tânia Lucas, Bárbara Henriques, Rodrigo David, Joana Ferreira, Javier Fernandez, António Figueira for all the joy and good environment in the lab.

To “Papucho”, for the inspiration, for his personal example, for being always by my side, for the common sense and thoughtfulness, for the good advice, for teaching me to appreciate the simple things in life, like having a good conversation tasting a good wine, and specially for believing in me and in my work. Thanks for a clear understanding of the importance and role of science in the future of human destiny. I certainly owe much of what I am to your attention and care.

I am also grateful to my Mother, who is no longer with us, but who would certainly be proud of my work. Wherever you are, you will always be in my heart.

To my dear aunt – Tatia, for her joy, for her constant encouragement and support along this long path. You are such a beautiful person.

To my siblings, Guilherme Romão, Catarina Chaves and Mateus Romão, that are always so close to me. Thanks for the brotherhood and for the great times where we keep sharing our life adventures.

To Inês Sá for being with me during this final phase and for having pushed me up to finalize this important challenge. For being such a wonderful person, so beautiful, so simple, so nice to me. For your cute family that treats me so warmly.

To my older friends Catarina Graça, Susana Cruz, Flávia Araújo and Diana Fernandes for the long and forever friendship. For patience, for the dinners, for the endless laughter in our evenings.

To my “migas mais lindas” Márcia Tavares e Vanessa Almeida for always being with me during all this time. For the laughs, for the stories, for the shared moments since university times. You became part of me.

To my dears Raquel Saramago, Tiago Corona and Andreia Rijo for how much you made me grow as a person. I am so thankful for having you in my existence.

To Joana Guilherme, for sharing with me these difficult and stressful times during the PhD until the very end of the thesis submission.

Last but not the least, thanks to the members of Rodon Biologics, specially Inês Pinto, Diana Querido, Luís Nogueira, Manuel Matos, Ana Rita Ricardo and Phil Cunnah for receiving me just after my PhD lab work, exactly on the beginning of my thesis writing, and for the great scientific inputs that keeps me a scientific enthusiast.

To everyone, even those not mentioned here because of my forgetfulness, my thanks for everything.

Dissertation Abstract

Alzheimer's disease (AD) is the most prominent cause of dementia and is accompanied by chronic neuroinflammation, protein aggregation and formation of amyloids. During inflammation important modulators of inflammatory responses are implicated, including cytokines and chemokines, among which are S100 proteins. Expression levels of S100 proteins are increased in inflammatory diseases and neurodegenerative disorders such as AD, where they are found around amyloid plaques. This was suggestive of a functional link with Aβ aggregation, in agreement with the newly uncovered activity of S100B as a chaperone suppressor of amyloid formation. This PhD thesis aimed at investigating the role and S100 proteins as potential modifiers of proteostasis in pathophysiological states, resorting to different model systems - from brains of animal models to isolated proteins and peptides, combining cellular, molecular, biophysical, and biochemical techniques. First the distribution of S100 proteins in the brains of AD *APP23* mice models was investigated. Results showed that in the brain of *wild type* mice, S100A6 and S100B are mostly expressed in astrocytes, while low expression of S100A8 was found in neurons and glial cells *in vitro*. Analysis of *APP23* mice brains revealed increased expression of S100A8 in neurons and co-localization of S100 proteins with Aβ plaques. *In vitro* assays showed that S100A6, S100A8, S100A9, S100A8/A9, delay Aβ aggregation, similarly to S100B. This regulatory activity is similar to that of molecular chaperones, which highlights the potential of S100 proteins as regulators of proteostasis in pathophysiological states. Next, the focus was on the S100A9 protein which is abundant in the brain and has been linked with amyloid formation and deposition in neurodegenerative disorders. We investigated the self-assembly of the S100A9 protein and characterized the formation of polymeric structures formed by this protein, combining biophysical spectroscopies and biochemical assays, outlining the steps of a possible mechanism of functional assembly of this protein with relevance in health and disease.

Key words: Protein Folding and aggregation; Protein Biophysics; Alzheimer's disease; Calcium proteins; Molecular Chaperones

Resumo da Dissertação

As proteínas S100 constituem uma família conservada em vertebrados, composta por +20 proteínas que ligam cálcio através de dois motivos EF e que ocorrem sobretudo como homo-dímeros. São proteínas multifuncionais, com atividade dependente e independente da ligação de cálcio, e que desempenham funções intra- e extracelulares. Intracelularmente estão envolvidas na regulação celular, como a diferenciação, proliferação e apoptose, e na homeostase de cálcio. Extracelularmente, as proteínas S100 interagem com recetores pro-inflamatórios como *RAGE* e *TLR4*, ativando a microglia e os astrócitos reativos, induzindo a cascata inflamatória. Apesar da elevada homologia estrutural entre os membros da família das S100, as suas funções não são intercambiáveis. Além disso, a concentração e estado de oligomerização das proteínas S100 também é determinante para sua função biológica. Considerando a variedade de funções em que estão implicadas, não é surpresa que a sua desregulação estar associada a inúmeras doenças. De facto, diferentes padrões de expressão das proteínas S100 estão associados a várias condições patológicas como doenças neurodegenerativas, cancros e doenças autoimunes, encontrando-se tipicamente sobre expressas. Algumas proteínas S100 como S100A1, S100A6, S100A8, S100A9, S100A8/A9 e S100B, expressas no sistema nervoso central, estão associadas com a severidade de doenças neurodegenerativas como as doenças de Alzheimer e Parkinson. A doença de Alzheimer (DA) é uma doença neurodegenerativa e a maior causa de demência no mundo, que afeta milhões de pessoas, resultando num declínio das funções cognitivas. Os principais fatores bioquímicos envolvidos na doença são a neuroinflamação crónica, a acumulação do péptido Aβ em placas amiloides extracelulares e da proteína tau em emaranhados neurofibrilares dentro dos neurónios. A neuroinflamação leva à morte de células neuronais, à perda de sinapses e a danos no tecido neuronal. Durante a evolução da doença de Alzheimer o processo inflamatório resulta na produção de citocinas pro-inflamatórias entre as quais estão as proteínas S100, que desempenham funções desde fases iniciais da patologia neurodegenerativa, daqui resultando um crescente interesse no estudo destas proteínas.

Esta tese de doutoramento teve como objetivo investigar o papel das proteínas S100 como potenciais modificadores da proteostase em estados fisiopatológicos, recorrendo a diferentes sistemas modelo – desde cérebros de modelos animais a proteínas e péptidos isolados, combinando técnicas celulares, moleculares, biofísicas e

bioquímicas. Em particular, e dado que várias proteínas S100 estão presentes no cérebro e estão envolvidas em processos neurodegenerativos, este trabalho visou também investigar o seu impacto na doença de Alzheimer.

Para tal, começamos por estudar os níveis de expressão e localização cerebral específicas das proteínas S100, nomeadamente S100A6, S100A8 e S100B, recorrendo a modelos animais da doença de Alzheimer. Estudos em cérebros de ratinhos *wild type* revelaram que as proteínas S100 têm, de facto, níveis de expressão diferentes: enquanto que as proteínas S100A6 e S100B estão sobre expressas em astrócitos, a proteína S100A8 mostra um baixo nível de expressão tanto em neurónios como nas células da glia. Imagens de fluorescência *in vivo* confirmam expressões distintas em diferentes regiões do cérebro: as proteínas S100A6 e S100B mostram um padrão de expressão em todas as regiões do cérebro, com maior incidência no córtex e no cerebelo, enquanto a proteína S100A8 tem expressão muito baixa em todo o cérebro. Em contrapartida os cérebros de ratinhos transgénicos *APP23* mostram que a expressão da proteína S100A8 está aumentada em células neuronais e que as proteínas S100A6, a S100A8 e S100B estão co-localizadas com as placas amiloides constituídas por Aβ. Neste ponto postulamos que níveis elevados de expressão e distribuição espacial entre as proteínas S100 e as placas de Aβ possam resultar de relações funcionais entre estes mediadores de inflamação (proteínas S100) e os processos patofisiológicos da DA, podendo indiciar mecanismos moleculares importantes que relacionam a cascata neuroinflamatória com a agregação proteica.

Utilizando métodos de fluorescência de tioflavina T, capazes de monitorizar o processo cinético de agregação da proteína Aβ, investigou-se a possibilidade das proteínas S100 regularem a formação de fibras patológicas. Os resultados obtidos evidenciaram que as proteínas S100A6, S100A8, S100A9, S100A8/A9, inibem a agregação de Aβ42, tal como a da previamente estudada proteína S100B, presumivelmente através de interações proteína:proteína transientes. Através de análise mecanísticas verificou-se que diferentes proteínas S100 podem influenciar de forma diferente a agregação do péptido Aβ42. Por outro lado, estes resultados sugerem que as proteínas S100 contribuem para a manutenção da homeostasia proteica na doença de Alzheimer. Em fases iniciais da patologia, as proteínas S100 parecem ter efeitos benéficos dado que atrasam a agregação do péptido Aβ; contudo, em fases mais avançadas da doença, nas quais se tem já acumulação de proteínas agregadas, a sua atividade pro-inflamatória torna-se preponderante e a sua ação biológica torna-se agravante. Não é de excluir que deste agravamento possa também fazer parte co-

agregação com o péptido Aβ, no que poderia ser um mecanismo de inativação dos chaperões S100 através de perda de função por agregação. Estes resultados abrem novas perspetivas relativamente ao uso de proteínas desta família como moduladores terapêuticos que podem atrasar a formação de agregados de Aβ, que por sua vez podem atrasar o início e a progressão da doença de Alzheimer.

Algumas proteínas S100 podem formar oligómeros (tetrâmeros, hexâmeros, octâmetros, *etc*) funcionais, dependendo das condições fisiológicas, nomeadamente das suas concentrações relativas e a presença de iões metálicos, tais como cálcio e zinco, onde este último é um ligando adicional de algumas destas proteínas. Em particular, a proteína S100A9, que está implicada em neurodegeneração tendo elevados níveis de expressão durante os períodos de infamação que pode levar a formação e deposição amiloide, forma estruturas descritas na literatura como sendo amilóide, mas cuja natureza estrutural permanece por esclarecer. Assim, neste trabalho investigou-se a formação e estrutura destes filamentos formados pela proteína S100A9. Descobrimos que a proteína S100A9 tem a particularidade de formar estruturas poliméricas únicas sob incubação em condições fisiológicas e a elevadas concentrações, semelhantes às fisiológicas. Estes filamentos são muito estáveis e a sua análise estrutural recorrendo a métodos biofísicos revela que são constituídas por homo-dimeros nativos da proteína S100A9, mantendo uma conformação nativa com predominância de hélices α, característica da proteína S100A9 nativa, apesar de apresentarem um ligeiro aumento em folhas-β. Além disso, verificou-se que estas estruturas filamentosas resultam de um processo de interação entre moléculas S100A9 que se podem dissociar de forma reversível. Este modelo de automontagem, até agora único para a S100A9 entre a família das S100, poderá estar relacionado com uma extensão desordenada de amino ácidos na região C-terminal, que é única nesta proteína entre todas as S100, e que pode mediar a formação desta estrutura filamentosa, que não demonstra características amilóide prototípicas, como anteriormente se pensava. Esta observação indicia um possível mecanismo funcional de *self-assembly* através do qual se torna possível o armazenamento extracelular ou aumento de atividade biológica desta proteína, entre outras possibilidades.

Em suma, o trabalho desenvolvido nesta tese de doutoramento sugere que as proteínas S100, nomeadamente as S100A6, S100A8, S100A9 e S100A8/A9, podem afetar a progressão da doença de Alzheimer, atuando como chaperões moleculares no estágios iniciais da doença, prevenindo ou atrasando a agregação do péptido $A\beta_{42}$. Esta interação suporta a interligação entre neuro inflamação, onde são sobre expressas as

proteinas S100, e a formação das placas amiloides de Aβ em Alzheimer. Além disso, foram propostos novas potenciais funções da proteína S100A9.

Palavras Chave: Agregação e Enrolamento de Proteínas; Biofísica de Proteínas; Doença de Alzheimer; Proteínas que ligam Cálcio; Chaperões Moleculares

Thesis manuscripts

#1 - S. Hagmeyer, M. A. **Romão**, J. S. Cristóvão, A. Vilella, M. Zoli, C. M. Gomes, A. M. Grabrucker, Distribution and Relative Abundance of S100 Proteins in the Brain of the APP23 Alzheimer's Disease Model Mice. Frontiers in Neuroscience 13, (2019); published online Epub2019-June-20 (10.3389/fnins.2019.00640).

#2 - Figueira, A., **Romão**, M.A., Cristóvão, J.S., Gomes, C.M. (2022) Brain expressed S100 proteins act concertedly to suppress amyloid-β aggregation by targeting diverse microscopic mechanisms (in preparation)

#3 Romão, M.A., et al (2022) Nanoscale analysis of self-assembled pseudo-amyloid fibrils formed by native globular protomers (in preparation)

Other manuscripts not included in the thesis

#4 R. Loera-Valencia, M. A. M. Ismail, J. Goikolea, M. Lodeiro, L. Mateos, I. Björkhem, E. Puerta, M. A. **Romão**, C. M. Gomes, P. Merino-Serrais, S. Maioli and A. Cedazo-Minguez (2021) Hypercholesterolemia and 27-Hydroxycholesterol Increase S100A8 and RAGE Expression in the Brain: a Link Between Cholesterol, Alarmins, and Neurodegeneration. Molecular Neurobiology, 10.1007/s12035-021-02521-8

#5 J. S. Cristóvão, M. A. **Romão**, R. Gallardo, J. Schymkowitz, F. Rousseau, C. M. Gomes, Targeting S100B with Peptides Encoding Intrinsic Aggregation-Prone Sequence Segments. Molecules 26, (2021)10.3390/molecules26020440

#6 Ammendola, S., Secli, V., Pacello, F., Mastropasqua, M. C., Romão, M. A., Gomes, C. M., Battistoni, A. (2022) Zinc-binding metallophores protect *Pseudomonas aeruginosa* from calprotectin-mediated metal starvation. FEMS Microbiology Letters. in press

Abbreviations

Aβ – Amyloid-beta
AD – Alzheimer's disease
AFM – Atomic Force microscopy
ALS – Amyotrophic lateral sclerosis
ANS – 8-Anilino-1-naphthanesulfonic acid
APP – amyloid precursor protein
APR – aggregation prone region
CAM – cell adhesion molecule
CD – circular dichroism spectroscopy
CICR – calcium-induced/calcium release
CNS – central nervous system
CP – Calprotectin
CR – Congo Red
CTF – C-terminal fragments
Cryo-EM – cryo-electron microscopy
DAMPs – damage-associated molecular pattern
DLS – Dynamic Light Spectroscopy
DNA – Deoxyribonucleic acid
DTT – Dithiothreitol
EDTA – Ethylenediaminetetraacetic acid
EMMPRIN – extracellular matrix metalloproteinase inducer
EOAD – early onset dementia
ERK – extracellular signal-regulated protein kinase
FAD – familial AD
FTAA – formyl thiophene acetic acid
FTD – frontotemporal dementia
FTIR – Fourier transform infrared spectroscopy
HD – Huntington disease
HEPES - 4-(2-hydroxyethyl)-1-piperazineethanesulfonic acid
HSP – heat shock protein
HSF – heat shock factor
IDP – Intrinsically disorder protein
LCO – luminescent conjugated oligothiophene
IL – Interleukin
LOAD – late onset AD
MAPK – Mitogen-Activated Protein Kinase
MMP – matrix metalloproteinase
MSA – multiple sequence alignment
NF-κB – nuclear factor κB
NMR – Nuclear magnetic resonance
ND – neurodegenerative disease
NTS – neurofibrillary tangles
OA – osteoarthritis
PD – Parkinson's disease
PQC – protein quality control
PN – Proteostasis network
PSEN – Presenilin
RA – rheumatoid arthritis
ROS – reactive oxygen species
sAD – sporadic AD
TDP-43 – TAR DNA-binding protein 43
UPS – ubiquitin proteosome system
RAGE – receptor for advanced glycation end products
SAXS – Small-angle X-ray scattering
SEC – Size exclusion chromatography
$t_{1/2}$ – half-time reaction
TBI – traumatic brain injury
TCEP – Tris(2-carboxyethyl) phosphine)
TEM – transmission electron microscopy
TLR4 – tool-like receptor4
ThT – Thioflavin-T
TNF – Tumor necrosis factor
WT – wild type

List of figures

List of Tables

Table of Contents

Thesis outline

This dissertation is focused on investigations to establish S100 proteins as novel modifiers of proteostasis in pathophysiological states and is organised in six chapters.

The first two introductory chapters are aimed to overview the state of the art regarding protein misfolding, proteostasis and human disease and to introduce the characteristics of the proteins from the S100 family and the evidence for their role as modifiers of cellular proteostasis and proteotoxicity.

Chapter 1 provides a general introduction to the topic of protein folding, proteostasis and amyloid diseases. Through brief yet comprehensive sections, this chapter covers the fundamentals of protein folding, discusses how protein misfolding and aggregation arises with a focus on amyloids, whose generic structural features are discussed. The mechanisms operating in cells that are responsible for protein quality control and maintenance of proteostasis are overviewed and the generic features of amyloid neurodegenerative diseases are covered.

Chapter 2 reviews the characteristics of S100 proteins, with a focus on their biochemical and structural features, including metal binding properties and oligomerization. The physiological functions of S100 proteins are discussed and their participation in disease states and potential applications as biomarkers is comprehensively reviewed.

The following chapters present the results obtained and include topical introductions regarding the themes under investigation. These chapters cover results obtained using different model systems - from brains of animal models to isolated proteins and peptides, combining cellular, molecular and biophysical experimental techniques, and include published results.

Chapter 3 focuses on the role of S100 proteins in Alzheimer's disease and on the study of their distribution and in the brains of AD mice models. It presents an introduction to Alzheimer's disease and available animal models, discussing the involvement of S100 proteins in the pathology. Results presented in this chapter have been published in thesis manuscript #1.

Chapter 4 follows up on previous these results, notably on the observation that multiple S100 proteins delay the aggregation of Amyloid β, to carry out a systematic investigation of the possible action of these proteins as anti-aggregation chaperones in human brain. it provides a typical introduction to the mechanisms of amyloid aggregation and its analysis using kinetic

methods. Results presented in this chapter are included in thesis manuscript #2, in preparation.

Chapter 5 reports investigations on the self-assembly of the S100A9 protein, whose anti aggregation activity has been established in the previous chapter, into native-like fibrils. The introduction reports previous findings on the involvement of S100A9 in Alzheimer's disease and its presumed potential to form amyloid fibrils is critically discussed. Results presented in this chapter are included in thesis manuscript #3, in preparation.

Chapter 6 provides a general conclusion of the thesis results discussing the significance of the biology of S100 proteins as novel players in proteostasis.

Chapter I: General Introduction – Proteostasis in health and disease

---

1. Introduction – Protein Folding, Proteostasis and Amyloid Diseases

1.1. Fundamentals of protein folding

One of the biggest modern scientific challenges is to understand the biological complexity of living organisms, which are a highly evolved system made up of a wide number of molecular networks. These networks enable and control all the processes that take place in the cell and proteins are the key elements. Proteins are the most abundant macromolecules in the cell and, besides chemical processes, proteins are responsible for the control of all molecular interactions characteristic of living systems.

Proteins are composed by a specific polypeptide sequence made of amino acid residues, called primary sequence, which contains information that dictate its unique native and functional three-dimensional structure, as postulated by Christian Anfinsen (1916-1995) [1]. The conversion of the protein encoded sequence into its native structure is called protein folding and is fundamental in biology due to the high dependence of all biological processes on the protein machinery. In accordance with Anfinsen's experiments on ribonuclease A during the 1960's [1, 2], the native state of a protein is reached downhill to its lowest free energy corresponding to the most thermodynamically stable conformation [2]. This means that all information about the folding of a protein is encoded on its amino acid sequence. Getting knowledge about the sequence should be enough to unequivocally determine the folded structure of any protein, in any medium and, consequently, its interaction and catalytic properties and folding mechanism. However, considering the degrees of freedom of polymeric nature of proteins, the heterogeneity of amino acid side chains and the variety of possible interactions stabilizing the folded conformation, deciphering the rules underlying protein folding is a very hard task. However, this conundrum has been partly overcome with recently developed machine learning methods, including AlphaFold, which allow highly accurate protein structure predictions [3].

The high number of degrees of freedom in the conformation of a polypeptide brings other known biological paradox introduced by Cyrus Levinthal (1922-1990) in the late 1960's, known as Levinthal's Paradox [4, 5]. Levinthal focused his research work on the investigation of the kinetics and dynamics of the protein folding process. He postulated that, if the protein folding is truly a two-state reaction without intermediates occurring during the process, then finding the native folded state of a protein by a random search among all possible configurations would take an enormously long time [4] Therefore, he concluded that in nature proteins do not sample all possible configurations since they fold very fast (from milliseconds

to up to a few seconds). Since the folding process is usually extremely efficient and fast, Levinthal suggested that proteins fold through a specific folding pathways [4]. Levinthal also postulated that protein folding is speeded up and guided by the rapid formation of local interactions between the certain residues that determine further the global folding. This means that local amino acid side chains form stable interactions and serve as nucleation points to the folding process [4, 6]. Some folding intermediates and partially folded protein states observed during folding kinetics experiments recreate some features of such transition state.

During folding towards the native state, proteins do not randomly explore the conformational space, but rather undergo cooperative, sequential folding of smaller domains, markedly reducing the high dimensionality of the folding process, allowing the final structure to be obtained in milliseconds [7]. To describe the protein folding process and energetics of the different conformers along the process, an energy diagram is often depicted – the so-called energy landscape funnel diagram (Fig. 1). To gain functional activity, most proteins must fold into well-defined three-dimensional structures. Folding reactions are highly complex and heterogeneous, relying on the cooperation of many weak, non-covalent interactions that participate in the stabilization of the monomeric entities [8]. The energy landscape diagram is shaped like a funnel because it maps all possible conformations of a protein as a function of their free energy, which narrows to the energetically most favorable conformer [8-10].

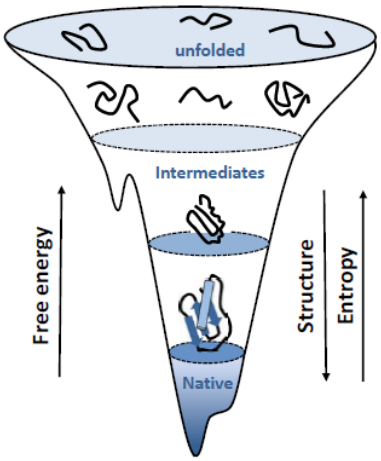

Figure 1 – Folding funnel diagram protein folding. Energy diagram representing the protein folding process from unfolded to the native state. As a protein folds, it gets more structured, while the configurational free energy and entropy lower. From [10]

The folded/unfolded state of a protein is dictated by the balance between entropy, which indicates the degrees of freedom of a system, and enthalpy, which relates with the energetics of the system. If on the one hand, the unfolded state of a protein corresponds to the higher conformational entropy state (as unfolded proteins are linear polymers of tens to hundreds amino acids), on the other hand, a folded protein comprises a multiplicity of

interactions which constitute an enthalpic gradient towards the native state. The interactions responsible for the folding of proteins to their native conformations include hydrophobic interactions, hydrogen bounds and electrostatic interactions, first described by Kauzmann [11]. They are sometimes referred to as “weak interactions”; however, they are a very significant number of individual interactions in folded proteins. Folded conformations can additionally be stabilized by other contributors such as disulphide bridges, oligomerization, cofactors and/or post-translational modifications. In the native state, the set of possible conformations gets narrower, due to favorable intramolecular interactions, decreasing the entropy as structural organization increases, decreasing the degrees of freedom on the polypeptide within each conformer. The final balance between the two energetic components that have opposite directions will be marginally stable towards the native state. This gives rise to an important property for the dynamic behavior of the proteins allowing them to acquire some conformational flexibility which is also required for many protein functions like cargoes transportation, regulatory functions, signaling pathogen invasion and enabling neuronal communication [12].

These principles are slightly different for the so called intrinsically disordered proteins (IDPs), also called intrinsically unfolded proteins [13]. These proteins, or domains within proteins lack an organized tertiary structure, and feature a considerable structural heterogeneity and flexibility, playing an important role in protein-protein interactions and in signaling reactions [14]. IDPs have been suggested to display folding energy landscapes in which wide arrays of conformers can be populated, with relatively flat energy regions, and appear to involve transitions to higher energy states. Entropic effects of IDPs contributed by solvent play an especially important role in driving folding, as opposed to enthalpic effects [9, 15]. Many of these proteins and regions are not persistently unfolded and undergo folding-upon-binding when they interact with physiologic partners.

1.2. Protein misfolding and amyloid aggregation

Protein folding in the cell is tightly controlled by protein quality control (PQC) systems in the cell (discussed in the next section) as protein folding may be disrupted by adverse biochemical, physical, and biological factors, including genetic mutations. Genetic defects causing modifications on the primary sequence of the proteins may affect the folding pathway and the stability of the native state, generating partly folded states. Molecular crowing in cells may also favor unspecific intermolecular interactions formed conformers leading to protein self-assembly into either amorphous or highly organized structures, as amyloid fibrils [16] (Fig.2).

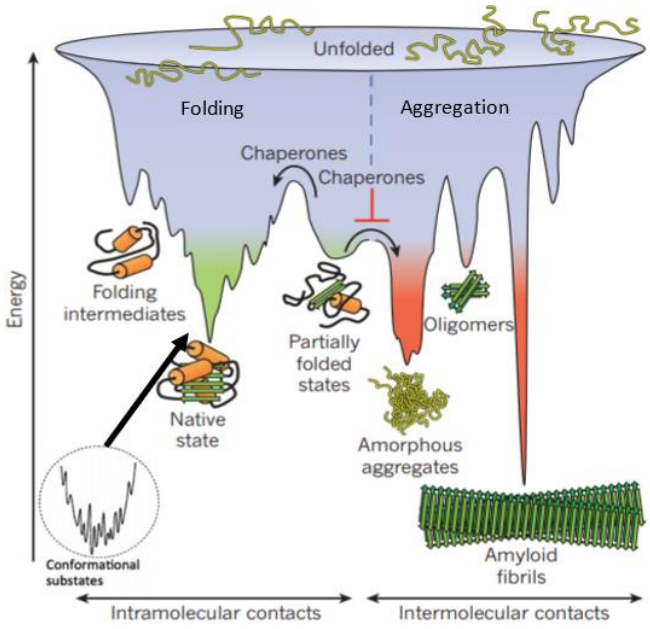

Figure 2 - Energy landscape diagram for protein folding and aggregation of a typical small globular protein. On the left is represented the folding process from the unfolded polypeptides in random conformations where the entropy is maximal, towards the native state via intramolecular contacts. Unfolded proteins are highly flexible and hydrated. During the process structure is gradually acquired, the energy decreases, and the conformers sample different regions of the conformational space, experiencing progressive decrease in free energy until the native state is formed. On the right is represented the aggregation process where the unfolded or partially unfolded conformations proceed towards the formation of aggregates and/or amyloid fibrils via intermolecular contacts. Fibrillar aggregation typically occurs by nucleation-dependent polymerization. It may initiate from intermediates populated during de novo folding or after destabilization of the native state (partially folded states) and is normally prevented by molecular chaperones. Amyloidogenic conformers are very stable having very low free energy. Adapted from [8, 9]

Fibrillar aggregation typically occurs by nucleation-dependent polymerization. It may initiate from intermediates populated during *de novo* folding or after destabilization of the native state (partially folded states) and is normally prevented by molecular chaperones. Amyloidogenic conformers are very stable, having a very low free energy, as depicted in the right-hand side of Fig 2, which represents the aggregation process where the unfolded or partially unfolded conformations towards the formation of amyloid fibrils via intermolecular contacts.

In the context of protein folding *vs* protein misfolding, is important to focus on the physicochemical principles of self-organization, with special emphasis on the kinetic competition of folding and aggregation that led nature to evolve folding catalysis and chaperones. The problematic conformation of the proteins is the partially folded or misfolded, which are the ones that tend to aggregate in a concentration-dependent manner. These states typically expose hydrophobic amino-acid residues and regions of unstructured polypeptide

backbone to the solvent — features that become buried in the native state. Like intramolecular folding, aggregation is largely driven by hydrophobic interactions. Indeed, the protein aggregation (self-assembly) process may involve misfolding of a native protein or spontaneous self-assembly of a disordered peptide resulting in the exposure of aggregation prone regions (APR) which are 10-15 residue long segments comprising amino acids with high hydrophobicity, low charge and high propensity to adopt β-sheet structures [17]. These events constitute aggregation hotspots that will generate stable interprotein contacts. Self-assembly of these conformers, driven by APR interactions drives the formation of β-sheet/ β-harpin containing conformers, often accompanied by an increase in compactness and size [16] . During the process of aggregation, the free energy change depends on the peptide monomer concentration. At low concentrations, the monomeric state is favored and at high concentrations the aggregated state is favored because of the large barrier that needs to be overcome to form aggregates, making them highly stable structures [18, 19]. Aggregation starts with nucleation when proteins/polypeptides self-assemble forming a growing core. When this aggregation nucleus crosses a critical mass threshold, reversibility of association is lost, and protein molecules form large aggregates. The transition from the native state to an amyloid conformation can be direct or involve multiple steps or stages, represented in Fig. 3. Protein aggregation can yield different types of conformers, which may include partially or completely unfolded proteins and intermediates, oligomers, unordered amorphous aggregates or highly ordered fibrils called amyloids [18]. Generically they are enriched in a cross-β structure [20], yet fluctuate in sequence, time and conditions [21]. One specific form of aggregated proteins is amyloid conformation, which is very stable, but its formation can still be reversible [22].

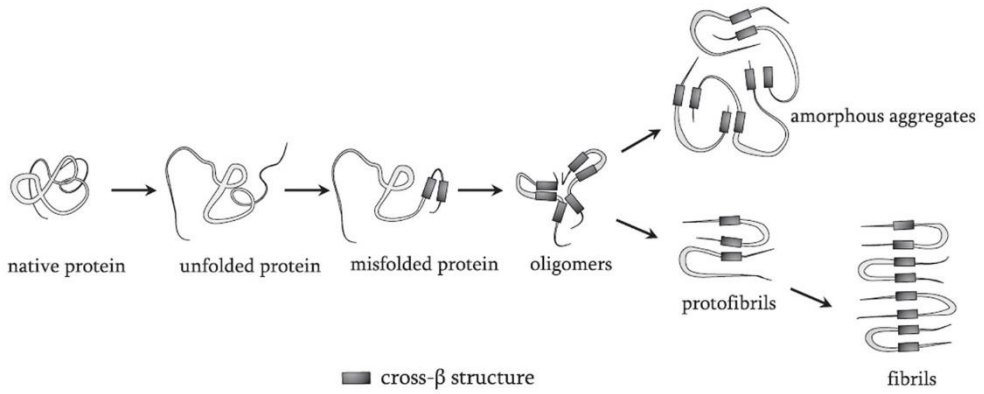

Figure 3 –**Protein misfolding and aggregation**. Under certain circumstances, for example pH or temperature change, proteins undergo conformational changes that result in unfolding and partial misfolding that is associated with the tendency to aggregate. During aggregation, proteins can obtain a range of different structural appearances, which are generally enriched in cross-β structure, including intermediates varying from unordered amorphous aggregates to ordered fibrils that are called amyloid. From [18]

The definition of amyloid is based on structural and biophysical properties. Amyloids are highly ordered protein aggregates defined by β-strands that run perpendicular to the long fibril axis in the so called cross-β structure [8, 13]. Due to its unique three-dimensional structure, amyloid folds only upon intermolecular contacts and the structure repeats itself at the atomic level, accompanied by a characteristic diffraction pattern with a meridional reflection at 4.7 Å and an equatorial reflection (i.e., 90° off the other reflection) at ~8–11 Å [23]. Because of its structure, it can grow by recruiting corresponding amyloid peptide/protein and thus has the capacity to become an infectious protein agent. Amyloids can be routinely detected by the binding of some dyes, such as Congo Red and Thioflavin-T and their derivatives[24], which are very specific for this type of structures. Determining the structure of amyloids has become very challenging: for X-ray crystallography due to the low solubility and for NMR due to its large size. As a result, other techniques, as atomic force microscopy, solid state NMR, transmission electron microscopy (TEM) and cryo-electron microscopy (cryo-EM), shown in Fig. 4, become more important tools to reveal the morphology and structures of amyloid fibrils implicated in some of the gravest of human diseases [25]. Amyloids have a submicroscopic structure, i.e. bundles of straight and rigid fibrils ranging in width from 60 to 130 Å and in length from 1.000 to 16.000 Å, as determined by Cryo electron microscopy studies [26].

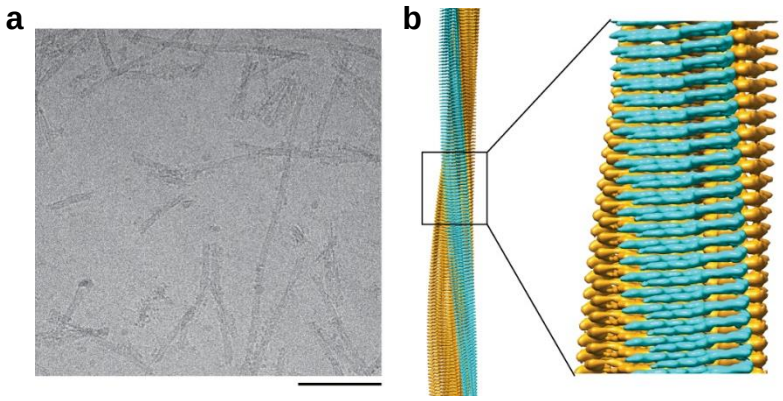

Figure 4 –Cryo-EM structure of ATTR amyloid fibril. a) Cryo-EM image of extracted fibrils. Scale bar = 200nm. b) side view of the reconstructed 3D map. N-terminal density in cyan, C-terminal density in orange. Adapted from [25]

Over the years, it has become clear that many different peptide and protein molecules are able to self-assemble into amyloid fibrils, sharing the common cross-β sheet structure and that are associated with a range of increasingly prevalent clinical disorders, including Alzheimer's and Parkinson's diseases [27]. Understanding the molecular architecture of amyloid fibrils may be an important step towards development of therapeutic interventions based on targeting the fibrils themselves or the processes that generate them.

1.3. Protein quality control and Proteostasis

Proteostasis, from protein homeostasis, is defined by the balanced cellular synthesis and folding and clearance of diverse old, misfolded, and damaged proteins. Newly synthesized proteins are at great risk of aberrant folding and misfolding, potentially forming toxic species. To avoid these dangers, different cellular organelles activate stress programs, which modulate gene expression, to respond to the accumulation of these misfolded proteins. These changes reduce the expression of various genes to attenuate aggregation and induce the production of chaperones, which act in concert to restore functional proteins and proteostasis [28, 29].

The proteostasis network (PN) consists of machineries that assure the balance between synthesis, folding, and clearance. Of its various components, chaperones (including heat shock proteins, HSPs), and chaperonins are the key to ensure the production and persistence of functional and correctly folded proteins (i.e. to maintain proteostasis) [29]. The heat-shock response is the first mechanism that was identified as a cellular response to the accumulation of misfolded proteins in the cytosol [30]. Chaperones are present in all cell types and cellular compartments to ensure that the folding is efficient by reducing the probability of competing reactions, particularly aggregation. Collectively, they can mediate and interact with nascent proteins to stabilize them, or assist with the correct folding into their active conformation, without being present in the protein's final structure [29] (Fig. 5)

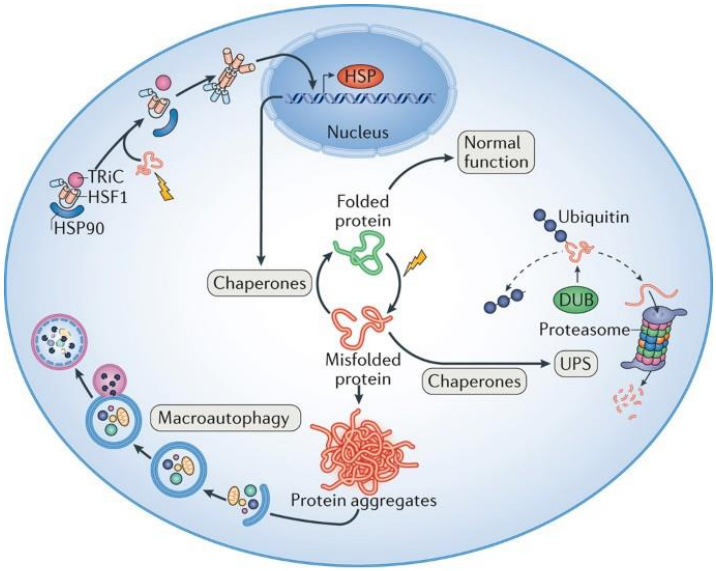

Figure 5 –Overview of proteostasis network. Representation of PQC system: stress causes misfolding of nascent proteins or damage to functional proteins, often resulting in the exposure of hydrophobic surfaces leading to aggregates formation. Subsequence binding of chaperones either initiate refolding or prevents protein aggregation. Under no stress conditions, heat shock factor protein 1 (HSF1) monomers are associated with a chaperon-complex that includes heat-shock protein (HSP)90 and T-complex protein1 ring complex (TRiC). During misfolding, chaperones dissociate from the complex and bind to unfolded proteins. When refolding is not possible, chaperones keep the misfolded proteins in a soluble state, so that protein-degradation system can dispose of it. Ubiquitin–proteasome system (UPS)-mediated proteolysis is the primary degradation system that can remove

soluble (chaperone-presented) misfolded, oxidized, mutant, or otherwise-damaged proteins. The UPS also degrades normal proteins that are no longer needed, providing temporal regulation of protein activity. If the proteins cannot be maintained in a soluble state, autophagy is the primary route to clear the aggregated proteins. DUB, deubiquitinating enzymes.

HSPs are able not only to protect proteins as they fold but also to rescue or inhibit protein misfolding and even aggregation, enabling them to have a second chance to fold correctly. HSPs, typically having hydrophobic binding sites, could recognize and bind tightly to surface-exposed hydrophobic residues of aberrant proteins, thereby sequestrating abnormal proteins and preventing their mutual interaction and subsequent unfavourable aggregation.

Folding, misfolding and unfolding are crucial for many events of cellular activity as trafficking, translocation across membranes, secretion, immune responses and regulation of the cell cycle [16]. Although the amino acid sequences of molecular chaperones and the biological environments in which they function have coevolved to maintain peptides and proteins in their soluble states, in some circumstances they can convert into non-functional and potentially damaging protein aggregates. Intermediates and aggregates which escaped the cellular quality-control mechanism will accumulate in the cell and, besides shifting the folding route towards a dead-end kinetic and energetic trap, leads to cell dysfunction and affects the proteostasis in the cell, leading to disease states [13, 16]. Such folding intermediates are the rule for proteins larger than 100 amino acids (~90% of all proteins in a cell), which have a strong tendency to undergo rapid hydrophobic collapse into compact globular conformations. The collapse may lead either to disorganized globules lacking specific contacts and retaining large configurational entropy or to intermediates that may be stabilized by non-native interactions (misfolded states) [8]. However, the problem starts when proteins fail to fold correctly, which can bring several biological consequences, arising the misfolded proteins possibly leading to misfolded diseases [13].

1.4. Neurodegenerative amyloid diseases

Protein aggregation and formation of amyloids is a hallmark phenomenon that is associated with a wide range of increasingly common human disorders, also known as amyloid diseases, such as Alzheimer's disease (AD) and Parkinson's disease (PD).[31] The formation of these fibrillar aggregates can result from combination of genetic and environmental factors, which is triggered by exposure of aggregation prone regions promoting the self-assembly into an ordered amyloid core. Amyloids can be secreted to the extracellular environment generating deposits, protein inclusions and pathology spreading [32]. The accumulation of toxic

aggregated proteins (including amyloid, amorphous or native-like assemblies) both inside and outside neurons in specific regions of the brain, have links with human neurodegenerative -age-related- diseases, including AD and PD, as well as several other pathologies (Table 1).

Table 1. Amyloid diseases caused by Protein Aggregation: location and affected tissues.

Disease	Aggregation proteins	Location	Affected tissues (region)
Alzheimer's disease (AD)	B-Amyloid (amyloid plaques)	Extracellular	Brain (Cerebral cortex)
	Tau (neurofibrillary tangles)	Intracytoplasmic intraneuronal	Whole Brain
Huntington disease (HD)	Huntingtin	Intranuclear neuronal	
Prion disease	Prion	Extracellular	Brain (grey matter) and peripheral nervous system
Parkinson's disease (PD)	α-synuclein	Intracytoplasmic	Brain (substancia nigra, brain stem)
Amytrophic lateral	SOD1, FUS, TDP-43	Intraneuronal	Motor neurons
Sclerosis (ALS)	Ubiquitin positive proteins		

Notably, despite the involvement of distinct proteins in different neurodegenerative diseases (NDs), the process of protein misfolding and aggregation is remarkably similar. The same type of toxic amyloid fibrillar deposits, formed by different proteins, also progress differently in the brain, affecting the appearance of the different lesions among diseases (Fig 6).

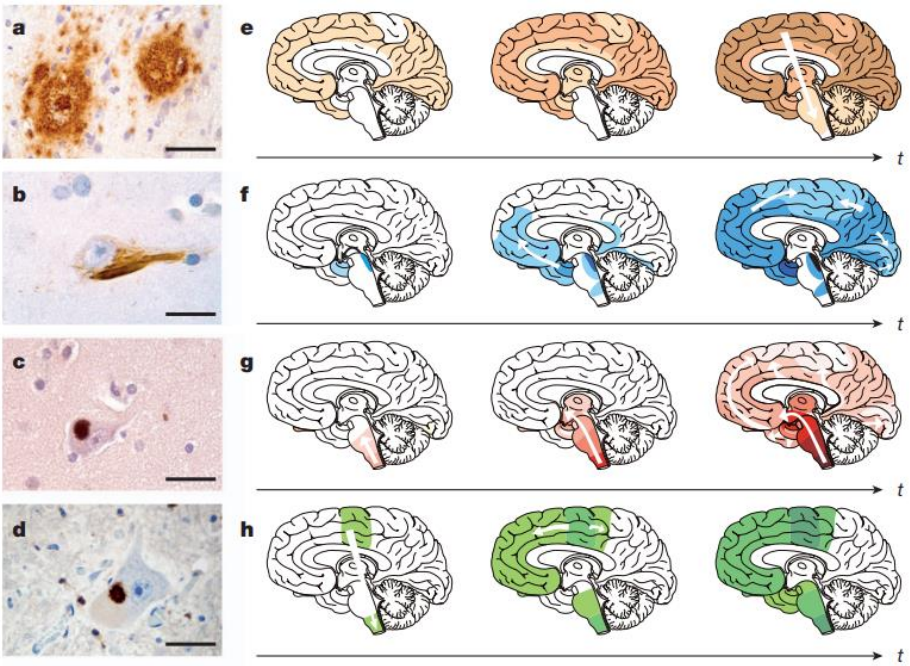

Figure 6 – **Disease progression in the brain in neurodegenerative diseases.** Proteins adopt an amyloid conformation and spread within the brain in different ways. a) Aβ deposits (amyloids plaques) in the neocortex of a patient with Alzheimer's disease. b) Tau inclusions (neurofibrillary tangles) in a neocortical neuron of a patient with Alzheimer's disease. c) α-synuclein in neocortical neuron from a patient with Parkinson's disease. d) TDP-43 inclusion in a motoneuron of the spinal from a patient with amyotrophic lateral sclerosis. Scale bars are 50mm in a and 20mm in b-d. e-h) progression of specific proteinaceous lesions in neurodegenerative diseases over

time (t) inferred from post-mortem analysis of brains. e) and f) Aβ deposits and tau inclusions in AD brains. g) α-syn inclusions in PD-brains and h) TDP-43 inclusions for ALS brains. Three stages are shown for each disease, with white arrows indicating the putative spread of the lesions. From [33].

Aggregates can gradually change in structure and composition over time, especially in cells where the initial aggregate-inducing protein species can sequester and sometimes irreversibly trap other proteins [9, 34]. Aggregate toxicity will depend on a few aspects including the reactive surface, localization, compartmentalization, and stability of the aggregates [9]. The mechanisms of aggregate toxicity include physical damage to membranes; hindrance of transport-processes including axonal transport and nucleocytoplasmic trafficking; co-aggregation of essential proteins like transcription factors, chaperones and components of PQC network; or aberrant metal binding sites that either promote peptide cross-linking or the formation of reactive oxygen species via Fenton reactions [1, 2, 9]. These events will lead to cellular dysfunction, damage of the network of synaptic connections, selective brain mass loss, and brain damage, hallmark events in NDs [35].

Amyloid fibril formation can be associated with loss of function and/or gain of toxic function due to toxicity arising from the formation of oligomers that disrupt membranes and seed further aggregation as well as from the accumulation of highly stable amyloid fibrils that disrupt the proteostasis network. These gain-of-toxic-function diseases are typically age related and are caused by the accumulation of amyloid or amyloid like aggregates of the disease protein. Thus, the age-related decline in proteostasis and specifically in the inability to upregulate chaperones in response to conformational stresses would trigger disease manifestation and, in turn, accelerate proteostasis collapse [28, 29].

In conclusion, maintaining proteostasis through proper PQC largely determines health, and ageing inevitably causes gradual failures in PQC and proteostasis. Proteins that aggregate in disparate neurodegenerative disorders share molecular properties of nucleation, growth, multiplication and spread. Getting knowledge about each of these phenomena, as well as the disease mechanisms and aggregates and amyloids structures and functions, presents potential therapeutic targets. For example, reducing the production or stimulating the removal of amyloidogenic proteins [36], stabilize the native conformation of an amyloidogenic protein [37]102, or stabilizing existing aggregates could be strategies for new therapeutic approaches.

2. References

1. Anfinsen, C.B., *Principles that govern the folding of protein chains.* Science, 1973. **181**(4096): p. 223-30.
2. Anfinsen, C.B. and E. Haber, *Studies on the reduction and re-formation of protein disulfide bonds.* J Biol Chem, 1961. **236**: p. 1361-3.
3. Tunyasuvunakool, K., et al., *Highly accurate protein structure prediction for the human proteome.* Nature, 2021. **596**(7873): p. 590-596.
4. Levinthal, C., *How to fold graciously.* Mossbauer Spectroscopy in Biological Systems Proceedings, 1969. **67**: p. 22-24.
5. Zwanzig, R., A. Szabo, and B. Bagchi, *Levinthal's paradox.* Proc Natl Acad Sci U S A, 1992. **89**(1): p. 20-2.
6. Levinthal, C., *Molecular model-building by computer.* Sci Am, 1966. **214**(6): p. 42-52.
7. Englander, S.W. and L. Mayne, *The nature of protein folding pathways.* Proc Natl Acad Sci U S A, 2014. **111**(45): p. 15873-80.
8. Hartl, F.U., A. Bracher, and M. Hayer-Hartl, *Molecular chaperones in protein folding and proteostasis.* Nature, 2011. **475**(7356): p. 324-32.
9. Raskatov, J.A. and D.B. Teplow, *Using chirality to probe the conformational dynamics and assembly of intrinsically disordered amyloid proteins.* Sci Rep, 2017. **7**(1): p. 12433.
10. Gomes, C.M., *Protein misfolding in conformational disorders.* Curr Top Med Chem, 2012. **12**(22): p. 2459.
11. Kauzmann, W., *Some factors in the interpretation of protein denaturation.* Adv Protein Chem, 1959. **14**: p. 1-63.
12. Ribrault, C., K. Sekimoto, and A. Triller, *From the stochasticity of molecular processes to the variability of synaptic transmission.* Nat Rev Neurosci, 2011. **12**(7): p. 375-87.
13. Chiti, F. and C.M. Dobson, *Protein Misfolding, Amyloid Formation, and Human Disease: A Summary of Progress Over the Last Decade.* Annu Rev Biochem, 2017. **86**: p. 27-68.
14. Dunker, A.K., et al., *Function and structure of inherently disordered proteins.* Curr Opin Struct Biol, 2008. **18**(6): p. 756-64.
15. Granata, D., et al., *The inverted free energy landscape of an intrinsically disordered peptide by simulations and experiments.* Sci Rep, 2015. **5**: p. 15449.
16. Dobson, C.M., *Protein folding and misfolding.* Nature, 2003. **426**(6968): p. 884-90.
17. Beerten, J., J. Schymkowitz, and F. Rousseau, *Aggregation prone regions and gatekeeping residues in protein sequences.* Curr Top Med Chem, 2012. **12**(22): p. 2470-8.
18. Herczenik, E. and M.F. Gebbink, *Molecular and cellular aspects of protein misfolding and disease.* FASEB J, 2008. **22**(7): p. 2115-33.
19. Nelson, R., et al., *Structure of the cross-beta spine of amyloid-like fibrils.* Nature, 2005. **435**(7043): p. 773-8.
20. Rousseau, F., J. Schymkowitz, and L. Serrano, *Protein aggregation and amyloidosis: confusion of the kinds?* Curr Opin Struct Biol, 2006. **16**(1): p. 118-26.
21. Huang, T.H., et al., *Alternate aggregation pathways of the Alzheimer beta-amyloid peptide. An in vitro model of preamyloid.* J Biol Chem, 2000. **275**(46): p. 36436-40.
22. Wetzel, R., *Kinetics and thermodynamics of amyloid fibril assembly.* Acc Chem Res, 2006. **39**(9): p. 671-9.
23. Riek, R., *The Three-Dimensional Structures of Amyloids.* Cold Spring Harb Perspect Biol, 2017. **9**(2).
24. Rambaran, R.N. and L.C. Serpell, *Amyloid fibrils: abnormal protein assembly.* Prion, 2008. **2**(3): p. 112-7.
25. Schmidt, M., et al., *Cryo-EM structure of a transthyretin-derived amyloid fibril from a patient with hereditary ATTR amyloidosis.* Nat Commun, 2019. **10**(1): p. 5008.
26. Cláudio M Gomes, P.F.N.F., *Protein Folding*. 2019, SringerBriefs in Molecular Sciecnce.
27. Cohen, S.I., et al., *From macroscopic measurements to microscopic mechanisms of protein aggregation.* J Mol Biol, 2012. **421**(2-3): p. 160-71.
28. Dubnikov, T., T. Ben-Gedalya, and E. Cohen, *Protein Quality Control in Health and Disease.* Cold Spring Harb Perspect Biol, 2017. **9**(3).
29. Henning, R.H. and B. Brundel, *Proteostasis in cardiac health and disease.* Nat Rev Cardiol, 2017. **14**(11): p. 637-653.

30. Morimoto, R.I., *Regulation of the heat shock transcriptional response: cross talk between a family of heat shock factors, molecular chaperones, and negative regulators.* Genes Dev, 1998. **12**(24): p. 3788-96.
31. Gomes, C.M., W. Hoyer, and J. Luo, *Editorial: The Biochemistry of Amyloids in Neurodegenerative Diseases, Volume I.* Front Neurosci, 2021. **15**: p. 819481.
32. Carvalho, S.B.C., I.; Botelho, H. M.; Yanamandra, K.; Fritz, G.; Gomes, C. M.; Morozova-Roche, L. A., *Structural Heterogeneity and Bioimaging of S100 Amyloid Assemblies*, in *Bionanoimaging: Protein Misfolding and Aggregation*. 2013.
33. Jucker, M. and L.C. Walker, *Self-propagation of pathogenic protein aggregates in neurodegenerative diseases.* Nature, 2013. **501**(7465): p. 45-51.
34. Mogk, A., B. Bukau, and H.H. Kampinga, *Cellular Handling of Protein Aggregates by Disaggregation Machines.* Mol Cell, 2018. **69**(2): p. 214-226.
35. Soto, C. and S. Pritzkow, *Protein misfolding, aggregation, and conformational strains in neurodegenerative diseases.* Nat Neurosci, 2018. **21**(10): p. 1332-1340.
36. Eisenberg, D. and M. Jucker, *The amyloid state of proteins in human diseases.* Cell, 2012. **148**(6): p. 1188-203.
37. Johnson, S.M., et al., *The transthyretin amyloidoses: from delineating the molecular mechanism of aggregation linked to pathology to a regulatory-agency-approved drug.* J Mol Biol, 2012. **421**(2-3): p. 185-203.

Chapter II: The S100 protein family: structure, function, and biological activities

1. The S100 protein family

1.1. Phylogeny and distribution of S100 proteins

General aspects, phylogeny, and sequence features

The S100 protein family consists of 24 members which are only found in vertebrates. They represent the largest subgroup within the Ca^{2+}-binding EF-hand superfamily, sharing significant structural similarities at both genomic and protein levels. The term S100 was firstly introduced in 1965 upon finding of two neuronal protein family members, S100A1 and S100B, and alludes to its solubility (S) in saturated (100%) ammonium sulphate [1] from a bovine brain fraction. The majority of human S100 proteins (S100A1 to S100A16) are organized in a gene cluster located in chromosomal region 1q21 [2], and the different genes are result of several gene duplication events. The remaining family member genes are distributed on chromosome 4 (S100P), 5 (S100Z), 21 (S100B) and the X chromosome (S100G) [3]

In humans, more than twenty S100 homologue proteins have been already identified. A multiple sequence alignment (MSA) of S100 family show highly conserved residues and/or regions among almost all S100s, shown in red, and in blue are shown the less conserved ones (Fig.1).

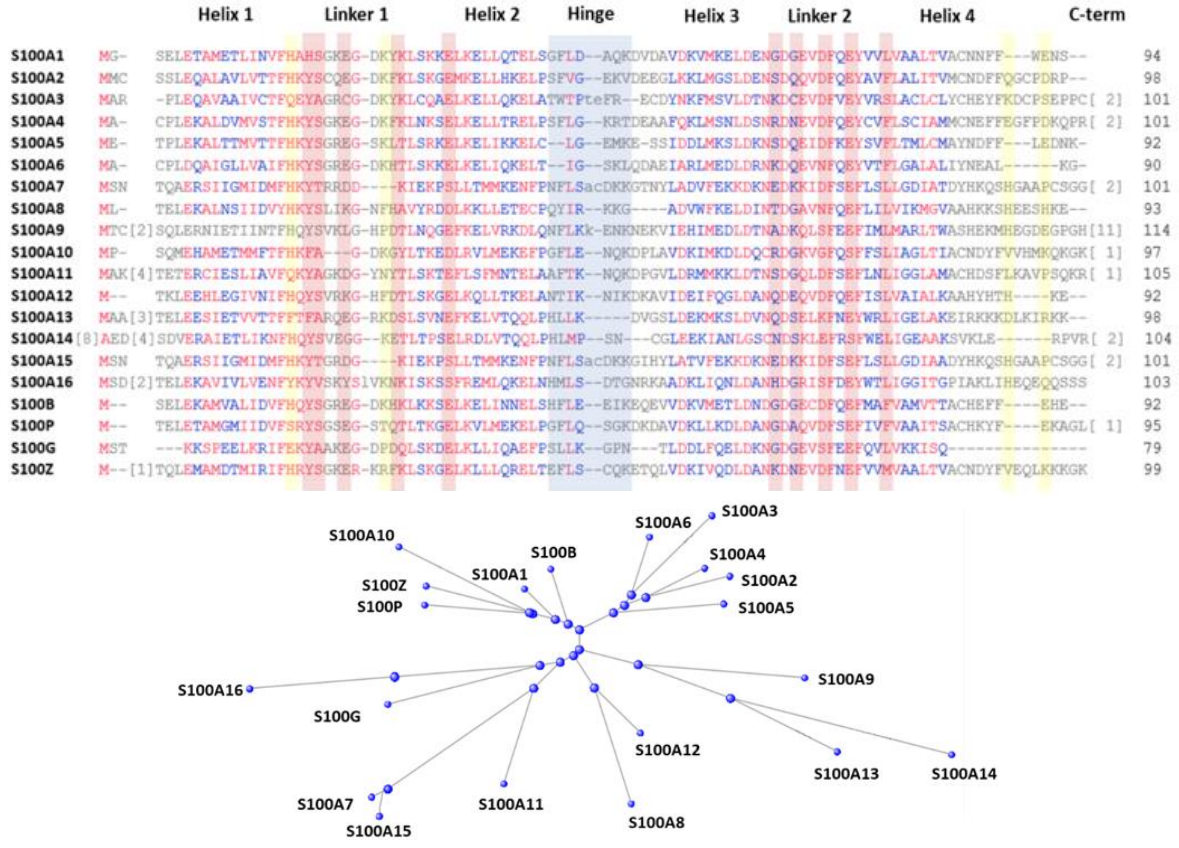

Figure 1 – Sequence and phylogeny features in S100 protein family. **A.** Sequence alignment of human S100 proteins. Multiple sequence alignment columns with no gaps are colored in blue or red: red letters indicate

the conservative residues, and the blue letters indicates the ones that differs; unaligned columns are compressed into the bracket form: [X], where X denotes the number of residues for a sequence in the unaligned range. In Red boxes, are represented the residues involved in binding Calcium, and in yellow, the residues involved in binding transition metals. **B.** Phylogenetic tree of human S100 protein family calculated from the alignment shown in A Phylogenetic tree was based upon multiple sequence alignments of S100 proteins, to determine clusters of similar S100 proteins. S100 protein sequences were extracted from UniProt, https://www.uniprot.org/.

The sequence homology among S100s varied between 22 and 57%, which is mainly due to the variance at the hinge region and C-terminus, the regions associated with their function [4, 5]. This type of alignment allows us to infer on functional and evolutionary relationships between sequences as well as help identify members of gene families. With the same data, a phylogenetic tree was constructed (Fig.1). With the phylogenetic analysis we can address the evolutionary relationships among the family based upon similarities and differences in their genetic characteristics. Among the different S100 sequences, amino acid identity ranges from 20% to 60% [6].

Distribution of S100 proteins in the human body

Although S100 proteins are exclusively expressed in vertebrates, each has a unique expression and distribution profile amongst different tissues and cell types (Fig.2), as well as a specific subcellular localization, underlining their high degree of specialization.

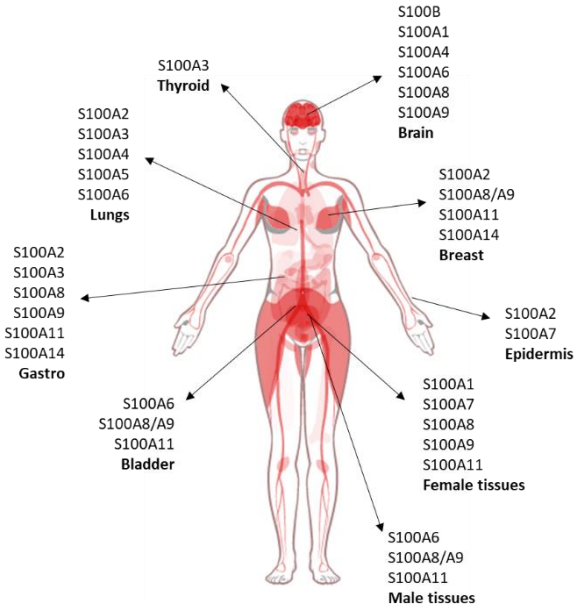

Figure 2 – Protein expression and tissue specific pattern distribution of S100 proteins. Distribution of S100 protein family specific expression patterns over the human body.

Due to their variability in primary sequences and localization in the human body, it is expected that S100 are involved in a multitude of cellular processes. Those may include cell cycle control, cell growth, differentiation, and motility, discussed below. Considering their possible diverse functions, is not surprising that they can are implicated in many human

diseases characterized by altered expression levels in a specific tissue or cell, as in different types of cancers [7, 8], in neurodegenerative diseases such as Alzheimer's disease (AD) [9], in inflammation and in autoimmune diseases [7, 8]

1.2. The structure of S100 proteins

General structural characteristics

Each S100 protein domain is about 10-12kDa in size and contains two EF-hand structural motifs, arranged in a back-to-back manner connected by a flexible linker, with a characteristic high degree of α-helical content [10], as shown in Fig. 3. The EF-hand located at *C-terminus* contains the classical Ca^{2+}-binding motif, with a 12 amino acid long loop, flanked by helices III and IV, where Ca^{2+} is coordinated mainly by amino acids side chain. On the *N-terminus* EF hand, there is a loop with 14 amino acids flanked by helices I and II, where Ca^{2+} is mainly coordinated by backbone carbonyls [11].

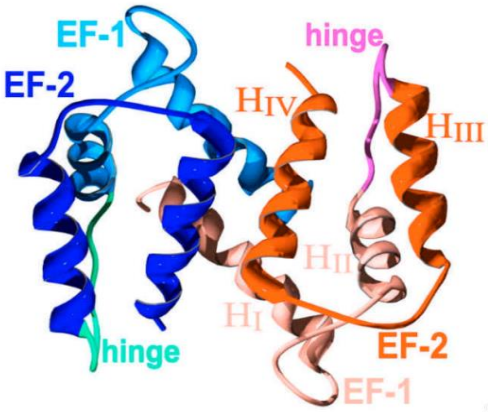

Figure 3 – Dimeric structure of S100 proteins. Monomers are depicted in blue and orange. Each monomer contains two EF-hand connected by a hinge region. From [12]

Ca^{2+}-binding and structural consequences

The conformational properties, function, and oligomerization state of S100 proteins are modulated by metal ion binding. In the metal-free state, the helices of both EF-hands in each monomer adopt antiparallel conformation masking the target protein interaction site. Upon Ca^{2+} binding, there are structural changes involving motions of the two helices flank the Ca^{2+} binding residues (specifically a shift by a 90° degrees movement of helix III), exposing a hydrophobic surface responsible for protein stabilization and facilitate interaction with targets [5, 13] (Fig.4). This surface is formed by residues of the hinge region, helix III and the *C-terminus*, and, curiously, are the regions which exhibit the largest variation in amino acid sequence throughout S100 family. Helices I and IV barely move during the calcium binding, maintained the dimeric state. The highly conserved regions between different S100s are located in these helices, from both monomers, which correspond to the dimer interface, and that are the basis for building a

compact four helix bundle as core structure for both homo and heterodimers [5]. Also, helices I and IV comprise regions with higher aggregation propensity, contiguous to locally disordered segments [14].

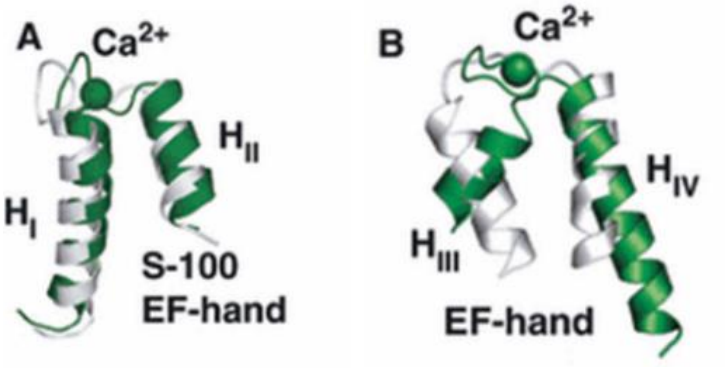

Figure 4 – Structural change of S100 proteins upon calcium binding. Calcium-driven conformational changes at the EF-hands in S100 proteins. Structure of the N-terminal, S100-specific EF-hand **(A)** and the C-terminal, canonical EF-hand **(B)** in the metal-free (lighter) and Ca^{2+}-bound (darker) form of S100A6. The EF-hand flanking helices (H_I–H_{IV}) are identified. From [5]

Generally, dimeric S100 proteins can bind up to four Ca^{2+} (K_d = 20–500μM) with strong positive cooperativity [11]. In the absence of a protein target, S100 proteins exhibit modest Ca^{2+}-binding affinities that are well below intracellular calcium concentrations (which is around 100nM [15]). However, Ca^{2+}-binding affinities increase by 5–300-fold in the presence of peptide and protein targets [16]. Ca^{2+} binding to S100s may be crucial for its functions and also for the formation of heterodimers, as exemplified for $(S100A8/A9)_2$ tetramers [17]. In the absence of Ca^{2+}, the EF-hands can instead accommodate Mg^{2+} ions. The reported affinities for Mg^{2+} ions are rather low, having only a minor effect on Ca^{2+} binding. Like other EF-hand proteins, Ca^{2+} binding-conformational changes leads to the ability to bind another metal-ions, as Zn^{2+}, Mg^{2+}, Mn^{2+} and Cu^{2+} at secondary binding sites [5, 18].

Additional metal ions binding sites

In addition to Ca^{2+}, many S100 proteins (such as S100A2, S100A3, S100A6, S100A7, S100A8／A9, S100A12, and S100B) also bind zinc with high affinity (K_d= 4nM to 2mM) [19]. Each of these S100s, in general, binds two Zn^{2+} ions per homodimer which are coordinated by residues from both subunits, stabilizing the dimer [20]. The binding occurs invariability at dimer interface. Zn^{2+}-binding to S100 proteins can be divided into two groups: one involves Cys residues and the other involves only side chains of His, Glu and Asp residues. Zn^{2+} coordination leads to a stabilization and extension of the C-terminal helix, changing the orientation of residues involved in target binding. There is evidence for a crosstalk between Ca^{2+} and Zn^{2+} binding to S100 proteins. For example, in S100B and S100A12, Zn^{2+} biding leads to an increase in Ca^{2+} affinity [21], whereas in S100A12 an opposite effect of Zn^{2+}

decreasing Ca^{2+} affinity was observed, pointing to an interplay of the metal ions in the activation of S100s [22]. This increase in Ca^{2+} affinity may be due to the His residue located in the Ca^{2+}-binding loops, which are part of Zn^{2+} coordinated residues, that may help to stabilize Ca^{2+}-bound conformation, thereby increasing Ca^{2+} affinity. Other Zn^{2+} coordinating residues are in the *C-terminus* of the S100 proteins and Zn^{2+} coordination leads to stabilization of the C-terminal helix, changing the orientation of the residues involved in target binding. As expected from these structural changes, Zn^{2+} binding modulates target binding properties of different S100 proteins [5]. Additionally, some S100 proteins members, as S100A5 [23], S100A12 [24, 25] and S100B [26], also bind Cu^{2+} and this binding occur frequently at the same sites as Zn^{2+}but with different affinity (K_d=0,46 -55 µM) [23, 27]. Overall, metalation state influence S100 protein conformation, modulation of folding, oligomeric state and presumably functions.

Quaternary structures – Oligomerization

S100 family members typically form homodimers, with the exception for the S100G which is monomeric and for the S100A8/A9 which appears in nature as a heterodimer [28], in a strictly Ca^{2+}-dependent manner [29]. Other heterodimers were reported *in vitro* like S100A1/A4 [30], S100A4/A9 [31], S100A1/P [32], and S100B/A6 and S100B/A11 [33] and the formation of these and tetrameric species is, in some cases, promoted by Ca^{2+}binding. [34]. Besides dimers, also other S100s conformations such as tetramers, hexamers, octamers, and higher oligomeric states were already found [6]. S100s tetramers (S100B [34]) , S100A2 [22], and S100A8/A9 [29]), hexamers (S100B [34], S100A12 [20, 35]), and octamers (S100B [34]), exhibit distinct signaling properties and functional and structural diversity from the homodimers, as functional oligomers [5] (Fig.5).

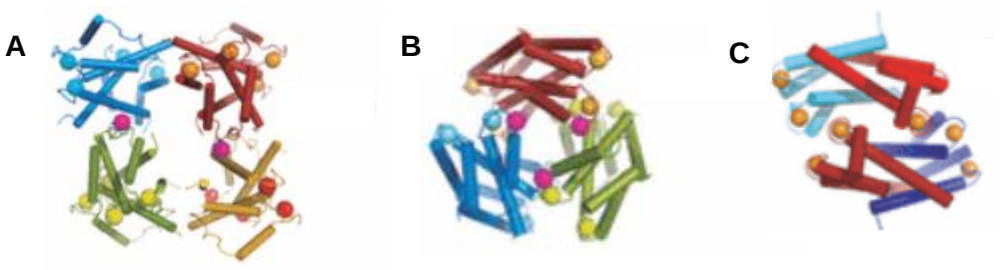

Figure 5 - S100 oligomeric structures. Example of S100 different multimeric states, as S100B octamer, 2H61; (A), S100A12 hexamer, 1GQM (B) and S100A8/A9 tetramer, 1XK4 (C). Each dimer in S100B or S100A12 is shown in an individual colour. S100A8 is shown in red, S100A9 in blue. Bound Ca^{2+} ions are shown as spheres; intersubunit Ca^{2+} ions are shown as magenta spheres. From [5]

Oligomeric proteins are probably more abundant in nature than monomers. There is strong evolutionary pressure for monomeric proteins to associate into oligomers [36]. The oligomers consist of noncovalently associated subunits and can also be either stable or only transiently formed during their specific functional cycle. Oligomerization can be achieved in different ways: two or more monomers form dimers, trimers tetramers *etc.*; tetramerization can be result of addition of monomers to dimers, trimers, etc.; or dimers of dimers, as occurs in tetramers of glyceraldehyde-3-phosphate dehydrogenase and yeast pyruvate decarboxylase [37, 38]. Higher order oligomerization of S100 proteins is mostly non-covalent (S100B covalent tetramers have been described) and can be promoted by low affinity metal binding sites at the exterior surface of the dimer. Both Ca^{2+} and transition metals (particularly Zn^{2+}) have been shown to stimulate oligomerization *in vitro*, and crystal structures have revealed a range of oligomeric states (Fig. 6). As mentioned above, Ca^{2+}-binding leads to conformational changes allowing the exposure of the aggregation prone regions (APRs) at the dimer interface. Under normal conditions, these APRs are protected from aggregation because they are buried in the hydrophobic core of S100 protein domains [39] or interaction sites. Moreover, they are flanked by intrinsically disorder regions (IDR), but, when exposed, can form oligomers and amyloids which can therefore influence downstream signaling and overall cell proteostasis [14]. However, the probability of aggregation-nucleation regions become solvent exposed increases with disease-state conditions, as mutations, physiological stress, or age-related dysregulations. In those conditions, APRs starts to self-assemble into β-structures which can undergo from small soluble oligomeric assemblies to large insoluble inclusions [40].

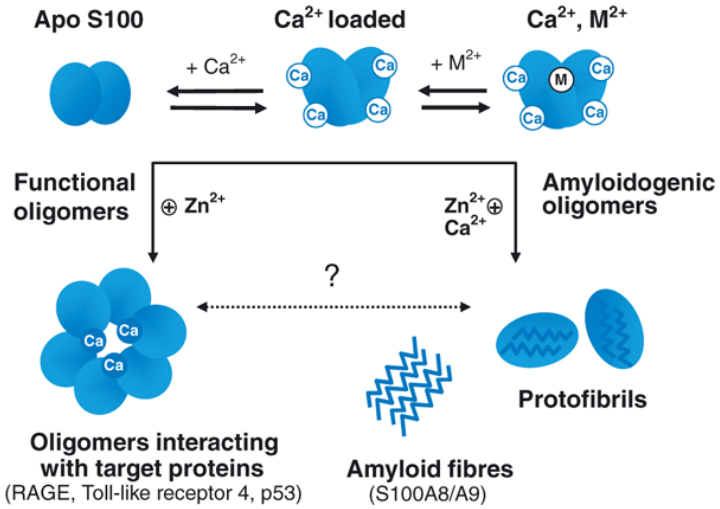

Figure 6 – Oligomerization of S100 proteins. A scheme of interconversion pathways of S100 proteins, evidencing the conformational change upon Ca^{2+} and other metal ions (M^{2+}) binding, and possible routes for oligomerization pathways. From [5]

In some circumstances, more highly oligomerized S100 protein may be more functionally efficient. Tetrameric S100A8/A9 has been introduced as one of the S100 functional

oligomers in a Ca^{2+} or Zn^{2+}-dependent manner [41]. In some cases high concentrations of S100s are required for activation whereas other functions depend on very low amounts [42], indicating different receptor affinities, different extents of ligand-induced receptor oligomerization or requirements of coreceptors [28]. Oligomerization thus seems to be determinant to S100s biological function and signaling. This occurrence raised the interest in S100 protein biology and pathology, as S100 oligomers and amyloids may have yet unknown roles in human disease, possibly by interfering with physiological S100 functions [5, 43]. Together, these facts suggest that S100 may undergo amyloid-like, fibrillar and oligomeric conformations under specific conditions, and that, clearly, metal ions play a determinant role in the process.

1.3. Function of S100 proteins in health and disease

Expression levels and localization

Expression of S100 proteins is carefully regulated to ensure the maintenance of immune homeostasis [44]. Epigenetic mechanisms play a vital role in the regulation of S100 gene expression, with methylation of DNA as a common method of transcriptional repression, and DNA hypomethylation as a significant expression inducer of several S100 members [45]. As an example, the S100A8/A9 heterodimer (termed calprotectin or CP) is constitutively expressed in certain immune cells including monocytes, neutrophils, and dendritic cells [46]. However, upon activation, it is also expressed in fibroblasts or mature macrophages [47], among other cell types. In neutrophils, 45% of the cytosolic proteins are constituted with S100A8 and S100A9, whereas the proportion in only 1% in monocytes [48]. Increasing evidence indicates that several S100 expression patterns differs between physiological and pathological conditions. For example, S100A8 and S100A9 expression could be upregulated by a number of conditions such as oxidative stress, specific cytokines, and growth factors in many types of cells [49]. In the case of S100A12, in physiological conditions, it is expressed in neutrophils, monocytes, and early macrophages [3, 49] but, under inflammation, can be detected in endothelial and epithelial cells, and pro-inflammatory macrophages [50]. Interleukins (ILs) also can significant increase S100s expression levels, as S100A9, by p38 MAPK pathway [51], and S100A7 in keratinocytes [52], and Calprotectin in tumor-infiltrated myeloid cells [53].

Functions dependent and independent of Ca^{2+} binding

Despite a high degree of structural similarity, S100 proteins are not functionally interchangeable. S100 family members modulate complex cellular responses through a multitude of protein:protein interactions, including regulation of cell apoptosis, cytoskeleton organization, cell proliferation, differentiation, migration/invasion, Ca^{2+} homeostasis , protein phosphorylation and inflammation in different cell types [28] [54-56]. (Fig 5). These functions can be either calcium-dependent or calcium-independent. Functionally, S100s are distributed into three main subgroups: a first group includes S100s proteins that only exert intracellular regulatory effects; a second group comprises S100s with intracellular and extracellular functions; and in a third group S100 proteins mainly possess extracellular regulatory effects. On the first subgroup, we have, for example, S100A1 which is predominantly expressed in striated muscle [57] and only exerts intracellular effects related with Ca^{2+} recycle and calcium-induced/calcium release (CICR) cascade [58]. For the second subgroup, additionally to intracellular roles, some S100 are released into extracellular environment and may exert extracellular functions. As examples we have S100B which can activate extracellular signal-regulated protein kinase (ERK) and nuclear factor κB (NF-κB) by binding to its cell surface receptor – receptor for advanced glycation end products – RAGE [59]. The third subgroup includes for instance S100A15 which mainly exerts extracellular regulatory functions.

In resting cells, S100 proteins are localized intracellularly. However, as mentioned before, in some instances, a particular S100 protein can be induced in pathological circumstances in a cell type that does not express it in normal physiological conditions. They are released to the extracellular space where can induce autoimmune conditions and inflammatory disorders [28, 60, 61]. Extracellularly, S100 proteins exert regulatory activities on monocytes, macrophages, microglia, neutrophils, lymphocytes, endothelial and vascular smooth muscle cells, neurons, astrocytes, Schwann cells and epithelial cells, thereby participating in innate and adaptive immune responses, cell migration and chemotaxis, tissue development and repair, and leukocyte and tumor cell invasion [28]. They are also involved in key cellular processes, for example, as pro-inflammatory cytokines and as signaling molecules, by the interaction with intracellular receptors, which are dependent of a dynamic cellular range of concentrations and oligomeric states. Additionally, S100s also have a role in inflammation and migration, through interactions with a variety of target proteins including enzymes, cytoskeletal subunits, receptors, transcription factors and nucleic acids [56] (Fig. 7). Some of their key regulatory functions are described in **Table 1**, as well as their involvement in disease states.

Table 1- S100 proteins: Intra and extracellular functions involved disease pathologies.

S100 Protein	Intracellular function	Extracellular Function	Involved disease
S100A1	Interact with sarcoplasmic reticulum Ca^{2+}-ATPase and RyR2 in the heart [61]	Promote Ca^{2+} flow into cultured ventricular cardiomyocytes [62], lengthen action potentials and enlarge action potential-induced Ca^{2+} transients in neurons [63].	Involved in breast cancer [41] S100A1 deficiency results in abnormal SR Ca^{2+} content and fluxes, deterioration of cardiac performance and heart failure. Cardiomyopathy [64]
S100A2	Bind to p53 transactivation domain and potentiate p53 as a tumor-suppressing protein [65]	Implicate in chemotaxis of eosinophils and calcification of cartilage/bone [66]	Downregulated in many cancers but upregulated in some. Involved in oral [67] lung cancer [68] Tumor suppression [69] Other functions still unclear [70]
S100A3	Epithelial cell differentiation, Ca^{2+} -dependent hairs in the formation of the skin barrier [71] Prevent hair from oxidative damage with affluent Cys [72]	Unknown	Involved in prostate cancer [73] Involved in HCC tumorigenesis and tumor aggressiveness [74]
S100A4	Induces MMP expression and interacts with cytoskeletal proteins, tropomyosin ad actin to promote cell migration [75]	Key role in tumor cell survival and metastasis [76]. Activates NF-kB, inducing production of pro-inflammatory cytokines and migration of neutrophils [77] Stimulate production of cytokine thereby impacting allergic inflammation [78]. Motivate cardiac myocyte growth, survival, and differentiation [76]. Downregulate the pro-apoptotic Bax and the angiogenesis inhibitor thrombospondin-1 genes, and facilitate production of MMPs in endothelial and tumor cells [77]	Empowers expression of metastasis in breast cancer [75, 79, 80], in lung cancer [81], prostate cancer [82], brain cancer [83], bladder cancer [83], thyroid cancer [84], among others.
S100A5	Is found in a small subset of amniote tissues but little is known about the biological roles. May be involved in inflammation and olfactory signaling [85]	Unknown	Upregulated in bladder cancers [86] and recurrent grade I meningiomas [87], but its pathological significance is still unclear
S100A6	Participate in cell proliferation, cytoskeletal dynamics and tumorigenesis [88] Inhibit the interaction between heat shock proteins (Hsp70 and Hsp90) and Sgt1 or Hop to favor apoptosis in some cells [89]	Stimulates insulin release from pancreatic islet cells [88] Regulate allergic responses via inhibiting histamine that are released by mast cells [88]. Activates RAGE and promote apoptosis and generation of ROS in neuroblastoma cells [9]	Involved in Gastric cancer [90] Associated with impaired axons in ALS [91] Possible involvement in nervous system pathologies, as AD, ALS, PD and HD [92] Upregulated in AD [53]
S100A7	Signals through RAGE to activate NF-κB, inducing production of pro-inflammatory cytokines and migration of neutrophils, monocytes, and macrophages [93] [94]	Involved in antimicrobial responses and innate immunity [95] Adheres to, and reduces E. coli survival [95] Zn2+--binding S100A7/RAGE is required for chemotactic activity for lymphocytes, monocytes, and granulocytes [96] S100A7 can cooperate with S100A15 thereby aggravating inflammatory response and promote ROS production from neutrophils [97] Prevent generation of amyloidogenic peptides in Alzheimer's disease [98]	Overexpressed in inflammatory skin diseases [99] Overexpression induces leukocyte infiltration linked to inflammatory skin diseases such as psoriasis [100] Aggressive features in breast cancer [93, 101]
S100A8	Implicated in myeloid cell differentiation [102] Stimulate keratinocyte differentiation *via* inhibiting telomerase activity and exerts anti-inflammatory effects [103] Scavenge intracellular ROS generated by neutrophils and may stabilize NO in these cells [104] Suppress NADPH oxidase activation and transnitrosylate hemoglobin by S-nitrosylation of S100A8 [105] Regulate transendothelial migration of neutrophils by reducing p38 mitogen-activated protein kinase (MAPK)-dependent phosphorylation of S100A9 in neutrophils [105]	Involved in regulation of inflammation [106] Murine and human S100A8 is chemotactic for leukocytes (at picomolar concentrations) [107] and for neutrophils (depending on oxidation state) [108], respectively. Mitigate inflammation response by scavenging oxidant and generating functional modifications [53], [54], [55]. Induce generation of TNF-α and IL-1β by binding to TLR-4, inhibited by S100A9 [109] Can inhibit MMP activity, suggesting an auto-regulatory mechanism [110] Scavenges intracellular ROS and stabilizes NO in neutrophils, protecting from oxidative damage in inflammatory lesions [109]	Overexpressed in inflammatory and autoimmune conditions. Involved in thyroid cancer [111] Precede the formation of AD plaques in mice models [112]

S100A9	Abolish S100A8-induced reduction in telomerase activity [103] Inhibits myeloid (dendritic cell and macrophage) differentiation and accumulation of myeloid-derived suppressor cells in pathological responses by intracellular ROS generation, contributing to tumor growth [113] Reduce microtubule polymerization and F-actin cross-linking via the S100A8/S100A9 complex [105] As a substrate of p38 MAPK, phosphorylation of S100A9 regulates exocytosis by promoting cytoskeletal reorganization [114] Regulates S100A8/A9 activities	Involved in leukocyte migration, chemotactic for neutrophils [115] Induces TNF-α, IL-1β, IL-6, IL-8 in macrophages in NF-kB activation [116] In the presence of Zn^{2+} and Ca^{2+} S100A9 is a RAGE ligand and a TLR-4 ligand and may contribute to the pathogenesis of autoimmune diseases[117] Mediate dystrophic calcification [118] Anti-inflammatory properties [119] Suppresses macrophage activation following uptake of apoptotic neutrophils, *in vitro* [120]	Anti-inflammatory in healthy state, while oxidative stress activates its pro-inflammatory functions. Contributes to the pathogenesis of autoimmune diseases [121] Involved in prostate cancer [122], brain cancer [123], lymphoma [122] and melanoma [124] Associated with osteoclast generation and bone degradation [125] Involved in AD, contributing to amyloid plaque formation together with Aβ [126, 127], and PD, co-aggregating with α-syn [128].
S100A8/A9 (Calprotectin)	Inhibits myeloid cell differentiation [102] and interacts with nuclear factors [129] Transports unsaturated fatty acids and promote NADPH oxidase activation in phagocytes by interaction with p67*phoxand* and Rac-2, and enhance ROS levels [130] Induces microtubule polymerization and F-actin cross-linking	Anti-microbial properties mediated by chelation of Zn^{2+} and Mn^{2+} [131] Contributes to the anti-invasive properties of skin [132] S100A8/A9 amyloid deposition in aging prostate [49] Activate proinflammatory cytokine production by human monocytes and macrophages via the NF-κB and p38 MAPK pathways [116] Promotes tumor development via RAGE-mediated production of inflammatory mediators [133] Inhibits MMPs by sequestering Zn^{2+} from their active sites [110] Released calprotectin may promote endothelial apoptosis [134]	Abundant in atherosclerosis [118] and cardiovascular events [135] Overexpression promotes resistance to TNF-α-induced apoptosis and induces malignant progression through ROS production. Involved in prostate cancer [49, 136] and colon tumor [137]
S100A10	Enhance and assists the binding of certain membrane proteins (e.g. actin-binding protein AHNAK) to annexin 2 by forming ternary complex with them, which facilitates the transport of S100A10 to the plasma membrane [138, 139] Plays important roles in angiogenesis and endothelial cell function	Heterotetrametric complexes with annexin-2 serve as extracellular binding partners for pathogen and host proteins [140] Related to promyelocytic leukemia by promoting tPA-dependent plasmin generation [140] Important role in angiogenesis *in vivo,* pointing a role in endothelial cell function [141] Mediates macrophages recruitment into tumor sites in response to inflammatory stimuli [142] Essential for the migration of tumor-promoting macrophages into tumor site *in vivo* [143]	Downregulated in depressive-like states. Implication in the action of antidepressant drugs and electroconvulsive seizures due to its interaction with serotonin [139] Involved in lung cancer [143] and ovarian cancer [144]
S100A11	When phosphorylated, Ca^{2+}-bound S100A11 inhibits cell growth through activation of cell cycle modulator p21 WAF1/CIP1 [145] Bind to Rad54B (a DNA-dependent ATPase) participated in recombinational repair of DNA damage [146] Stimulate cell growth by enhancing the levels of EGF protein family [147]	Prohibit fertilization by acting on cumulus cells in mice [148] Promote chondrocyte hypertrophy differentiation and matrix catabolism by binding to RAGE and activating the p38 MAPK pathway [149] Stimulates RAGE-dependent type X collagen and IL-8 production [149]	Signal through RAGE to activate p38 MAPK, accelerating chondrocyte hypertrophy and matrix catabolism to promote osteoarthritis progression [150] Involved in lung cancer [151, 152], thyroid cancer [153] and pancreatic cancer [154]
S100A12	Regulate interactions between cytoskeletal elements and membranes [155] Overexpression causes several vascular smooth muscle cell (VSMC) dysfunctions in human aortic aneurysms by regulating mitochondrial function and promoting the production of proMMP2, phosphorylation and nuclear transport of Smad2 [156]	Constitutively expressed by neutrophils Inhibits growth and motility of filarial parasites [25] Enhances Zn^{2+} activity [157] Induce pro-inflammatory cytokine production from master cells [158] but it does not occur in human monocytes or macrophages [159] Bind to RAGE exerting a role in promoting remodeling of atherosclerotic plaque and nodular calcification in vascular smooth muscle cells [160]	Expression in epithelial cells is associated with growth arrest. Overexpression linked to leukocyte influx [156] Involved in thyroid and colorectal cancer [161]
S100B	Stimulates cell proliferation and migration and inhibits apoptosis and differentiation [162]. Lack of S100B downregulation may maintain cell proliferation with potential beneficial effects during development and tissue regeneration, and detrimental effects during tumorigenesis. Regulates Ca^{2+} homeostasis [163]	Different effects on neurons, astrocytes and microglia depending on the concentrations [17] Up to a few nanomolar amounts, behaves like a neurotrophin protecting neuronal cells against neurotoxic stimuli, whereas at micromolar doses it kills neurons through excess ERK1/2 stimulation and ROS production and/or potentiation of neurotoxic effects of β-amyloid, *via* RAGE engagement [17, 164] Stimulates astrocyte proliferation at low doses and promotes inflammatory activities at high doses [17, 164] Overexpression of S100B accelerates AD-like pathology, in transgenic mice [165]	Involved in brain, cartilage and muscle repair, activation of astrocytes in brain damage and neurodegenerative processes, cardiomyocyte remodeling after infarction and in melanoma genesis and gliomagenesis. High levels of expression in AD [166, 167] and PD [54]

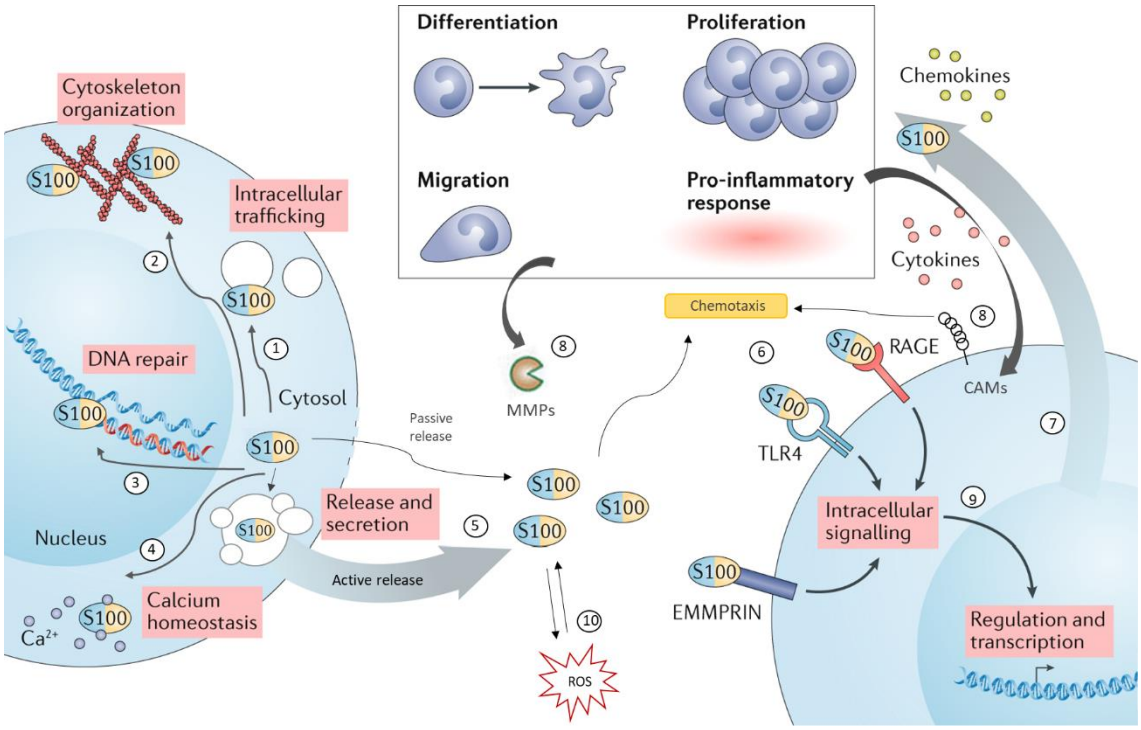

Figure 7 – Role of S100 proteins intra and extracellular. S100 proteins have different functions in cell housekeeping and inflammation. Intracellular functions extend to specific cell functions such as membrane protein recruitment and trafficking (1), cytoskeleton assembly and organization (2) transcriptional regulation and DNA repair (3) and Ca^{2+} homeostasis (4.). Release of S100 proteins occurs either passively upon cell damage or actively following cell activation (5). Once released into the extracellular space, S100 proteins interact with RAGE, TLR4 (6) and EMMPRIN. Upon binding to their receptors, proinflammatory pathways are activated promoting cell migration, proliferation, and differentiation (7). S100 protein-induced signaling pathways also lead to the expression of MMPs and CAMs, thereby promoting chemotaxis and tissue remodeling (8). S100s intracellular signaling results in gene regulation and transcription to restore proteostasis (9). Certain S100 proteins, such as S100A8/A9, are extremely sensitive to oxidation (10). Their redox state acts as a molecular switch from proinflammatory function to protective wound-healing and antioxidant function. In return, oxidation sensitive S100 proteins are believed to act as scavengers of ROS and NO and thereby prevent oxidative stress. CAM – cell adhesion molecule, MMP – matrix metalloproteinase, ROS – reactive oxygen species, EMMPRIN – extracellular matrix metalloproteinase inducer, RAGE – receptor for advances glycation end products, TLR4 – tool-like receptor4. Adapted from [169, 170]

Several S100 proteins can act as damage-associated molecular pattern recognition factors (DAMPs) in the adaptive and innate immune systems [28] and are known to be recruited to sites of inflammation [171]. DAMPs are linked with cell death and tissue damage through induction of inflammatory responses, including rheumatoid arthritis (RA), osteoarthritis (OA) and atherosclerosis [28], or production of biological active molecules [4, 172]. Proinflammatory responses are triggered via binding to pattern recognition receptors expressed on epithelial cells and innate and adaptive immune cells After cell damage/stress or activation of immune cells including neutrophils and macrophages, S100 proteins in extracellular space exert regulatory effects on several different cell types. They can activate

both immune and endothelial cells by binding to receptors for advanced-glycation end products (RAGE) and toll-like receptors (TLR), or other receptors. These interactions are mediated upon calcium and zinc binding [173, 174].

S100s interaction with TLR4, leads to an intracellular signaling pathway.NF-κB and inflammatory cytokine production which is responsible for activating the innate immune system, and with RAGE, propagating cellular dysfunction in several inflammatory disorders and tumors. Upon activation of proinflammatory pathways, cell migration, proliferation and differentiation are promoted, contributing to the expression of MMPs (matrix metalloproteinases) and CAMs (Cell adhesion molecules), very important proteins for the cleavage of cell surface receptors and degrade extracellular matrix and maintaining tissue structure and function.

Metal ions also influence S100s binding and interactions with receptors, such as for S100B, where Ca^{2+} promotes tetramerization and tighter interaction with RAGE [34]. Moreover, Ca^{2+} and Zn^{2+} binding to S100A9 is both required for interaction with receptors such as RAGE or TLR-4 [7, 8, 175]. There is evidence showing that binding of CP, as well as S100A8 and S100A9, to TLR4 triggers a signaling cascade that modulates processes such as inflammation, cell proliferation, differentiation, and tumor development via NF-κB activation [173, 176]. Calprotectin is the most-well studied of the S100 proteins in the immune response; it has been shown to function in the response to a range of microbial pathogens via a mechanism termed “nutritional immunity”, inhibiting growth by sequestering nutrient transition metals Zn^{2+} and Mn^{2+} [18]. Also, calprotectin binds and sequesters zinc, thus inhibiting matrix metalloproteinase and other zinc-dependent enzymes as well as interfering with microbial growth. Elevated CP in plasma levels may lead to severe dysregulation of zinc homeostasis. Besides, Zn^{2+} have an important role in conformation and oligomeric state of S100 family. [177].

Considering the multiplicity of functions associated with S100 proteins, it is not a surprise find these proteins deregulated expression and implicated in numerous human disorders. Various S100 proteins are found in body fluids, including serum, urine, seminal plasma, saliva, sputum, cerebrospinal fluid and in feces and abscess fluid, principally associated with active disease states. They have been implicated in the control of a wide number of intra and/or extracellular functions, including different types of cancers [7, 8], neurodegenerative disorders [94, 168] , inflammation and autoimmune diseases [7, 8, 16, 178, 179], and typically involves upregulation. Moreover, calcium remodeling of Ca^{2+}-homeostasis and dysregulation of Ca^{2+}-signaling in cells is closely associated with uncontrolled cell multiplication, an increase in cell migration, angiogenesis, invasion and cancer progression [180].

S100 proteins involvement in disease state and use as novel biomarkers

S100 proteins have received increasing attention due to their close association with many human diseases. Since several S100 proteins can be identified in body fluids, they may be used as biomarkers to detect specific diseases. Different expression levels of S100 protein family are associated with various pathological conditions, as neurological disorders as neurodegeneration and traumatic brain injuries [168], cancers [7, 56], inflammation and autoimmune diseases [179], and typically involves upregulations [178]. The complexity of the different expression patterns of alterations implies that S100 proteins have a little range of action between acting as both friend and foe and exert both pro- and anti- pathological actions.

In acute inflammation, there are generally elevated systemic levels of some S100s, as S100A8, S100A9 and/or S100A12, likely released from extravasating neutrophils and activated macrophages [28]. Proteins S100A4, S100A8/9, S100A11 and S100A12 have been found to be upregulated in the synovial tissue, synovial fluid, or serum of patients with RA [150, 181, 182]. Expression of S100A8/A9 was elevated in the synovium of a collagenase-induced OA mouse model [34], as well as in patients with sepsis, correlating with severity of disease [183]. S100A12 levels were also found to be significantly increased in the synovial fluid of patients with OA when compared to healthy controls [184].Increased serum levels of S100A6 have been reported in patients with gastric cancer[91]; S100A7 levels have been found to increase in cerebrospinal fluid and brain of patients with AD [99]; S100A12 presents elevated expression levels in patients with diabetes [185]; for individuals with obesity and coronary artery diseases augment CP serum levels have been observed [186]

Nowadays some of them are already used for some diagnosis: S100A1 in an early diagnostic of ischemic coronary diseases [65]; S100B in melanoma [187] and also associated with vitiligo progression [188]; S100A4 which is implicated in metastatic tumor progression [189], several S100s (A7,A8,A9,A12) are involved in chronic skin disease, psoriasis, being S100A12 the one with closest association with disease activity [190]; S100A9-positive inflammatory cells in cancer tissues correlates with a better prognosis in patients with gastric cancer [191]; S100A9 has also been used as a robust biomarker differentiating early stages of cognitive impairment of AD [128]; S100A8/A9 (calprotectin) which represents promising biomarkers to evaluate the risk potential of various types of cancer, rheumatic diseases and cystic fibrosis, among many other possibilities.S100A8 and S100A9 are associated with a number of chronic inflammatory diseases. Beside cancers, S100 proteins also have clinical relevance in brain injury and pathologies having been closely associated with neurodegenerative diseases, such as AD, down syndrome, and schizophrenia [192]. S100s

also play a crucial role triggering inflammation through interaction with receptors RAGE and TLR4, whose calprotectin was demonstrated to be an endogenous agonist [173]. Another way to use S100 as therapeutic approach is the usage of inhibitors for S100B and S100A1 which may delay the progression of AD [193, 194].

S100A8 and S100A9 expression is upregulated in invasive ductal carcinoma of breast, and that extracellular S100A8 and/or S100A9 also contribute to the formation of the pre-metastatic niche [195]. Additionally, S100A8/A9 heterodimer was the first of the S100 proteins family found to be amyloidogenic [41] namely in the ageing prostate, which were found in prostate amyloid deposits known as *corporea amylacea* [136] Yet the specific assembly mechanisms and global processes remains unclear. Moreover, S100A9 is abundant in the brain and has been found in diseased and aged tissues, in the form of punctiform histological inclusions in correlation with classical amyloid pathological hallmarks [127, 196-198], making it a robust biomarker of neurodegeneration, notably Alzheimer's Disease [128]. In the case of autoimmune disorders, S100A9 was newly introduced as a novel biomarker in psoriasis, being highly expressed in induced psoriasiform dermatitis mice [199].

Although gene therapy has not been used to modulate the expression of S100 family members in patients with cancer, it has been used in preclinical animal models, in which, as example, it beneficially upregulates S100A1 expression in heart disease [200]. A novel therapeutic strategy can involve S100 neutralizing antibodies. Already some antibodies targeting S100A8/A9, S100A4 and S100A7 [201] have demonstrated efficacy for a number of pathological conditions, namely cancer [16]. Other approaches to modulate S100 protein activity include S100A4- and S100P–neutralizing antibodies [202, 203], and peptibodies (peptide–Fc fusion proteins) directed against S100A8 and S100A9[204]; both approaches reduce tumor growth in murine cancer models.

Function-blocking antibodies directed towards receptors and ligands have been widely used as therapeutic agents for the treatment of numerous pathologies including cancers and in immune disorders [205, 206]. For example, function-blocking S100A9 antibodies can inhibit dextran sulfate sodium (DSS)-induced acute colitis and attenuate azoxymethane/DSS-induced colitis-associated cancer [207], reduce neutrophilic inflammation and airway reactivity in a murine asthma model [208], and diminish immune cell infiltration and preserve bone/collagen in a model of rheumatoid arthritis [209]. Also, in acute myeloid leukemia (AML), S100A8 antibodies, but not S100A9 antibodies, induce AML cell differentiation, reduce leukemic burden and increase survival [210]. In addition, peptibodies, peptide-Fc fusion proteins that target S100A8 and S100A9, reduce tumor burden in multiple cancer models [204]. Lastly, in murine models of breast cancer, S100A9 antibodies have been used in conjunction with single-photon

emission computed tomography (SPECT) for the in vivo detection of S100A8/A9 as a marker for the establishment of the pre-metastatic niche [195, 211]. Together, these studies highlight the potential use of S100A8 and S100A9 antibodies as both therapeutic and diagnostic reagents.

Some studies focused on S100A4 shows that it blocks monoclonal antibodies limit tumor metastasis and T cell recruitment in syngeneic mouse models of breast cancer [212] , to inhibit the growth of pancreatic tumors in immunocompromised mice [213], to decrease azoxymethane/DSS-induced colon inflammation and tumorigenesis [214] , and to reduce epidermal thickness in a mouse model of human psoriasis [16, 215].

Although the specificity of antibody-based therapies may reduce toxicity and off-target effects, their efficacy may be limited by their ability to target only extracellular S100 proteins. However, conformationally constrained inhibitory peptides directed against S100s, namely S100B, which are capable of penetrating cells, have been shown to reduce tumor growth in a melanoma xenograft model [7, 216]. Other common strategies for inhibiting S100 proteins exploit small molecules that block the hydrophobic cleft required for the recognition of S100 targets, preventing them to bind Ca^{2+} and other small molecules required for their biological functions. These small molecules can block interactions between S100 with RAGE and TLR4, reducing inflammatory responses and inhibition of metastasis [217].

The development of molecular probes, such as antibodies and small-molecule inhibitors, open new insights in therapeutic approaches in S100-involved cancers and other diseases. Despite considerable progress in S100 protein biology, there is currently little information on how post-translational modifications or heterodimer formation affect S100 signaling. A mechanistic examination of both S100 protein biology and biochemistry will be required to define how each family member contributes to the proliferation, metastasis, angiogenesis and immune evasion of cancers and other diseases.

Summing up, S100s have a very specific expression pattern levels for each cell compartment, needed for their correct functions. As much as we know about their involvement in different pathways, the more we can use them as biomarkers to identify and influence pathological states. Moreover, they become good potential drug targets, in the way that we can block or enhance their functions.

1.4. S100 proteins in neurodegeneration

Neurodegeneration refers to a slow and progressive atrophy and loss of function of neurons. is a process which leads to irreversible neuronal damage and death and a common

final pathway present in aging and neurodegenerative diseases (ND), such as Alzheimer's disease (AD), Parkinson's disease (PD) and amyotrophic lateral sclerosis (ALS). There is an increase recognition that inflammation plays a critical role in ND of the central nervous system (CNS). Simultaneously, a feedback and feedforward responses of vascular, astrocytes, and microglia demonstrates that ND involves many roles and interactions of different intermediates and cell types in the decline of brain homeostasis [218]. Additionally, metal ion homeostasis and calcium signaling are also implicated in disease pathogenesis. In the early stages of AD, calcium imbalance triggers neuronal apoptosis and formation of free radicals through mitochondrial dysfunction [167]. An increased neuroinflammatory response has been observed in AD, mediated by the binding of receptors RAGE and TLR4, activating microglia and reactive astrocytes, inducing the chronic expression and secretion of cytokines and chemokines – the so called alarmins or DAMPs – enhancing possibly loss of synapses and neurons[219]. Among these alarmins are S100 proteins, Fig. 8.

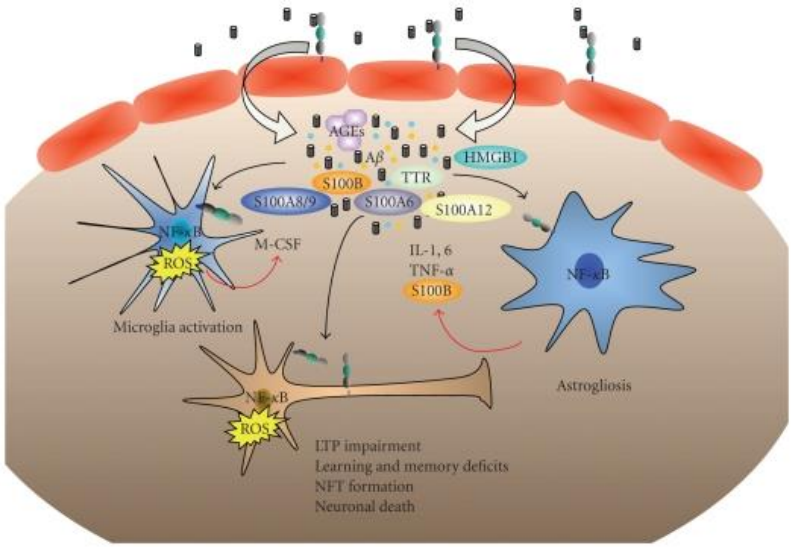

Figure 8 – **Crosstalk between activated microglia signals and its ligands in neuroinflammation, namely Alzheimer's disease.** Upon inflammation, overexpression of S100 proteins is activated. RAGE-mediated activation of glia cells results in the release of inflammatory cytokines. The brain becomes the site of intense inflammation and oxidative stress that facilitates formation of AGEs, and there is accumulation of S100 proteins during disease. Chronic RAGE activation triggers several AD-associated neuropathological features including microglia activation, the production of reactive oxygen species (ROS), neurite degeneration, and neuronal apoptosis ultimately leading to memory impairment. From [220]

S100 proteins influence cognitive processes in the healthy brain and play roles in development and neuronal maintenance. As DAMPs molecules, they play a role in the pathogenesis of neurodegenerative diseases. Some members of the S100 protein group such as S100B [165], S100A9, S100A8, S100A12, S100A1 [194], and the S100A8/A9 complex

[221] are thought to be closely associated to the severity of diseases such as Alzheimer's [167, 222] and Parkinson's [168].

Because S100 proteins are involved in diverse pathways in health state and the deregulated expression in response to stress in disease state, affecting other pathways, S100s gain significant interest. In view of the large number of tertiary and quaternary structures and the complex structure–functional relationship affecting S100s interactions with target proteins, it is tempting to speculate that this variability may account for the promiscuity of S100 proteins. Their involvement in neurodegeneration, more specifically in AD, will be discussed in the next chapter.

2. References

1. Moore, B.W., *A soluble protein characteristic of the nervous system.* Biochem Biophys Res Commun, 1965. **19**(6): p. 739-44.
2. Schafer, B.W., et al., *Isolation of a YAC clone covering a cluster of nine S100 genes on human chromosome 1q21: rationale for a new nomenclature of the S100 calcium-binding protein family.* Genomics, 1995. **25**(3): p. 638-43.
3. Ravasi, T., et al., *Probing the S100 protein family through genomic and functional analysis.* Genomics, 2004. **84**(1): p. 10-22.
4. Chang Xia, Z.B., Amelia C. Toomey, Jixin Zhong, Xiaoquan Rao, *S100 Proteins As an Important Regulator of Macrophage Inflammation.* Front. Immunol., 2018.
5. Fritz, G., et al., *Natural and amyloid self-assembly of S100 proteins: structural basis of functional diversity.* FEBS J, 2010. **277**(22): p. 4578-90.
6. Gilston, B.A., E.P. Skaar, and W.J. Chazin, *Binding of transition metals to S100 proteins.* Sci China Life Sci, 2016. **59**(8): p. 792-801.
7. Bresnick, A.R., D.J. Weber, and D.B. Zimmer, *S100 proteins in cancer.* Nat Rev Cancer, 2015. **15**(2): p. 96-109.
8. Salama, I., et al., *A review of the S100 proteins in cancer.* Eur J Surg Oncol, 2008. **34**(4): p. 357-64.
9. Boom, A., et al., *Astrocytic calcium/zinc binding protein S100A6 over expression in Alzheimer's disease and in PS1/APP transgenic mice models.* Biochim Biophys Acta, 2004. **1742**(1-3): p. 161-8.
10. Vogl, T., A.L. Gharibyan, and L.A. Morozova-Roche, *Pro-inflammatory S100A8 and S100A9 proteins: self-assembly into multifunctional native and amyloid complexes.* Int J Mol Sci, 2012. **13**(3): p. 2893-917.
11. Heizmann, G.F.a.C.W., *3D structures of the calcium and zinc binding S100 proteins.* Handbook of Metalloproteins, 2006.
12. Fritz, G., et al., *The crystal structure of metal-free human EF-hand protein S100A3 at 1.7-A resolution.* J Biol Chem, 2002. **277**(36): p. 33092-8.
13. Carvalho, S.B.C., I.; Botelho, H. M.; Yanamandra, K.; Fritz, G.; Gomes, C. M.; Morozova-Roche, L. A., *Structural Heterogeneity and Bioimaging of S100 Amyloid Assemblies*, in *Bionanoimaging: Protein Misfolding and Aggregation*. 2013.
14. Carvalho, S.B., et al., *Intrinsically disordered and aggregation prone regions underlie beta-aggregation in S100 proteins.* PLoS One, 2013. **8**(10): p. e76629.
15. Bagur, R. and G. Hajnoczky, *Intracellular Ca(2+) Sensing: Its Role in Calcium Homeostasis and Signaling.* Mol Cell, 2017. **66**(6): p. 780-788.
16. Bresnick, A.R., *S100 proteins as therapeutic targets.* Biophys Rev. , 2018. **10(6): 1617–1629**.
17. Leukert, N., et al., *Calcium-dependent tetramer formation of S100A8 and S100A9 is essential for biological activity.* J Mol Biol, 2006. **359**(4): p. 961-72.
18. Zackular, J.P., W.J. Chazin, and E.P. Skaar, *Nutritional Immunity: S100 Proteins at the Host-Pathogen Interface.* J Biol Chem, 2015. **290**(31): p. 18991-8.
19. Heizmann, C.W. and J.A. Cox, *New perspectives on S100 proteins: a multi-functional Ca(2+)-, Zn(2+)- and Cu(2+)-binding protein family.* Biometals, 1998. **11**(4): p. 383-97.
20. Moroz, O.V., et al., *The crystal structures of human S100A12 in apo form and in complex with zinc: new insights into S100A12 oligomerisation.* J Mol Biol, 2009. **391**(3): p. 536-51.
21. Dell'Angelica, E.C., C.H. Schleicher, and J.A. Santome, *Primary structure and binding properties of calgranulin C, a novel S100-like calcium-binding protein from pig granulocytes.* J Biol Chem, 1994. **269**(46): p. 28929-36.
22. Koch, M., et al., *Implications on zinc binding to S100A2.* Biochim Biophys Acta, 2007. **1773**(3): p. 457-70.
23. Schafer, B.W., et al., *Brain S100A5 is a novel calcium-, zinc-, and copper ion-binding protein of the EF-hand superfamily.* J Biol Chem, 2000. **275**(39): p. 30623-30.
24. Moroz, O.V., et al., *Structure of the human S100A12-copper complex: implications for host-parasite defence.* Acta Crystallogr D Biol Crystallogr, 2003. **59**(Pt 5): p. 859-67.
25. Hung, K.W., C.C. Hsu, and C. Yu, *Solution structure of human Ca(2+)-bound S100A12.* J Biomol NMR, 2013. **57**(3): p. 313-8.
26. Nishikawa, T., et al., *Identification of S100b protein as copper-binding protein and its suppression of copper-induced cell damage.* J Biol Chem, 1997. **272**(37): p. 23037-41.

27. Sivaraja, V., et al., *Copper binding affinity of S100A13, a key component of the FGF-1 nonclassical copper-dependent release complex.* Biophys J, 2006. **91**(5): p. 1832-43.
28. Donato, R., et al., *Functions of S100 proteins.* Curr Mol Med, 2013. **13**(1): p. 24-57.
29. Korndorfer, I.P., F. Brueckner, and A. Skerra, *The crystal structure of the human (S100A8/S100A9)2 heterotetramer, calprotectin, illustrates how conformational changes of interacting alpha-helices can determine specific association of two EF-hand proteins.* J Mol Biol, 2007. **370**(5): p. 887-98.
30. Wang, G., et al., *Mutually antagonistic actions of S100A4 and S100A1 on normal and metastatic phenotypes.* Oncogene, 2005. **24**(8): p. 1445-54.
31. Bjo, P., et al., *Common Interactions between S100A4 and S100A9 Defined by a Novel Chemical Probe.* PLoS ONE 2013. **8(5):e63012**.
32. Wang, G., et al., *Heterodimeric interaction and interfaces of S100A1 and S100P.* Biochem J, 2004. **382**(Pt 1): p. 375-83.
33. Deloulme, J.C., et al., *S100A6 and S100A11 are specific targets of the calcium- and zinc-binding S100B protein in vivo.* J Biol Chem, 2000. **275**(45): p. 35302-10.
34. Ostendorp, T., et al., *Structural and functional insights into RAGE activation by multimeric S100B.* EMBO J, 2007. **26**(16): p. 3868-78.
35. Xie, J., et al., *Hexameric calgranulin C (S100A12) binds to the receptor for advanced glycated end products (RAGE) using symmetric hydrophobic target-binding patches.* J Biol Chem, 2007. **282**(6): p. 4218-31.
36. Hugo M. Botelho, G.F., Cláudio M. Gomes, *Amyloid Proteins, Methods and Protocols - Analysis of S100 Oligomers and Amyloids*. 2nd ed. 2012.
37. White, M.R., et al., *A dimer interface mutation in glyceraldehyde-3-phosphate dehydrogenase regulates its binding to AU-rich RNA.* J Biol Chem, 2015. **290**(3): p. 1770-85.
38. Lu, G., et al., *The structural basis of substrate activation in yeast pyruvate decarboxylase. A crystallographic and kinetic study.* Eur J Biochem, 2000. **267**(3): p. 861-8.
39. Dobson, C.M., *Protein folding and misfolding.* Nature, 2003. **426**(6968): p. 884-90.
40. Beerten, J., J. Schymkowitz, and F. Rousseau, *Aggregation prone regions and gatekeeping residues in protein sequences.* Curr Top Med Chem, 2012. **12**(22): p. 2470-8.
41. Yanamandra, K., et al., *Amyloid formation by the pro-inflammatory S100A8/A9 proteins in the ageing prostate.* PLoS One, 2009. **4**(5): p. e5562.
42. R., D., *RAGE: a single receptor for several ligands and different cellular responses: the case of certain S100 proteins.* Curr Mol Med. , 2007. **7:711–24**.
43. Botelho, H.M., G. Fritz, and C.M. Gomes, *Analysis of S100 oligomers and amyloids.* Methods Mol Biol, 2012. **849**: p. 373-86.
44. Donato, R., *Intracellular and extracellular roles of S100 proteins.* Microsc Res Tech, 2003. **60**(6): p. 540-51.
45. Lindsey, J.C., et al., *Epigenetic deregulation of multiple S100 gene family members by differential hypomethylation and hypermethylation events in medulloblastoma.* Br J Cancer, 2007. **97**(2): p. 267-74.
46. Averill, M.M., et al., *S100A9 differentially modifies phenotypic states of neutrophils, macrophages, and dendritic cells: implications for atherosclerosis and adipose tissue inflammation.* Circulation, 2011. **123**(11): p. 1216-26.
47. Ingersoll, M.A., et al., *Comparison of gene expression profiles between human and mouse monocyte subsets.* Blood, 2010. **115**(3): p. e10-9.
48. Schiopu, A. and O.S. Cotoi, *S100A8 and S100A9: DAMPs at the crossroads between innate immunity, traditional risk factors, and cardiovascular disease.* Mediators Inflamm, 2013. **2013**: p. 828354.
49. Hsu K, C.C., Guenther BD, Sorenson BS, Khammanivong A, Ross KF, Geczy CL, Herzberg MC and . *ANTI-INFECTIVE PROTECTIVE PROPERTIES OF S100 CALGRANULINS.* Antiinflamm Antiallergy Agents Med Chem, 2009. **8(4)**: p. 290-305.
50. Mork, G., et al., *Proinflammatory cytokines upregulate expression of calprotectin (L1 protein, MRP-8/MRP-14) in cultured human keratinocytes.* Br J Dermatol, 2003. **149**(3): p. 484-91.
51. Bando, M., et al., *Mechanism of interleukin-1alpha transcriptional regulation of S100A9 in a human epidermal keratinocyte cell line.* Biochim Biophys Acta, 2013. **1829**(9): p. 954-62.
52. Glaser, R., et al., *Antimicrobial psoriasin (S100A7) protects human skin from Escherichia coli infection.* Nat Immunol, 2005. **6**(1): p. 57-64.
53. Kim, J.H., et al., *The role of myofibroblasts in upregulation of S100A8 and S100A9 and the differentiation of myeloid cells in the colorectal cancer microenvironment.* Biochem Biophys Res Commun, 2012. **423**(1): p. 60-6.

54. Santamaria-Kisiel, L., A.C. Rintala-Dempsey, and G.S. Shaw, *Calcium-dependent and -independent interactions of the S100 protein family.* Biochem J, 2006. **396**(2): p. 201-14.
55. Donato, R., et al., *S100B's double life: intracellular regulator and extracellular signal.* Biochim Biophys Acta, 2009. **1793**(6): p. 1008-22.
56. Donato, R., *Functional roles of S100 proteins, calcium-binding proteins of the EF-hand type.* Biochim Biophys Acta, 1999. **1450**(3): p. 191-231.
57. Engelkamp, D., et al., *S100 alpha, CAPL, and CACY: molecular cloning and expression analysis of three calcium-binding proteins from human heart.* Biochemistry, 1992. **31**(42): p. 10258-64.
58. Most, P., et al., *Distinct subcellular location of the Ca2+-binding protein S100A1 differentially modulates Ca2+-cycling in ventricular rat cardiomyocytes.* J Cell Sci, 2005. **118**(Pt 2): p. 421-31.
59. Leclerc, E., et al., *S100B and S100A6 differentially modulate cell survival by interacting with distinct RAGE (receptor for advanced glycation end products) immunoglobulin domains.* J Biol Chem, 2007. **282**(43): p. 31317-31.
60. Nefla, M., et al., *The danger from within: alarmins in arthritis.* Nat Rev Rheumatol, 2016. **12**(11): p. 669-683.
61. Xia, S., et al., *An Update on Inflamm-Aging: Mechanisms, Prevention, and Treatment.* J Immunol Res, 2016. **2016**: p. 8426874.
62. Rohde, D., et al., *S100A1: a multifaceted therapeutic target in cardiovascular disease.* J Cardiovasc Transl Res, 2010. **3**(5): p. 525-37.
63. Reppel, M., et al., *S100A1 enhances the L-type Ca2+ current in embryonic mouse and neonatal rat ventricular cardiomyocytes.* J Biol Chem, 2005. **280**(43): p. 36019-28.
64. Hernandez-Ochoa, E.O., et al., *Augmentation of Cav1 channel current and action potential duration after uptake of S100A1 in sympathetic ganglion neurons.* Am J Physiol Cell Physiol, 2009. **297**(4): p. C955-70.
65. Kiewitz, R., et al., *S100A1, a new marker for acute myocardial ischemia.* Biochem Biophys Res Commun, 2000. **274**(3): p. 865-71.
66. van Dieck, J., et al., *Posttranslational modifications affect the interaction of S100 proteins with tumor suppressor p53.* J Mol Biol, 2009. **394**(5): p. 922-30.
67. Balmain, N., et al., *Immunolocalization of S100A2 calcium-binding protein in cartilage and bone cells.* Cell Mol Biol (Noisy-le-grand), 2003. **49**(4): p. 485-6.
68. Tsai WC, T.S., Jin YT, Wu LW., *Cyclooxygenase-2 is involved in S100A2-mediated tumor suppression in squamous cell carcinoma.* Mol. Cancer Res, 2006. **4**: p. 539–547.
69. Bulk, E., et al., *S100A2 induces metastasis in non-small cell lung cancer.* Clin Cancer Res, 2009. **15**(1): p. 22-9.
70. Wicki, R., et al., *Repression of the candidate tumor suppressor gene S100A2 in breast cancer is mediated by site-specific hypermethylation.* Cell Calcium, 1997. **22**(4): p. 243-54.
71. Wolf, S., C. Haase-Kohn, and J. Pietzsch, *S100A2 in cancerogenesis: a friend or a foe?* Amino Acids, 2011. **41**(4): p. 849-61.
72. Kizawa, K., et al., *Specific citrullination causes assembly of a globular S100A3 homotetramer: a putative Ca2+ modulator matures human hair cuticle.* J Biol Chem, 2008. **283**(8): p. 5004-13.
73. Kizawa, K., et al., *Dissimilar effect of perming and bleaching treatments on cuticles: advanced hair damage model based on elution and oxidation of S100A3 protein.* J Cosmet Sci, 2005. **56**(4): p. 219-26.
74. Kang, M., et al., *S100A3 suppression inhibits in vitro and in vivo tumor growth and invasion of human castration-resistant prostate cancer cells.* Urology, 2015. **85**(1): p. 273 e9-15.
75. Tao, R., et al., *Role of S100A3 in human hepatocellular carcinoma and the anticancer effect of sodium cantharidinate.* Exp Ther Med, 2017. **13**(6): p. 2812-2818.
76. Boye, K. and G.M. Maelandsmo, *S100A4 and metastasis: a small actor playing many roles.* Am J Pathol, 2010. **176**(2): p. 528-35.
77. Forst, B., et al., *Metastasis-inducing S100A4 and RANTES cooperate in promoting tumor progression in mice.* PLoS One, 2010. **5**(4): p. e10374.
78. Zhang, G., et al., *Knockdown of S100A4 decreases tumorigenesis and metastasis in osteosarcoma cells by repression of matrix metalloproteinase-9.* Asian Pac J Cancer Prev, 2011. **12**(8): p. 2075-80.
79. Takenaga, K., Y. Nakamura, and S. Sakiyama, *Expression of a calcium binding protein pEL98 (mts1) during differentiation of human promyelocytic leukemia HL-60 cells.* Biochem Biophys Res Commun, 1994. **202**(1): p. 94-101.
80. Ismail, N.I., et al., *S100A4 overexpression proves to be independent marker for breast cancer progression.* Cancer Cell Int, 2008. **8**: p. 12.

81. Ismail, T.M., et al., *S100A4 Elevation Empowers Expression of Metastasis Effector Molecules in Human Breast Cancer.* Cancer Res, 2017. **77**(3): p. 780-789.
82. Liu, L., et al., *S100A4 alters metabolism and promotes invasion of lung cancer cells by up-regulating mitochondrial complex I protein NDUFS2.* J Biol Chem, 2019. **294**(18): p. 7516-7527.
83. Saleem, M., et al., *S100A4 accelerates tumorigenesis and invasion of human prostate cancer through the transcriptional regulation of matrix metalloproteinase 9.* Proc Natl Acad Sci U S A, 2006. **103**(40): p. 14825-30.
84. Kin-Hoe Chow, H.J.P., Joshy George, Keiko Yamamoto, Andrew D. Gallup, Joel H. Graber, Yuanxin Chen, Wen Jiang, Dennis A. Steindler, Eric G. Neilson, Betty Y.S. Kim, and Kyuson Yun, *S100A4 is a biomarker and regulator of glioma stem cells that is critical for mesenchymal transition in glioblastoma.* Cancer Res., 2017. **77**(18): p. 5360–5373.
85. M Zou, R.S.A.-B., H Al-Hindi, N R Farid, and Y Shi1, *S100A4 (Mts1) gene overexpression is associated with invasion and metastasis of papillary thyroid carcinoma.* Br J Cancer 2005. **93**(11): p. 1277–1284.
86. Wheeler, L.C. and M.J. Harms, *Human S100A5 binds Ca(2+) and Cu(2+) independently.* BMC Biophys, 2017. **10**: p. 8.
87. Yao, R., et al., *Expression of S100 protein family members in the pathogenesis of bladder tumors.* Anticancer Res, 2007. **27**(5A): p. 3051-8.
88. Hancq, S., et al., *S100A5: a marker of recurrence in WHO grade I meningiomas.* Neuropathol Appl Neurobiol, 2004. **30**(2): p. 178-87.
89. Lesniak, W., L.P. Slomnicki, and A. Filipek, *S100A6 - new facts and features.* Biochem Biophys Res Commun, 2009. **390**(4): p. 1087-92.
90. Slomnicki, L.P., B. Nawrot, and W. Lesniak, *S100A6 binds p53 and affects its activity.* Int J Biochem Cell Biol, 2009. **41**(4): p. 784-90.
91. Zhang J, Z.K., Jiang X. , *S100A6 as a potential serum prognostic biomarker and therapeutic target in gastric cancer. .* Dig. Dis. Sci. , 2014. **59**: p. 2136–2144.
92. Hoyaux, D., et al., *S100A6 overexpression within astrocytes associated with impaired axons from both ALS mouse model and human patients.* J Neuropathol Exp Neurol, 2002. **61**(8): p. 736-44.
93. Filipek, A. and W. Lesniak, *S100A6 and Its Brain Ligands in Neurodegenerative Disorders.* Int J Mol Sci, 2020. **21**(11).
94. Cristóvão, J.S., and Gomes, C. M. , *S100 proteins in Alzheimer's Disease.* Front. Neurosci., 2019. **13:463**.
95. Emberley, E.D., et al., *The S100A7-c-Jun activation domain binding protein 1 pathway enhances prosurvival pathways in breast cancer.* Cancer Res, 2005. **65**(13): p. 5696-702.
96. West N.R., W.P.H., *S100A7 (psoriasin) is induced by the proinflammatory cytokines oncostation-M and interleukine-6 in human breast cancer.* Oncogene, 2010. **29**(14): p. 2083-92.
97. Wolf, R., et al., *Chemotactic activity of S100A7 (Psoriasin) is mediated by the receptor for advanced glycation end products and potentiates inflammation with highly homologous but functionally distinct S100A15.* J Immunol, 2008. **181**(2): p. 1499-506.
98. Zheng, Y., et al., *Microbicidal protein psoriasin is a multifunctional modulator of neutrophil activation.* Immunology, 2008. **124**(3): p. 357-67.
99. Qin, W., et al., *S100A7, a novel Alzheimer's disease biomarker with non-amyloidogenic alpha-secretase activity acts via selective promotion of ADAM-10.* PLoS One, 2009. **4**(1): p. e4183.
100. Glaser, R., et al., *The antimicrobial protein psoriasin (S100A7) is upregulated in atopic dermatitis and after experimental skin barrier disruption.* J Invest Dermatol, 2009. **129**(3): p. 641-9.
101. Ekman, A.K., et al., *Overexpression of Psoriasin (S100A7) Contributes to Dysregulated Differentiation in Psoriasis.* Acta Derm Venereol, 2017. **97**(4): p. 441-448.
102. Nasser, M.W., et al., *S100A7 enhances mammary tumorigenesis through upregulation of inflammatory pathways.* Cancer Res, 2012. **72**(3): p. 604-15.
103. Lagasse, E. and I.L. Weissman, *Mouse MRP8 and MRP14, two intracellular calcium-binding proteins associated with the development of the myeloid lineage.* Blood, 1992. **79**(8): p. 1907-15.
104. Rosenberger, S., et al., *A novel regulator of telomerase. S100A8 mediates differentiation-dependent and calcium-induced inhibition of telomerase activity in the human epidermal keratinocyte line HaCaT.* J Biol Chem, 2007. **282**(9): p. 6126-35.
105. Lim, S.Y., et al., *S-nitrosylated S100A8: novel anti-inflammatory properties.* J Immunol, 2008. **181**(8): p. 5627-36.

106. Vogl, T., et al., *MRP8 and MRP14 control microtubule reorganization during transendothelial migration of phagocytes.* Blood, 2004. **104**(13): p. 4260-8.
107. Passey, R.J., et al., *A null mutation in the inflammation-associated S100 protein S100A8 causes early resorption of the mouse embryo.* J Immunol, 1999. **163**(4): p. 2209-16.
108. Lackmann, M., et al., *Identification of a chemotactic domain of the pro-inflammatory S100 protein CP-10.* J Immunol, 1993. **150**(7): p. 2981-91.
109. Goyette, J. and C.L. Geczy, *Inflammation-associated S100 proteins: new mechanisms that regulate function.* Amino Acids, 2011. **41**(4): p. 821-42.
110. van Lent, P.L., et al., *S100A8 causes a shift toward expression of activatory Fcgamma receptors on macrophages via toll-like receptor 4 and regulates Fcgamma receptor expression in synovium during chronic experimental arthritis.* Arthritis Rheum, 2010. **62**(11): p. 3353-64.
111. Isaksen, B. and M.K. Fagerhol, *Calprotectin inhibits matrix metalloproteinases by sequestration of zinc.* Mol Pathol, 2001. **54**(5): p. 289-92.
112. Ashley N Reeb, W.L., Will Sewell, Laura A Marlow, Han W Tun, Robert C Smallridge, John A Copland, Kyle Spradling, Rebecca Chernock, Reigh-Yi Lin, *S100A8 is a novel therapeutic target for anaplastic thyroid carcinoma.* J Clin Endocrinol Metab, 2015. **100**(2): p. 232-42.
113. Lodeiro, M., et al., *Aggregation of the Inflammatory S100A8 Precedes Abeta Plaque Formation in Transgenic APP Mice: Positive Feedback for S100A8 and Abeta Productions.* J Gerontol A Biol Sci Med Sci, 2017. **72**(3): p. 319-328.
114. Cheng, P., et al., *Inhibition of dendritic cell differentiation and accumulation of myeloid-derived suppressor cells in cancer is regulated by S100A9 protein.* J Exp Med, 2008. **205**(10): p. 2235-49.
115. Lominadze, G., et al., *Myeloid-related protein-14 is a p38 MAPK substrate in human neutrophils.* J Immunol, 2005. **174**(11): p. 7257-67.
116. Ryckman, C., et al., *Proinflammatory activities of S100: proteins S100A8, S100A9, and S100A8/A9 induce neutrophil chemotaxis and adhesion.* J Immunol, 2003. **170**(6): p. 3233-42.
117. Sunahori, K., et al., *The S100A8/A9 heterodimer amplifies proinflammatory cytokine production by macrophages via activation of nuclear factor kappa B and p38 mitogen-activated protein kinase in rheumatoid arthritis.* Arthritis Res Ther, 2006. **8**(3): p. R69.
118. Leclerc, E., et al., *Binding of S100 proteins to RAGE: an update.* Biochim Biophys Acta, 2009. **1793**(6): p. 993-1007.
119. McCormick, M.M., et al., *S100A8 and S100A9 in human arterial wall. Implications for atherogenesis.* J Biol Chem, 2005. **280**(50): p. 41521-9.
120. Sroussi, H.Y., J. Berline, and J.M. Palefsky, *Oxidation of methionine 63 and 83 regulates the effect of S100A9 on the migration of neutrophils in vitro.* J Leukoc Biol, 2007. **81**(3): p. 818-24.
121. De Lorenzo, B.H., et al., *Macrophage suppression following phagocytosis of apoptotic neutrophils is mediated by the S100A9 calcium-binding protein.* Immunobiology, 2010. **215**(5): p. 341-7.
122. Björk P, B.A., Vogl T, Stenström M, Liberg D, Olsson A, et al., *Identification of Human S100A9 as a Novel Target for Treatment of Autoimmune Disease via Binding to Quinoline-3-Carboxamides.* PlOS Biology, 2009. **7**(4): p. e1000097.
123. Kallberg, E., et al., *S100A9 interaction with TLR4 promotes tumor growth.* PLoS One, 2012. **7**(3): p. e34207.
124. Chen, S., et al., *Comparative proteomics of glioma stem cells and differentiated tumor cells identifies S100A9 as a potential therapeutic target.* J Cell Biochem, 2013. **114**(12): p. 2795-808.
125. Toshihiko Hibino, M.S., Shoko Miyamoto, Mami Yamamoto, Akira Motoyama, Junichi Hosoi, Tadashi Shimokata, Tomonobu Ito, Ryoji Tsuboi, Nam-Ho Huh, *S100A9 is a novel ligand of EMMPRIN that promotes melanoma metastasis.* Cancer Res, 2013. **73**(1): p. 172-83.
126. Dapunt U, G.T., Maurer S, Stegmaier S, Prior B, Hansch GM, et al. , *Neutrophil-derived MRP-14 is up-regulated in infectious osteomyelitis and stimulates osteoclast generation.* J Leukoc Biol 2015. **98**: p. 575–82.
127. Wang, C., et al., *The role of pro-inflammatory S100A9 in Alzheimer's disease amyloid-neuroinflammatory cascade.* Acta Neuropathol, 2014. **127**(4): p. 507-22.
128. Horvath, I., et al., *Pro-inflammatory S100A9 Protein as a Robust Biomarker Differentiating Early Stages of Cognitive Impairment in Alzheimer's Disease.* ACS Chem Neurosci, 2016. **7**(1): p. 34-9.
129. Horvath, I., et al., *Co-aggregation of pro-inflammatory S100A9 with alpha-synuclein in Parkinson's disease: ex vivo and in vitro studies.* J Neuroinflammation, 2018. **15**(1): p. 172.

130. Kuwayama, A., et al., *Appearance of nuclear factors that interact with genes for myeloid calcium binding proteins (MRP-8 and MRP-14) in differentiated HL-60 cells.* Blood, 1993. **81**(11): p. 3116-21.
131. Kerkhoff, C., et al., *The arachidonic acid-binding protein S100A8/A9 promotes NADPH oxidase activation by interaction with p67phox and Rac-2.* FASEB J, 2005. **19**(3): p. 467-9.
132. Kehl-Fie, T.E., et al., *Nutrient metal sequestration by calprotectin inhibits bacterial superoxide defense, enhancing neutrophil killing of Staphylococcus aureus.* Cell Host Microbe, 2011. **10**(2): p. 158-64.
133. Gebhardt, C., et al., *RAGE signaling sustains inflammation and promotes tumor development.* J Exp Med, 2008. **205**(2): p. 275-85.
134. Ehlermann, P., et al., *Increased proinflammatory endothelial response to S100A8/A9 after preactivation through advanced glycation end products.* Cardiovasc Diabetol, 2006. **5**: p. 6.
135. Frangogiannis, N.G., *S100A8/A9 as a therapeutic target in myocardial infarction: cellular mechanisms, molecular interactions, and translational challenges.* European Heart Journal, 2019. **40**(32): p. 2724–2726.
136. Gharibyan, A.L., D. Raveh, and L.A. Morozova-Roche, *S100A8/A9 amyloidosis in the ageing prostate: relating ex vivo and in vitro studies.* Methods Mol Biol, 2012. **849**: p. 387-401.
137. Ichikawa, M., et al., *S100A8/A9 activate key genes and pathways in colon tumor progression.* Mol Cancer Res, 2011. **9**(2): p. 133-48.
138. Rescher, U. and V. Gerke, *S100A10/p11: family, friends and functions.* Pflugers Arch, 2008. **455**(4): p. 575-82.
139. Svenningsson, P. and P. Greengard, *p11 (S100A10)--an inducible adaptor protein that modulates neuronal functions.* Curr Opin Pharmacol, 2007. **7**(1): p. 27-32.
140. O'Connell, P.A., et al., *Regulation of S100A10 by the PML-RAR-alpha oncoprotein.* Blood, 2011. **117**(15): p. 4095-105.
141. Surette, A.P., et al., *Regulation of fibrinolysis by S100A10 in vivo.* Blood, 2011. **118**(11): p. 3172-81.
142. O'Connell, P.A., et al., *S100A10 regulates plasminogen-dependent macrophage invasion.* Blood, 2010. **116**(7): p. 1136-46.
143. Phipps, K.D., et al., *Plasminogen receptor S100A10 is essential for the migration of tumor-promoting macrophages into tumor sites.* Cancer Res, 2011. **71**(21): p. 6676-83.
144. Wang, L., et al., *S100A10 silencing suppresses proliferation, migration and invasion of ovarian cancer cells and enhances sensitivity to carboplatin.* J Ovarian Res, 2019. **12**(1): p. 113.
145. Sakaguchi, M., et al., *PKCalpha mediates TGFbeta-induced growth inhibition of human keratinocytes via phosphorylation of S100C/A11.* J Cell Biol, 2004. **164**(7): p. 979-84.
146. Murzik, U., et al., *Rad54B targeting to DNA double-strand break repair sites requires complex formation with S100A11.* Mol Biol Cell, 2008. **19**(7): p. 2926-35.
147. Sakaguchi, M., et al., *S100A11, an dual mediator for growth regulation of human keratinocytes.* Mol Biol Cell, 2008. **19**(1): p. 78-85.
148. Hanaue, M., et al., *Characterization of S100A11, a suppressive factor of fertilization, in the mouse female reproductive tract.* Mol Reprod Dev, 2011. **78**(2): p. 91-103.
149. Cecil, D.L. and R. Terkeltaub, *Transamidation by transglutaminase 2 transforms S100A11 calgranulin into a procatabolic cytokine for chondrocytes.* J Immunol, 2008. **180**(12): p. 8378-85.
150. Andres Cerezo, L., et al., *Calgizzarin (S100A11): a novel inflammatory mediator associated with disease activity of rheumatoid arthritis.* Arthritis Res Ther, 2017. **19**(1): p. 79.
151. Hao, J., et al., *Selective expression of S100A11 in lung cancer and its role in regulating proliferation of adenocarcinomas cells.* Mol Cell Biochem, 2012. **359**(1-2): p. 323-32.
152. Sato, H., et al., *Therapeutic potential of targeting S100A11 in malignant pleural mesothelioma.* Oncogenesis, 2018. **7**(1): p. 11.
153. Anania, M.C., et al., *S100A11 overexpression contributes to the malignant phenotype of papillary thyroid carcinoma.* J Clin Endocrinol Metab, 2013. **98**(10): p. E1591-600.
154. Xiao, M., et al., *S100A11 promotes human pancreatic cancer PANC-1 cell proliferation and is involved in the PI3K/AKT signaling pathway.* Oncol Lett, 2018. **15**(1): p. 175-182.
155. Vogl, T., et al., *S100A12 is expressed exclusively by granulocytes and acts independently from MRP8 and MRP14.* J Biol Chem, 1999. **274**(36): p. 25291-6.
156. Hofmann Bowman, M., et al., *S100A12 mediates aortic wall remodeling and aortic aneurysm.* Circ Res, 2010. **106**(1): p. 145-54.
157. Cole, A.M., et al., *Calcitermin, a novel antimicrobial peptide isolated from human airway secretions.* FEBS Lett, 2001. **504**(1-2): p. 5-10.

158. Yang, Z., et al., *S100A12 provokes mast cell activation: a potential amplification pathway in asthma and innate immunity.* J Allergy Clin Immunol, 2007. **119**(1): p. 106-14.
159. Goyette, J., et al., *Pleiotropic roles of S100A12 in coronary atherosclerotic plaque formation and rupture.* J Immunol, 2009. **183**(1): p. 593-603.
160. Hofmann Bowman, M.A., et al., *S100A12 in vascular smooth muscle accelerates vascular calcification in apolipoprotein E-null mice by activating an osteogenic gene regulatory program.* Arterioscler Thromb Vasc Biol, 2011. **31**(2): p. 337-44.
161. Xiaojie Wang, Z.S., Wei Tian, Chenghao Piao, Xiaochen Xie, Jin Zang, Shiqiao Peng, Xiaohui Yu & Yiwei Wang, *S100A12 is a promising biomarker in papillary thyroid cancer.* Scientific Reports, 2020. **10**(1724).
162. Hachem, S., et al., *Expression of S100B during embryonic development of the mouse cerebellum.* BMC Dev Biol, 2007. **7**: p. 17.
163. Xiong, Z., et al., *Enhanced calcium transients in glial cells in neonatal cerebellar cultures derived from S100B null mice.* Exp Cell Res, 2000. **257**(2): p. 281-9.
164. Sorci, G., et al., *S100B Protein, A Damage-Associated Molecular Pattern Protein in the Brain and Heart, and Beyond.* Cardiovasc Psychiatry Neurol, 2010. **2010**.
165. Mori, T., et al., *Overexpression of human S100B exacerbates cerebral amyloidosis and gliosis in the Tg2576 mouse model of Alzheimer's disease.* Glia, 2010. **58**(3): p. 300-14.
166. Hagmeyer, S., et al., *Distribution and Relative Abundance of S100 Proteins in the Brain of the APP23 Alzheimer's Disease Model Mice.* Front Neurosci, 2019. **13**: p. 640.
167. Cristovao, J.S. and C.M. Gomes, *S100 Proteins in Alzheimer's Disease.* Front Neurosci, 2019. **13**: p. 463.
168. Steiner, J., et al., *S100B protein in neurodegenerative disorders.* Clin Chem Lab Med, 2011. **49**(3): p. 409-24.
169. Bertheloot, D. and E. Latz, *HMGB1, IL-1alpha, IL-33 and S100 proteins: dual-function alarmins.* Cell Mol Immunol, 2017. **14**(1): p. 43-64.
170. Austermann, J., C. Spiekermann, and J. Roth, *S100 proteins in rheumatic diseases.* Nat Rev Rheumatol, 2018. **14**(9): p. 528-541.
171. Striz, I. and I. Trebichavsky, *Calprotectin - a pleiotropic molecule in acute and chronic inflammation.* Physiol Res, 2004. **53**(3): p. 245-53.
172. Newton, K. and V.M. Dixit, *Signaling in innate immunity and inflammation.* Cold Spring Harb Perspect Biol, 2012. **4**(3).
173. Vogl, T., et al., *Mrp8 and Mrp14 are endogenous activators of Toll-like receptor 4, promoting lethal, endotoxin-induced shock.* Nat Med, 2007. **13**(9): p. 1042-9.
174. Nacken, W. and C. Kerkhoff, *The hetero-oligomeric complex of the S100A8/S100A9 protein is extremely protease resistant.* FEBS Lett, 2007. **581**(26): p. 5127-30.
175. Leclerc, E. and S.W. Vetter, *The role of S100 proteins and their receptor RAGE in pancreatic cancer.* Biochimica Et Biophysica Acta-Molecular Basis of Disease, 2015. **1852**(12): p. 2706-2711.
176. Loser, K., et al., *The Toll-like receptor 4 ligands Mrp8 and Mrp14 are crucial in the development of autoreactive CD8+ T cells.* Nat Med, 2010. **16**(6): p. 713-7.
177. Kerkhoff, C., et al., *Zinc binding reverses the calcium-induced arachidonic acid-binding capacity of the S100A8/A9 protein complex.* FEBS Lett, 1999. **460**(1): p. 134-8.
178. Heizmann, C.W., *S100 proteins: Diagnostic and prognostic biomarkers in laboratory medicine.* Biochim Biophys Acta Mol Cell Res, 2019. **1866**(7): p. 1197-1206.
179. Foell, D. and J. Roth, *Proinflammatory S100 proteins in arthritis and autoimmune disease.* Arthritis Rheum, 2004. **50**(12): p. 3762-71.
180. Monteith, G.R., N. Prevarskaya, and S.J. Roberts-Thomson, *The calcium-cancer signalling nexus.* Nat Rev Cancer, 2017. **17**(6): p. 367-380.
181. Klingelhofer, J., et al., *Up-regulation of metastasis-promoting S100A4 (Mts-1) in rheumatoid arthritis: putative involvement in the pathogenesis of rheumatoid arthritis.* Arthritis Rheum, 2007. **56**(3): p. 779-89.
182. Baillet, A., et al., *Synovial fluid proteomic fingerprint: S100A8, S100A9 and S100A12 proteins discriminate rheumatoid arthritis from other inflammatory joint diseases.* Rheumatology (Oxford), 2010. **49**(4): p. 671-82.
183. van Zoelen, M.A., et al., *Expression and role of myeloid-related protein-14 in clinical and experimental sepsis.* Am J Respir Crit Care Med, 2009. **180**(11): p. 1098-106.
184. Wang, L.C., et al., *S100A12 levels in synovial fluid may reflect clinical severity in patients with primary knee osteoarthritis.* Biomarkers, 2013. **18**(3): p. 216-20.

185. Oesterle, A. and M.A. Bowman, *S100A12 and the S100/Calgranulins: Emerging Biomarkers for Atherosclerosis and Possibly Therapeutic Targets.* Arterioscler Thromb Vasc Biol, 2015. **35**(12): p. 2496-507.
186. Mortensen, O.H., et al., *Calprotectin--a novel marker of obesity.* PLoS One, 2009. **4**(10): p. e7419.
187. Gogas, H., et al., *Biomarkers in melanoma.* Ann Oncol, 2009. **20 Suppl 6**: p. vi8-13.
188. Birlea, S.A., *S100B: Correlation with Active Vitiligo Depigmentation.* J Invest Dermatol, 2017. **137**(7): p. 1408-1410.
189. Ambartsumian, N., J. Klingelhofer, and M. Grigorian, *The Multifaceted S100A4 Protein in Cancer and Inflammation.* Methods Mol Biol, 2019. **1929**: p. 339-365.
190. D Wilsmann-Theis, J.W., D Holzinger, J Roth 2, S Koch, S Schnautz, T Bieber, J Wenzel, *Among the S100 proteins, S100A12 is the most significant marker for psoriasis disease activity.* J Eur Acad Dermatol Venereol, 2016. **30**(7): p. 1165-70.
191. Fan, B., et al., *Presence of S100A9-positive inflammatory cells in cancer tissues correlates with an early stage cancer and a better prognosis in patients with gastric cancer.* BMC Cancer, 2012. **12**: p. 316.
192. Gazzolo, D., et al., *The Ca(2+)-Binding S100B Protein: An Important Diagnostic and Prognostic Neurobiomarker in Pediatric Laboratory Medicine.* Methods Mol Biol, 2019. **1929**: p. 701-728.
193. Roltsch E, H.L., Young KA, Marks A, Zimmer DB., *PSAPP mice exhibit regionally selective reductions in gliosis and plaque deposition in response to S100B ablation.* J Neuroinflammation 2010. **16;7:78**.
194. Afanador, L., et al., *The Ca2+ sensor S100A1 modulates neuroinflammation, histopathology and Akt activity in the PSAPP Alzheimer's disease mouse model.* Cell Calcium, 2014. **56**(2): p. 68-80.
195. Eisenblaetter, M., et al., *Visualization of Tumor-Immune Interaction - Target-Specific Imaging of S100A8/A9 Reveals Pre-Metastatic Niche Establishment.* Theranostics, 2017. **7**(9): p. 2392-2401.
196. Gruden, M.A., et al., *The misfolded pro-inflammatory protein S100A9 disrupts memory via neurochemical remodelling instigating an Alzheimer's disease-like cognitive deficit.* Behav Brain Res, 2016. **306**: p. 106-16.
197. Wang, C., et al., *S100A9-Driven Amyloid-Neuroinflammatory Cascade in Traumatic Brain Injury as a Precursor State for Alzheimer's Disease.* Sci Rep, 2018. **8**(1): p. 12836.
198. Wang, C., et al., *Proinflammatory and amyloidogenic S100A9 induced by traumatic brain injury in mouse model.* Neurosci Lett, 2019. **699**: p. 199-205.
199. Xin Wang, X.L., Nian Liu HongXiang Chen, *Prediction of crucial epigenetically-associated, differentially expressed genes by integrated bioinformatics analysis and the identification of S100A9 as a novel biomarker in psoriasis.* Int Jornal of Molecular medicine 2019. **45: 93-102**.
200. Weber, C., et al., *Therapeutic safety of high myocardial expression levels of the molecular inotrope S100A1 in a preclinical heart failure model.* Gene Ther, 2014. **21**(2): p. 131-8.
201. Padilla, L., et al., *S100A7: from mechanism to cancer therapy.* Oncogene, 2017. **36**(49): p. 6749-6761.
202. Klingelhofer, J., et al., *Anti-S100A4 antibody suppresses metastasis formation by blocking stroma cell invasion.* Neoplasia, 2012. **14**(12): p. 1260-8.
203. Dakhel, S., et al., *S100P antibody-mediated therapy as a new promising strategy for the treatment of pancreatic cancer.* Oncogenesis, 2014. **3**: p. e92.
204. Qin, H., et al., *Generation of a new therapeutic peptide that depletes myeloid-derived suppressor cells in tumor-bearing mice.* Nat Med, 2014. **20**(6): p. 676-81.
205. Hofmann, K., A.K. Clauder, and R.A. Manz, *Targeting B Cells and Plasma Cells in Autoimmune Diseases.* Front Immunol, 2018. **9**: p. 835.
206. Konig, M., et al., *Tregalizumab - A Monoclonal Antibody to Target Regulatory T Cells.* Front Immunol, 2016. **7**: p. 11.
207. Zhang, X., et al., *Suppression Colitis and Colitis-Associated Colon Cancer by Anti-S100a9 Antibody in Mice.* Front Immunol, 2017. **8**: p. 1774.
208. Lee, T.H., et al., *Role of S100A9 in the development of neutrophilic inflammation in asthmatics and in a murine model.* Clin Immunol, 2017. **183**: p. 158-166.
209. Cesaro A, A.N., Plante A, Pagé N, Tardif MR, Tessier PA, *An inflammation loop orchestrated by S100A9 and calprotectin is critical for development of arthritis.* PLoS One, 2021. **7**(9).
210. Laouedj M, T.M., Gil L, Raquil MA, Lachhab A, Pelletier M, Tessier PA, Barabé F, *S100A9 induces differentiation of acute myeloid leukemia cells through TLR4.* Blood. , 2017. **129**: p. 1980-1990.

211. Becker, A., et al., *Optical in vivo imaging of the alarmin S100A9 in tumor lesions allows for estimation of the individual malignant potential by evaluation of tumor-host cell interaction.* J Nucl Med, 2015. **56**(3): p. 450-6.
212. Grum-Schwensen, B., et al., *S100A4-neutralizing antibody suppresses spontaneous tumor progression, pre-metastatic niche formation and alters T-cell polarization balance.* BMC Cancer, 2015. **15**: p. 44.
213. Hernandez, J.L., et al., *Therapeutic targeting of tumor growth and angiogenesis with a novel anti-S100A4 monoclonal antibody.* PLoS One, 2013. **8**(9): p. e72480.
214. Zhang, J., et al., *S100A4 promotes colon inflammation and colitis-associated colon tumorigenesis.* Oncoimmunology, 2018. **7**(8): p. e1461301.
215. Zibert, J.R., et al., *Significance of the S100A4 protein in psoriasis.* J Invest Dermatol, 2010. **130**(1): p. 150-60.
216. Dhar, A., et al., *Simultaneous inhibition of key growth pathways in melanoma cells and tumor regression by a designed bidentate constrained helical peptide.* Biopolymers, 2014. **102**(4): p. 344-58.
217. Jennbacken, K., et al., *Inhibition of metastasis in a castration resistant prostate cancer model by the quinoline-3-carboxamide tasquinimod (ABR-215050).* Prostate, 2012. **72**(8): p. 913-24.
218. De Strooper, B. and E. Karran, *The Cellular Phase of Alzheimer's Disease.* Cell, 2016. **164**(4): p. 603-15.
219. Venegas, C. and M.T. Heneka, *Danger-associated molecular patterns in Alzheimer's disease.* J Leukoc Biol, 2017. **101**(1): p. 87-98.
220. Leclerc, E., E. Sturchler, and S.W. Vetter, *The S100B/RAGE Axis in Alzheimer's Disease.* Cardiovasc Psychiatry Neurol, 2010. **2010**: p. 539581.
221. Chang, K.A., H.J. Kim, and Y.H. Suh, *The role of S100a9 in the pathogenesis of Alzheimer's disease: the therapeutic effects of S100a9 knockdown or knockout.* Neurodegener Dis, 2012. **10**(1-4): p. 27-9.
222. Chaves, M.L., et al., *Serum levels of S100B and NSE proteins in Alzheimer's disease patients.* J Neuroinflammation, 2010. **7**: p. 6.

Chapter III: S100 proteins in AD and their distribution in AD mice models

Part of this chapter has been published in †Hagmeyer S, †Romão MA, Cristóvão JS, Vilella A, Zoli M, Gomes CM and Grabrucker AM (2019) Distribution and Relative Abundance of S100 Proteins in the Brain of the APP23 Alzheimer's Disease Model Mice. Front. Neurosci. 13:640. doi: 10.3389/fnins.2019.00640. [†These authors have contributed equally to this work]

Part of this work was carried out during a research training visit to the WG Molecular Analysis of Synaptopathies at the Department of Neurology, Neurocenter of Ulm University, Germany. The following experiments were performed by Simone Hagmeyer: RNA extraction, amplification, and quantification, Zinpyr1 staining and S100s fluorescence quantitation.

1. Abstract

Alzheimer's disease is a the most common cause of dementia that affects millions of people. Deposition of Aβ peptide and phosphorylated tau protein into plaques and amyloids, and neuroinflammation, are the major biochemical hallmarks of the disease. Increasing evidence links proteins of the S100 family to the pathogenesis of Alzheimer's disease (AD). S100 proteins are EF-hand calcium-binding proteins with intra- and extracellular functions related to regulation of proliferation, differentiation, apoptosis, and trace metal homeostasis, and are important modulators of inflammatory responses. For example, S100A6, S100A8, and S100B expression levels were found increased in inflammatory diseases, but also in neurodegenerative disorders, and S100A8/A9 complexes may provide a mechanistic link between amyloid-beta (Aβ) plaque formation and neuroinflammation. On the other hand, S100B, a proinflammatory protein that is chronically up-regulated in AD and whose elevation precedes plaque formation, was recently shown to suppress Aβ aggregation. Here, we report expression of S100A6 and S100B in astrocytes and less so in neurons, and low level of expression of S100A8 in both neurons and glial cells *in vitro*. *In vivo*, S100A8 expression is almost absent in the brain of aged wildtype mice, while S100A6 and S100B are expressed in all brain regions and most prominently in the cortex and cerebellum. S100B seems to be enriched in Purkinje cells of the cerebellum. In contrast, in the brain of APP23 mice, a mouse model for Alzheimer's disease, S100B, S100A6, and S100A8 show co-localization with Aβ plaques, compatible with astrocyte activation, and the expression level of S100A8 is increased in neural cells. While S100A6 and S100B are enriched in the periphery of plaques where less fibrillar Aβ is found, S100A8 is more intense within the center of the inclusion. *In vitro* assays show that, similarly to S100B, S100A6, and S100A8 also delay Aβ aggregation suggesting a regulatory action over protein aggregation. We posit that elevated expression levels and overlapping spatial distribution of brain S100 proteins and plaques translates functional relationships between these inflammatory mediators and AD pathophysiology processes that uncover important molecular mechanisms linking the aggregation and neuroinflammation cascades.

2. Introduction

2.1. Brief perspective on Alzheimer's disease

Societal impacts

Alzheimer's disease (AD) is the most common neurodegenerative disease and cause of dementia worldwide, accounting for an estimated 60-80% of cases. It is estimated that

currently there are approximately 55 million people worldwide living with Alzheimer's disease or a related form of dementia [1, 2]. In 2021 in America, more than 6 million people of all ages have AD. According to "*Alzheimer's association*" an estimated 6.5 million American age 65 and older are living with AD in 2022 and this number could grow to 13.8 million by 2060. According About 1 in 9 age 65 and older has Alzheimer's and almost two-thirds are women [1]. Symptoms of the disease can first appear after age 60, and the risk increases with age, being the sixth-leading cause of death in the U.S. [2, 3]. Geographically, AD and dementia are most common in Western Europe (with North America close behind) and least common in Sub-Saharan Africa. In terms of ethnicity, African-Americans are about twice as likely to have Alzheimer's disease or other forms of dementia as white caucasians. Hispanics are about 1.5 times as likely to have Alzheimer's disease or other forms of dementia as caucasians. Statistically, one person in the U.S. develops AD every 66 seconds and projections point to this time decreases to 33 seconds [2, 3].

The progression of Alzheimer's disease is divided into three broad phases: preclinical AD, where there are no symptoms and brain changes are unnoticeable; mild cognitive impairment (MCI) due to AD and dementia due to AD, accompanied by brain changes and problems with memory and eventually physical disability (Fig. 1) AD dementia phase is further broken down into the stages of mild, moderate and severe, which reflect the degree to which symptoms interfere with one's ability to carry out everyday activities.

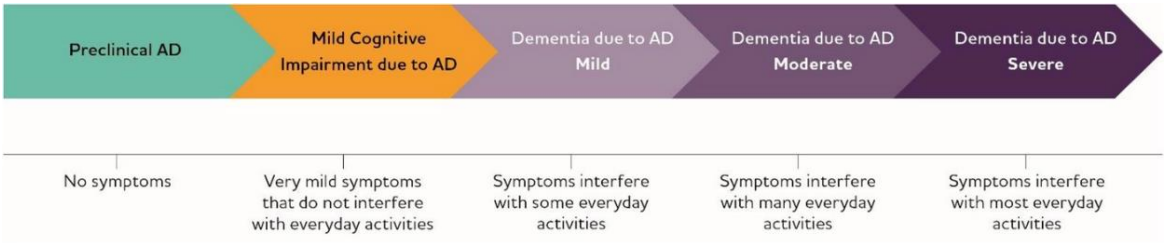

Figure 1 – Alzheimer's disease progression. AD progression is divided into three phases: preclinical AD, mild cognitive impairment due to AD and dementia due to AD. Although arrows are of equal size, the components of AD progression are not equal in duration. From [4]

Molecular hallmarks: amyloid β and tau aggregation

The hallmarks of Alzheimer's disease include atrophy of the cortex and hippocampus, the progressive accumulation of the Amyloid-beta peptide (Aβ) as extracellular plaques outside neurons in the brain, and of twisted intracellular strands composed by aggregated hyperphosphorylated tau protein as neurofibrillary tangles (NFTs) inside neurons. These occurrences are eventually accompanied by chronic neuroinflammation, followed by the death of neuronal cells and damage to brain tissue [4-6]. Simultaneously, a feedback and

feedforward responses of vascular, astrocytes, and microglia demonstrates that AD is a systems disorder which involves many roles and interactions of different intermediates and cell types in the decline of brain homeostasis [7]. AD is a slowly progressive brain disease that begins many years before symptoms emerge. It is in that time window – beginning of the disease and symptoms appearance – that scientist works to act on, towards preventing or delaying the severe progression of the disease.

AD is heterogeneous and multifactorial with sporadic (sAD) and familial (FAD) forms. Either increased production of Aβ and/or production of more aggregation prone species of Aβ (in case of FAD) or impaired clearance of Aβ (in the case of sAD) results in Aβ accumulation in the brain. The large majority of patients, ~95% of the cases, have the sporadic form or late onset dementia, LOAD, (mid -60s or later). This form is very complex and, besides environmental risk factors, is known a specific gene that directly increases the risk of AD, the APOE gene (and its forms APOE-e4, APOE-e2 and APOE-e3) responsible for encoding apolipoprotein E, representing about 40-65% of people diagnosed with AD [8-10]. The few remaining patients, less than 5% of all people with Alzheimer, have the familial form with early onset dementia, EOAD, (between 30s and mid -60s) and may present different symptoms. Autosomal-dominant forms of EFAD result from mutations in one of three genes encoding essential proteins for Aβ formation: the amyloid precursor protein (APP) and the Presenilins 1 and 2 (PSEEN1/2) [11, 12]. Presenilins are components of catalytic subunit of γ-secretase multicomplex, responsible for the cleavage of APP and formation of Aβ, and of these, presenilin-1 is by far the most common cause of early onset familial AD. Mutations in these three genes result in the production of abnormal proteins that are associated with the disease. Each of these mutations plays a role in the breakdown of APP, a membrane glycoprotein that plays an important role in range of biological activities, including neuronal development, neurogenesis, neurite outgrowth and guidance, synapses formation and repair, intracellular transport, and other aspects of neuronal homeostasis [13, 14]. APP proteolytic cleavage is part of a process that generates harmful forms of amyloid plaques by the accumulation of the Aβ peptide extracellularly, a hallmark of Alzheimer's disease, causing neuronal dysfunction. A schematic representation of the process is showed in Fig. 2.

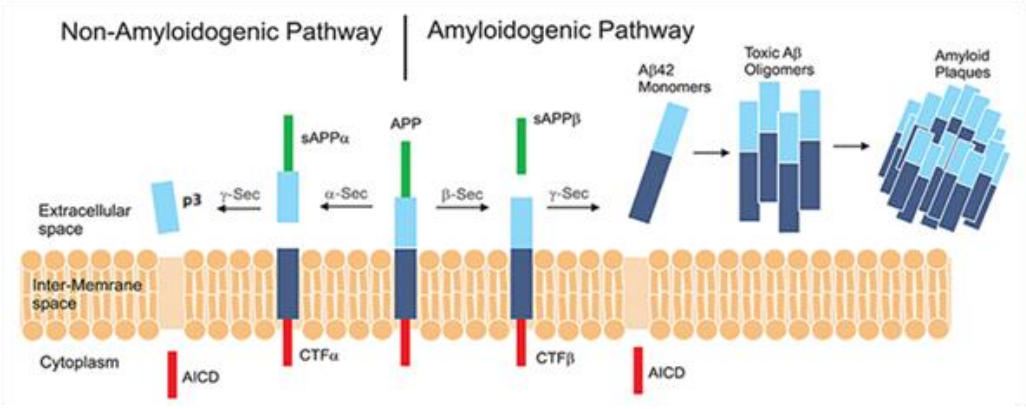

Figure 2 - Amyloid-β pathways that leads to AD. Schematic representation of Aβ amyloidogenic pathway: cleavage of APP by β-secretase and subsequently by γ -secretase results in the production of an amyloid plaque and sAPP-β release externally. The externally released Aβ fragment forms toxic oligomers and eventually packaged in amyloid plaques. The nonamyloidogenic pathway is initiated by α-secretase releasing sAPPα (secreted α-APP) into the intracellular space. The resulting CTF-α fragment is cleaved by γ -secretase in the intermembrane space resulting in both the AICD and p3 fragments that are both non-plaques forming elements. From [15]

Amyloid-β is secreted through sequential APP cleavage, by the β/γ-secretases, resulting in different Aβ species predominantly 38-42 amino acid long from the membrane into the extracellular space [16]. These Aβ peptides should be degraded by enzymes, as neprilysin and insulin degrading enzyme [17], but, in AD, the production and clearance of Aβ is imbalanced and triggers its deposition into amyloid plaques [18]. There are two most common isoforms Aβ40 and $Aβ_{42}$, with the more hydrophobicity and fibrillogenic being $Aβ_{42}$. Some experiments have shown correlations between $Aβ_{42}$/ $Aβ_{40}$ ratios, with a lower ratio associated with higher amyloid burden and steeper accumulation trajectories [19], greater cognitive decline [20], or increased risk of developing AD dementia [21]. There is an emerging consensus that the soluble oligomeric species of $Aβ_{42}$ (dimers, trimers, and small oligomeric aggregates but not monomers) are more neurotoxic than the previously implicated insoluble $Aβ_{42}$ mature fibrils and dense fibril meshes (senile plaques) [22, 23]. Aβ aggregates can be found as soluble oligomeric forms in APP-transgenic mice and human diseased brains [24]. Therefore, there is a possibility that aggregation of Aβ into plaques is a neuroprotective mechanism that eliminates the toxic oligomeric forms [5].

Beside Aβ, NFTs are also a translational hallmark of AD. NFTs are comprised of the microtubule-associated protein tau, in the form of filamentous tau polymers aggregates. Tau protein functions involves the binding to microtubules and assists with their self-assembly, formation and stabilization. However, when tau is hyperphosphorylated, is unable to bind to

the microtubules and become misfolded and unstable, leading to its disintegration. In addition to the well-known changes in phosphorylation state, tau undergoes multiple truncations and shifts in conformation as it transforms from an unfolded monomer to the structured polymer characteristic of NFT [25] (Fig. 3). These structures occur in the regions of the brain responsible for the various cognitive domains that are compromised during the course of AD. According to findings, the propagation of these tau tangles is closely tied to AD's clinical progression [26]. The presence of NFTs is also found in numerous other diseases knows as taupathologies.

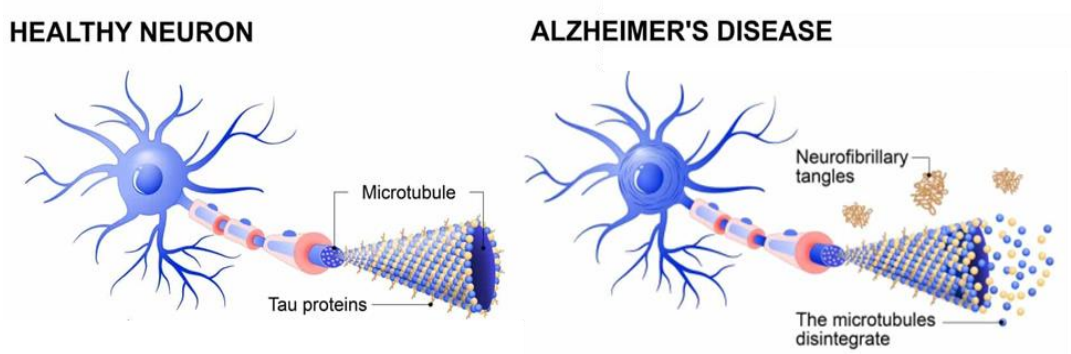

Figure 3 – Neurofibrillary tangles (NFTs) formation in AD. Schematic representation of microtubule-associated Tau protein in healthy neurons, and neurofibrillary tangles formation in Alzheimer's disease leading to microtubules disintegration. From [27]

Intraneuronal neurofibrillary tangles interfere with numerous intracellular functions. Because the tau pathology occurs within the cell bodies and processes of neurons and/or glia, it has always been assumed to be harmful [25]. Tau was found to be involved in certain genetic forms of frontotemporal dementia (FTD), suggesting that tau's aggregation into filaments results in a toxic gain of function much like that hypothesized for Aβ accumulation in AD. Overexpression of neurofilaments leads to accumulation and neuronal degeneration [25] and therefore it is likely that tau self-assembly causes neurodegeneration. In AD this process may be induced by Aβ [22], while in familial FTD it is caused by a Tau mutation, rather than an extracellular insult, which enhances tau filament formation. Findings such as these compel an understanding of the changes that drive, accompany, and sustain the formation of tau polymers in AD [28].

The deposition of these two proteins occurs and progresses in different parts of the brain: once Aβ amyloid plaques first appear in the neocortex and slowly progress through the striatum, brain stem cells and finally cerebellum [29], NFTs begin in the brain stem and progress towards the neocortex [30], in the opposite neuroanatomical direction from Aβ. Only in late stages of the disease, both aggregated proteins are present in the cortex. The genetic evidence obtained from the rare familial form of AD supports the hypothesis that the

accumulation of Aβ plaques is at the origin of the disease, and that Aβ pathology is initiated up to two decades before cortical tau pathology and the onset of clinical symptoms [31, 32].

2.2. S100 proteins and its involvement in Alzheimer's disease

While AD progresses, Aβ induces the chronic expression and secretion of cytokines and chemokines –DAMPS – enhancing Aβ generation and possibly loss of synapses and neurons [33]. Among these DAMPs are S100s whose multiple functions are tied to expression levels and intra- or extracellular localization [34-36] S100B, S100A9, S100A8, and S100A6 are among the most prominent brain expressed S100 proteins, which are all upregulated by aging and neuronal damage. Considering the involvement of S100 proteins in multiple regulatory functions in the brain, the fact that they have age- and damage- related expression, and a direct involvement in neuroinflammation, it is not surprising that they are implicated in molecular processes associated with AD pathogenesis. Fig. 4 depicts the intervention of S100s proteins in different pathways implicated in AD.

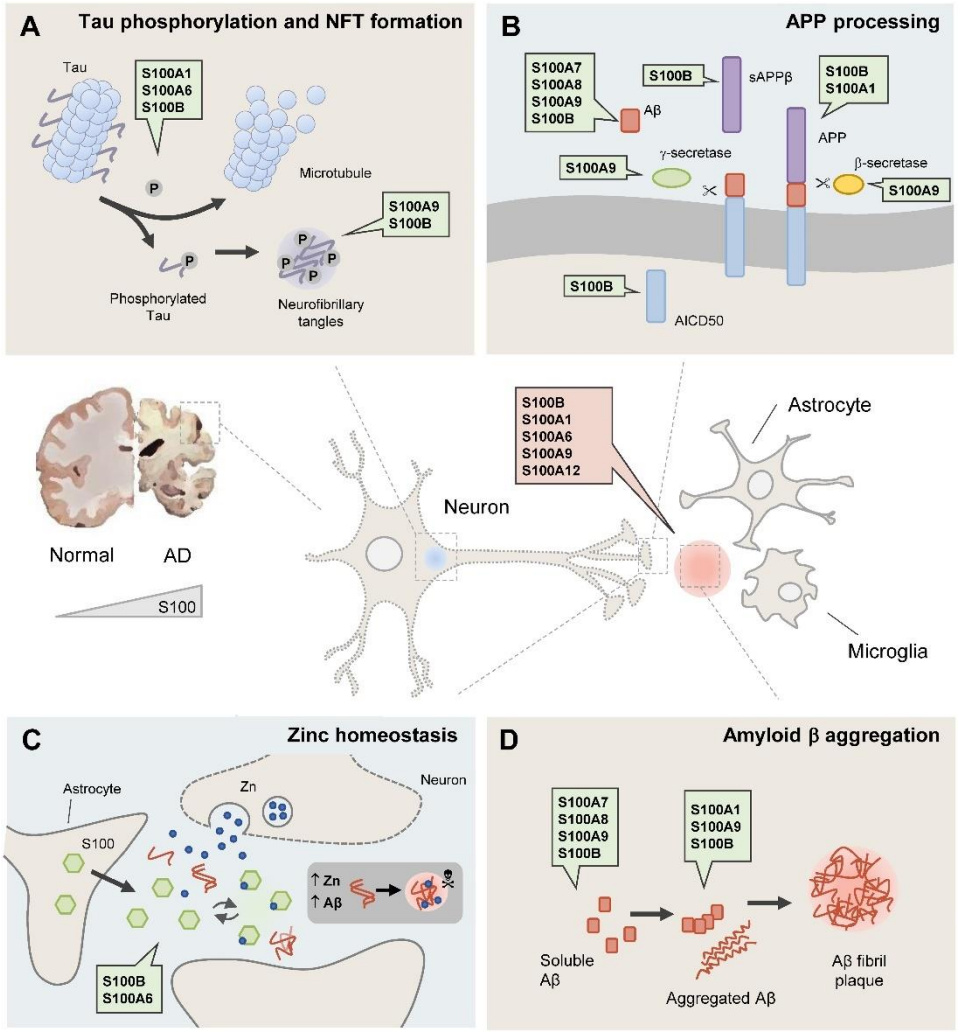

Figure 4 –S100 proteins are involved in a multitude of functions in Alzheimer's disease. In AD brain (central panel), neurons are damage due to the formation of intracellular neurofibrillary tangles (represented by the

blue dot) and extracellular amyloid species including ensembles of low molecular weight aggregates, protofibrils and fibrils (represented by the red dot) astrocyte and microglia become over activated resulting in some S100 proteins overexpression, being implicated in several molecular processes altered in AD. **(A)** Tau phosphorylation and NFT formation. S100A1, S100A6 and S100B are involved in the disassembly of microtubules and Tau release, while S100A9 and S100B are found within neurofibrillary tangles. **(B)** APP processing. Several S100 proteins are implicated in APP cleavage and its amyloidogenic processing. S100A9 regulates γ- and β-secretase expression and activity and S100B and S100A1 regulate APP levels. Moreover, S100A7, S100A8, S100A9 and S100B influence Aβ levels. **(C)** Zinc homeostasis. Due to their zinc-binding properties, S100B and S100A6 have zinc-buffering activities that are related to neuroprotective roles; and S100A6 reduces zinc levels and senile plaque load in PS/APP mouse brains. **(D)** Amyloid β aggregation. S100A1, S100A9, and S100B proteins can interact, modulate the aggregation and co-aggregate with the Aβ peptide. Several S100 proteins (S100B, S100A1, S100A6, S100A8, S100A9, and S100A12), are found within amyloid plaques and in astrocytes and/or microglia around amyloid deposits. From [37]

Understanding the physiology of S100 proteins in the context of their concentration – dependent activities and the investigation of the transition between their trophic roles (at nanomolar intracellular levels) and deleterious pro-inflammatory activities (at micromolar extracellular levels) is particularly challenging in the context of AD pathophysiology, as it can open new therapeutic opportunities.

S100B is one of the most abundant proteins in the brain (0.5%) and is constitutively produced by astrocytes at low levels. Brain injury and neurodegeneration result in astrocyte activation and increased expression of S100B, with its extracellular release and engagement of RAGE-mediated signaling and microglial activation [38]. Several evidences implicate S100B in AD pathogenesis: it is systematically elevated in AD patients and animal models [39-41], it is present in elevated amounts in astrocytes surrounding neuritic plaques preceding their appearance [42] and is suggested to regulate plaque formation. Knockout of S100B in the PS/APP AD mouse model selectively decreases plaque load in the cortical region [43] and its overexpression increases Aβ levels and deposits at early stages [44]. While elevated levels of extracellular S100B trigger AD aggravating roles as a pro-inflammatory enhancer, novel protective functions for S100B at lower levels and early disease stages are emerging. Recently we have established that S100B is a regulator of elevated zinc levels in the brain and that this metal-buffering activity is tied to a neuroprotective role, through an indirect effect on calcium levels and in inhibition of excitotoxicity [45]. Also, we have recently reported a calcium-tuned interaction between S100B and Aβ42 monomers, oligomers, and fibrils that suppresses Aβ42 aggregation and mitigates its cellular toxicity [46]. S100A6 is also upregulated in AD patients as well as in AD model mice [47-49]. The protein is found in clusters in astrocyte-positive regions within senile plaques. Its high affinity zinc binding properties led to the suggestion that

it may play a role in the regulation of the homeostasis of this metal ion in AD [47]. Interestingly, a zinc sequestering effect similar to that reported for S100B was recently elucidated: exogenous S100A6 protected cultured cells against Zn^{2+} toxicity and in APP/PS1 transgenic mice, increased S100A6 levels correlated with disaggregation of Aβ and decrease in plaque load [50]. Finally, S100A8 is also implicated in AD and its levels correlate with those of Aβ, being elevated in the hippocampus of Tg2576 and TgAPParc AD model mice [51]. Reciprocally, exposure of SH-SY5Y neuroblastoma cells to recombinant S100A8 increased Aβ42 and decreased Aβ40 production [51]. Studies in Tg2576 and TgAPParc AD mice brains indicate the presence of S100A8 inclusions distinct from corpora amylacea, that are formed independently of Aβ plaques [51], a feature which is likely tied to the self-assembly propensity of the S100 family members [52-54].

S100A9, also known as MRP14, has been shown to be involved in the progression of neurodegenerative and neuroinflammatory disorders [55-59] and to be strongly increased in brain lysates of AD [60, 61]. S100A9 was found to be present in activated glial and neurons positive for tau neurofibrillary tangles [62] and to be abundant in tissues surrounding amyloid deposits in AD [63], where is suggested that the increase of Aβ42 aggregation and deposition correlates with the elevation of S00A9 levels [63]. In some studies, it was possible to observe Aβ42 plaques and also isolated S100A9 plaques that are not colocalized, forming separate tissue deposits [56, 64]. In vitro biophysical approaches showed that S100A9 binds to Aβ40 through hydrophobic interactions [63, 65]. Kinetic assays suggested that S100A9 co-aggregates with Aβ40, promoting the formation of amyloid fibrils. The co-aggregation of S100A9 with Aβ42 was also referred to inhibit Aβ42 cytotoxicity [63]. Knockdown of S100A9 decreases cognition decline on Tg2576 mice and reduces amyloid plaque burden [60, 66]. S100A9 was found within amyloid plaques of sporadic and familial PS-1 AD brains [62, 63]. Also in Tg2576 AD mice, knockdown or knockout of S100A9 significantly reduced the neuropathology and greatly improved learning and memory [60], suggesting a link between S100A9 and AD pathology. However, the underlying structural and molecular details of such process remain enigmatic, and the characteristics of the fibrillar materials formed may differ from those of canonical amyloid fibrils. S100A8 was also found to be upregulated in AD patients [67]. Aggregates have also been suggested to precede the formation of AD plaques in mice models [51] S100 protein regulate several processes associated with AD but whose contribution and direct involvement in disease pathology remains to be fully established. S100A8 were found in microglial cells localized around amyloid plaques [61]. Also associated with amyloid plaques are S100A1 [68], S100A6 [50] S100A9 [62], S100A12 [62] and S100B [62]. Moreover, low levels of S100A9 inhibit Aβ42 cytotoxicity [37].

Like for AD, recent studies have shown that S100A9 is abundant in PD brain tissues both intracellularly and inside the Lewy bodies amyloid deposits, co-localized with in α-synuclein. In that study, they introduce the native S100A9, rather than its fibrils, as a player in α-synuclein aggregation, potentiating its amyloid formation [59]. Studies shows that in acute traumatic brain injury (TBI) S100A9 is upregulated and S100A9 deletion contribute to neuroprotection, improve TBI-impaired motor and cognitive function, and prevents neurodegeneration diminishing neuroinflammation [69]. Moreover, was recently published that on TBI mice models, S100A9 aggregates intracellularly into amyloid oligomers, and the self-assemblies occurs within minutes in acidic environments [70].

S100B as a novel type of anti-aggregation molecular chaperone

S100B is secreted from astrocytes and studies suggests that S100B can act both as a pro-inflammatory cytokine and as DAMP molecule, depending on its concentration. Most of the studies report mainly deleterious effects of S100s. Indeed, at micromolar concentrations S100B has deleterious effects inducing neuronal apoptosis but, at nanomolar concentration, S100B has neurotrophic effects, which lead to promotion of neuronal survival and neurite growth [37]. This open gates to introduction of some protective roles of S100 proteins. Early inflammatory responses start in a very-early stage of AD processes, most likely before amyloid plaques formation [71, 72]. This led us to the possibility of these inflammatory molecules, including S100, being involved at the early stages of AD pathology, even before the onset of the disease phenotypes.

Recently in our lab, we found that S100B has protective functions at early stages of inflammatory responses. Low levels of S100B have neuroprotective functions as a suppressor of Aβ aggregation and toxicity, protecting cells. Moreover, S100B was shown to regulate zinc homeostasis in neurons (Fig. 5) [73]. Was also demonstrated by biophysical and kinetic approaches, that substoichiometric S100B has dual function chaperon capable of suppressing the formation of toxic Aβ oligomers through both chelation of zinc and inhibition of protein aggregation [73].

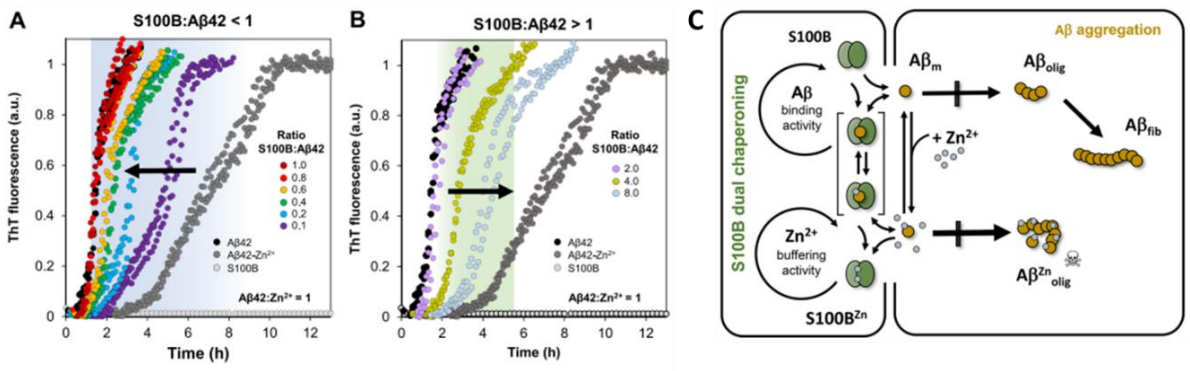

Figure 5 – Effect of S100B on $A\beta_{42}$ aggregation induced by Zn^{2+}-at different S100B:$A\beta_{42}$ molar ratios. The aggregation mechanism of 5μM $A\beta_{42}$ (black dotes) with equimolar Zn^{2+}in 50mM HEPES pH 7.4, at 37°C under quiescent conditions, in the presence of S100B in substoichiometric (A) or superstoichiometric (B) S100B:$A\beta_{42}$ molar ratios. (C) schematic representation of S100B dual function chaperon activity as a suppressor of Zn^{2+}induced Aβ toxicity. (n=3). From [73].

At substoichiometric S100B:$A\beta_{42}/Zn^{2+}$, the Zn^{2+} buffering activity predominates and the reaction half-time approaches that of 1:1 $A\beta_{42}/Zn^{2+}$ ($t_{1/2}$ = 7.0 ± 0.3 h, data not shown). Near equimolar conditions, half times converges to that of $A\beta_{42}$ alone ($t_{1/2}$ = 1.5 ± 0.1 h), indicating an inhibition on the formation of toxic $A\beta_{42}-Zn^{2+}$ oligomers [46, 73]. In superstoichiometric conditions, the inhibitory effect of S100B over $A\beta_{42}$ aggregation through binding of monomers and on-pathway oligomers prevails, denoted by the half time increase [46]. S100B is involved in dual chaperoning through Aβ binding and holdase-type inhibition of protein aggregation and zinc binding and buffering activity, which prevents deleterious Zn^{2+}-binding to Aβ and blocks the formation of toxic $A\beta-Zn^{2+}$ oligomers. It was also demonstrated that S100B delays the onset of Aβ42 aggregation and calcium binding-S100B to inhibit Aβ42 aggregation and toxicity [46].

Also found in our lab, it was demonstrated that S100B interacts with tau, in a Ca^{2+}-dependent manner, in living cells even microtubule-destabilizing conditions. The interaction inhibits aggregation of both full-length tau and of the microtubule binding domain. In agreement with the earlier findings that S100B has a role as an extracellular chaperone, its accumulation near tau positive inclusions, show to blocks proteopathic tau seeding (Fig. 6) [74].

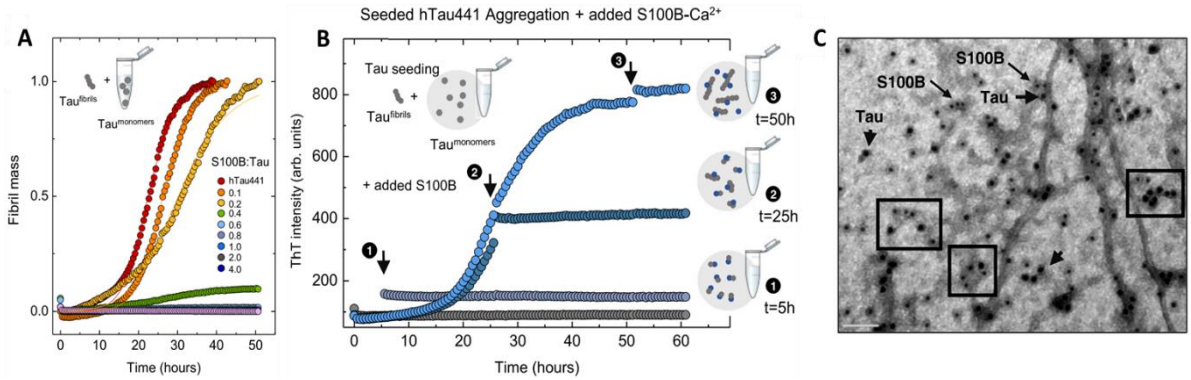

Figure 6 – Calcium binding S100B inhibits tau nucleation and co-localizes with tau fibrils and oligomers. A – Seeded fibril formation of 10 μM hTau441 (red) in 50 mM Tris pH 7.4, in the presence of 0.005% of preformed fibrils and 1.1 mM $CaCl_2$ at 37 °C under agitation, in the presence of 0.1 (orange), 0.2 (yellow), 0.4 (green), 0.6 (light blue), 0.8 (purple), 1.0 (blue), 2.0 (gray), and 4.0 (dark blue) molar equivalents of S100B. **B** – tau441-seeded aggregation in the same conditions as in **A**, with addition of equimolar S100B at 0 (gray), 5 (light blue, 1), 25 (dark blue, 2), and 50 (blue, 3) hours after aggregation start. Data are presented as mean values ± SD from n = 3 independent experiments except for samples with 0.0 and 0.1 equivalents of S100B for which n = 2. **C** - TEM image of tau aggregates grown in the presence of S100B-Ca2+ and immunogold labeled against S100B (10 nm, arrow) and tau (15 nm, arrowhead). Scale bar 100 nm. Independent experiments of immunogold labeling were performed three times. From [74].

Seeding with 0.005% of the full-length tau, hTau441, fibrils decrease the reaction half-time ca. 15h, from $t_{1/2}$ = 23.0 ± 0.2 h versus $t_{1/2}$ = 37.9 ± 1.3h, obtained in the unseeded reaction [74]. Some experiments also have shown that Ca^{2+} is required for the inhibitory action of S100B and this inhibition is highly increased in seeded assays [74]. Indeed, aggregation of hTau441 is completely abolished at a molar ratio hTau441:S100B > 0.6 (Fig. 6a), which was not the case in the unseeded assay. In Fig 6b, S100B-Ca^{2+} was added at different times along the aggregation reaction of hTau44: in the lag phase (t = 5 h), where monomeric tau predominates; at the reaction half-time (t = 25 h), where there is already a substantial amount of tau oligomers derived from monomers; and at the plateau stage (t = 50 h), when formed fibrils predominate. The S100B addition at the beginning abolish aggregation because of the interaction of the two proteins; at the middle, ThT intensity does not decrease, suggesting that S100B is also able to interact with tau oligomers and fibrils and that it does not cause fibril disassembly, which is confirmed when S100B is added at the end, when formed fibrils predominate, as there is no further change in the fibril mass. Interaction between S100B and tau fibrillar species and oligomers was confirmed by TEM using nanogold-conjugated anti-S100B and anti-tau antibodies, using hTau441 fibrillar materials formed at the plateau stage upon incubation in the presence of S100B-Ca2+. Is observed that S100B (labeled with 10-nm gold particles) binds

abundantly along the surface of tau fibrils (labeled with 15-nm particles) as well as to smaller tau aggregates and oligomeric materials.

Together, these findings establish Aβ and tau as clients of the S100B chaperone, providing evidence for neuro-protective functions of this inflammatory mediator across different neurodegenerative disorders.

2.3. Transgenic animal models of Alzheimer's Disease: an overview

Researchers interrogate biological mechanisms at multiple levels: first, at a fundamental level where the behavior of molecules is studied individually or in connection with other few molecules. Second, at a more complex level, the processes that involve the protein of interest in a network of hormones, circulating factors and cells, and crosstalk between cells, in healthy or diseased conditions. These two can be studied using *in vitro* approaches, for example cell culture, and give us some clues of *if* and *how* our molecule of interest interacts. These techniques have become very sophisticated to mimic the 3D and complex structures of tissues. But, when the exploration of physiological functions and systemic interactions between organs is required, a whole organism is necessary. It brings the third level, even more complex, which involves animal models to get a full description and understanding of the mechanisms.

Animal models have been used to address a variety of scientific questions, from basic science to the development and assessment of novel vaccines, or therapies. The use of animals for scientific purposes has been a longstanding practice in biology and medicine due to the remarkable anatomical and physiological similarities between humans and animals, particularly mammals. This usage has prompted researchers to investigate a large range of mechanisms before applying their discoveries to humans [75].

In Alzheimer's disease, as in many other diseases, experimental models are essential to further understand pathogenesis and to screen and validate preventive medications and novel therapeutics [76]. Various AD mouse models [77, 78] as well as other animal models including rats, non-human primates, *Drosophila*, and *Caenorhabditis elegans* [78] have been recently reviewed. In the absence of gene manipulations, no small animal models exist at present that sufficiently or consistently mimic clinical disease pathology for experimental and preclinical studies of AD (Fig. 7).

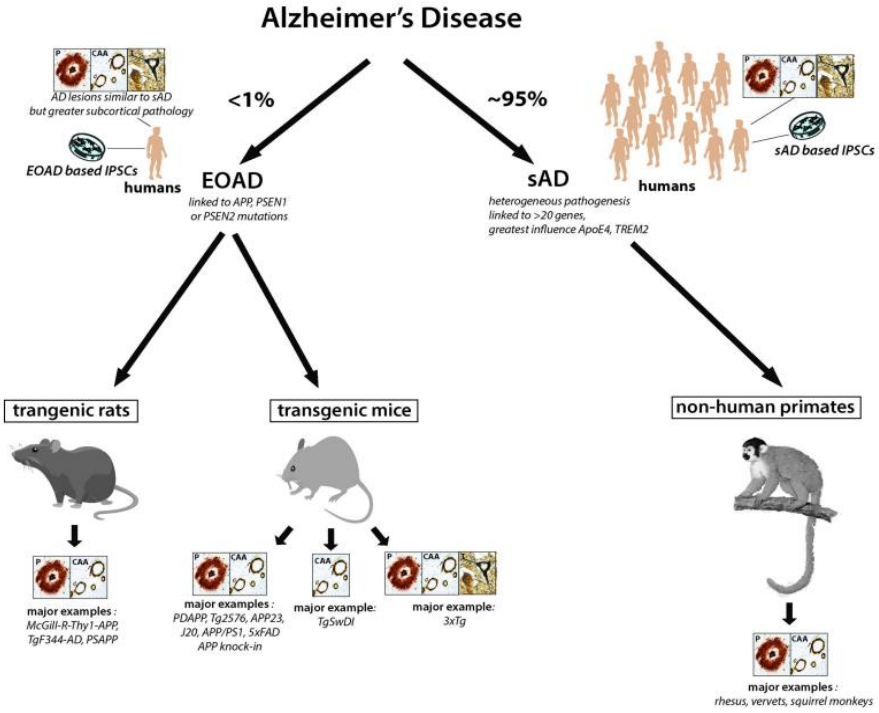

Figure 7 –Schematic of the major animal models of Alzheimer's disease. In AD less than 1% of the cases are early onset familial AD (EOAD), caused by autosomal dominant mutations in APP, PSEN1 or PSEN2. However, all major transgenic rodent models express these mutated forms of APP and PS1. In sporadic AD (sAD), the best animal models available are non-human primates. The consistent presence of the types of neuropathology present in each model is shown in the boxes; P: plaques; CAA; congophilic amyloid angiopathy (Aβ extracellular plaques in the brain) ; T: neurofibrillary tangles. We did not consider the presence of pretangle pathology in these animal models sufficient to indicate the presence of neurofibrillary tangle pathology. As such, only 3xTg mice express all 3 pathological hallmarks of AD. The specific types of animal models included in each category are examples of the most common animal models currently used in AD research. From [79]

FAD results in an earlier age of onset (EOAD) and different neuropathological features compared to sAD [80]. Phenotype widely varies and depends on the present mutation. FAD shows disproportionate subcortical Aβ42 accumulation, associated with enhanced striatal tau pathology [81], and different development of associated neuropathology such as TDP-43, compared to sAD. Differences between sAD and FAD may impact the translatability of therapeutic findings in transgenic mouse models that are largely based on over-expression of APP and PSEN1 containing FAD linked mutations [78].

In AD research community, the majority of used models are almost exclusively consisting of transgenic (Tg) mice. These mice models can consist of 3 approaches: overexpression of proteins associated with familial AD (FAD), mutant amyloid precursor protein (APP), or APP and presenilin (PS) [82]. All these mice exhibit AD pathology, but the overexpression paradigm may cause additional phenotypes unrelated to AD. At the time, the most practical approach are the genetically modified APP mouse models, which has 97% sequence homology with human APP (differences in three aminoacids [83]), results in the

formation and accumulation of amyloid β peptide (Aβ) as extracellular plaques (by expression of human *APP* alone or in combination with human *PSEN1*) and hyper-phosphorylated tau as intracellular neurofibrillary (by expression of human *MAPT*) [78, 82]. Differences between APP human and mice sequences impair Aβ aggregation and prevent the formation of amyloid plaques in wild-type mice. Therefore, expression of human APP is necessary for the formation of amyloid plaques in mice. Initial transgenic models expressed wild-type human APP in mice, however, while these transgenic mice had increased Aβ production, they failed to consistently show extensive AD associated neuropathology [83, 84]. Some of the currently used AD mice models and their most prominent features are listed in table 1.

Besides in FAD and sAD, Aβ and tau pathology are morphologically similar (rationalizing the use of mouse models with genetically engineered FAD mutations for understanding sAD). The potential mechanism of Aβ accumulation is the key main problem of all models. While on FAD Aβ deposition is primarily mainly caused by the increased production of Aβ>40 (except for intra-Aβ sequence mutations that alter its structural properties [85] or the Swedish mutation that increases all Aβ species by increasing cleavage at the β-site), Aβ deposition in sAD is likely partially caused by an aging-associated decrease in degradation/clearance of Aβ [82]. Resuming, while decreased Aβ degradation may be dominant in sAD, most APP mouse models have increased FAD-like production, and this should be considered and kept in mind during studies. In this chapter, APP23 mouse models were used to perform the assays, which have a 7-fold overexpression of mutant human APP with the Swedish double mutation. These mice develop extensive amyloid-β pathology. Aβ deposits are first observed at six months of age, and the formed plaques increase in size and number with age, occupying up to 25 percent of the neocortex and hippocampus in 24-month-old mice. Plaques are surrounded by activated microglia, astrocytes, and dystrophic neurites containing hyperphosphorylated tau, although neurofibrillary tangles are not observed. The APP23 line was considered a suitable model to analyze the localization of different S100s proteins in association with Aβ amyloid plaques in pathogenesis of Alzheimer's disease [86].

Table 1 – Alzheimer's disease mice models currently used and their characteristics.

Models	Mutation	Main features	Plaques	NFTs	Neurodegeneration	Gliosis
APP23 [87]	$APPK^{670N,M671L}$	Mid-life amyloid pathology (~12mo for homozygote, but note >24mo for heterozygote allele [77, 79, 88]	6mo: rare plaques in CTX [87]	None [87]	14–18mo: ↓ neurons in CA1, no change in CTX [89]	Fibrillar plaque associated astro- and microgliosis [8, 87]
			12mo: CTX, HIP, THAL, AMYG [76]			General astrocytosis [90, 91]
			Majority fibrillar			
Tg2576[92]	$APPK^{670N,M671L}$	Mid-life amyloid pathology (10-14mo) [88]	7 – 8mo: focal plaques in CTX [93]	None	None [94, 95]	Plaque associated astro- and microgliosis from 12 M [95-97]
			11–13mo: CTX, HIP, CER [92]			
			diffused and core			
APP/PS1 [6]	$APPK^{670N,M671L}$	Early-onset (~6mo) amyloid pathology [88]	1.5mo: CTX	None	17mo: ↓ neurons in DG, no change in CTX, CA1 [98]	Plaque-associated astroand microgliosis [99]
	$PSEN1^{L166P}$		3mo: CTX, HIP			
			3–5mo: THAL, STR, Brain stem			
			Majority fibrillar [99]			
3 x Tg [100]	$APPK^{670N,M671L}$	Early- to mid-life amyloid pathology plus hyperphosphorylated tau [88]	6–12mo: CTX, HIP [100]	12mo: First in CA1 neurons of HIP, later in CTX [100]	12mo: ↓ neurons in CTX [101]	General Astro and microgliosis in CA1 at 7mo [102]
	$PSEN1^{M146V}$		Diffuse and compact [100]			
	$MAPT^{P301L}$					
5xFAD [103]	$APPK^{670N,M671L}$	Juvenile-onset amyloid pathology (~3mo) [88]	2mo: CTX			
	APP^{V717I}		With age: HIP, THAL, spinal cord, brain stem, none in CER [103]	None [103]		9mo: focal ↓ neurons in CTX [103]
	APP^{V716V}					General and plaque associated astro- and microgliosis from 2mo [103]
	$PSEN1^{M146L}$					
	$PSEN1^{L286V}$					

3. Materials and Methods

Materials. Primary antibodies were purchased from Sigma Aldrich (Map2, S100B), Novus Biologicals [S100A8 (calgranulin A)], Abcam (GFAP, S100B, S100A6), and Covance (β-III Tubulin). Secondary antibodies Alexa488 and Alexa568 were purchased from Life Technologies. Secondary HRP antibodies were purchased from DAKO. Unless otherwise indicated, all other chemicals were obtained from Sigma-Aldrich.

Protein Expression and Purification. Human S100B, S100A6, and S100A8 were expressed in *E. coli* BL21(DE3) and purified to homogeneity using previously established protocols and quantitated using reported extinction coefficients [104, 105]. Apo S100B, S100A6, and S100A8 were prepared by incubation at 37°C for 2 h with a 300-fold excess of dithiothreitol (DTT) and 0.5 mM EDTA and eluted in a Superdex S75 (GE Healthcare). To remove contaminant trace metals all solutions were passed through Chelex resin (Bio-Rad). S100 protein solutions were prepared and stored in 50 mM Tris–HCl pH 7.4.

Hippocampal Culture from Rat Brain. Pregnant rats were purchased from Janvier Labs. The preparation of hippocampal cultures was performed as described before [106] from rat (embryonic day-18; E18). After preparation the hippocampal neurons were seeded on poly-l-lysine (0.1 mg/ml; Sigma-Aldrich) glass coverslips in a 24 well plate at a density of 3 × 10^4 cells/well. Cells were grown in Neurobasal™ medium (Life Technologies), complemented with B27 supplement (Life Technologies), 0.5 mM L-Glutamine (Life Technologies) and 100 U/ml penicillin/streptomycin (Life Technologies) and maintained at 37°C in 5% CO_2.

Immunocytochemistry. Cells were fixed with 4% paraformaldehyde (PFA)/4% sucrose/PBS at 4°C for 20 min. After washing 2× 5 min with 1× PBS with 0.2% Triton X-100 at RT, blocking was performed with 10% FBS in 1× PBS at RT for 1 h, followed by the primary antibody for 2 h at RT. After a 3× 5 min washing-step with 1× PBS, incubation with the secondary Alexa488 and/or Alexa568 antibody followed for 1 h at RT. The cells were washed again in 1× PBS for 10 min and cell nuclei stained with DAPI for 5 min. After washing with aqua bidestilled, coverslips were mounted using VectaMount (Vector Labs). Fluorescence images were obtained using an upright Axioscope microscope equipped with a Zeiss CCD camera (16 bits; 1280 × 1024 ppi) using Axiovision software (Zeiss) and ImageJ 1.51j.

Animals. Three and fifteen months-old male mice, *Mus musculus*, strain C57BL/6 and APP23 (maintained on the same background) were used. The animals were housed in plastic cages with stainless steel mesh lids under the standard laboratory condition with temperature 22–

24°C, food and water available *ad libitum*, humidity 55% ±10% and 12/12 h light/dark cycle (lights on at 7 AM).

Gene Expression Analysis. RNA was extracted using the Qiagen RNeasy lipid tissue kit according to the manufacturer's instructions. RNA concentrations were measured using a NanoDrop 2000 (Thermo Fisher Scientific). First strand synthesis and quantitative real-time-PCR amplification were performed in a one-step, single-tube format using the Rotor-Gene SYBR® Green RT-PCR kit from Qiagen according to the manufacturer's protocol in a total volume of 20 µl and gene specific QuantiTect Primer Assays (Qiagen). Thermal cycling and fluorescent detection were performed using the Rotor-Gene Q real-time PCR machine (model 2-Plex HRM) (Qiagen). Resulting data were analyzed using the HMBS gene as an internal standard to normalize transcript levels. All quantitative real-time PCR reactions were run in technical triplicates and mean cycle threshold (ct) -values for each reaction were taken into account for calculations. Ct values were calculated by the Rotor-Gene Q Software (version 2.0.2) and transformed into virtual mRNA levels according to the formula: virtual mRNA level = 10 × [ct(target) − ct(standard)]/slope of standard curve.

Histochemistry. Brain sections (14 µm thickness) were prepared from fresh snap-frozen brains using a cryostat (Leica CM 3050S) with the knife set at -23°C. Three sections of the brain of the same animal were collected on one microscope slide. For staining, the slices were thawed for 20 min at RT, fixed with PFA/4% Sucrose for 30 min at RT. After washing 10 min with 1× PBS, incubation with Triton 0.2% in 1× PBS for 2 h at RT was followed by incubation with Triton 0.05% for 10 min at RT. The slides were covered with Blocking Solution (BS)(10% FCS in 1× PBS) for 2 h at RT. The primary antibody was diluted in BS and applied over-night at 4°C. Subsequently, incubation for 3× 10 min with Triton 0.05% at RT was followed by incubation with the secondary antibody coupled to Alexa488 or Alexa568, diluted 1:500 in BS, at 37°C for 1.5 h. After a 3× 15 min washing step with Triton 0.05% and 1× 5 min with 1× PBS, cell nuclei were counterstained with DAPI and after the last washing step with 1× PBS for 5 min, cover slips were mounted using VectaMount. Zinpyr-1 staining was performed at a final concentration of 10 µM and incubation time of 1 h at RT. Subsequently, the sections were counterstained with DAPI. Images were taken with a Zeiss LSM710 confocal microscope. For image analysis, center and border zone of plaques were determined using ImageJ. Zinpyr1 signal intensity was measured of 50 plaques using the "plot profile" function along the diameter of a plaque crossing the center. A clear difference between center and border zone in Zinpyr1 fluorescence intensity can be observed with the border zone displaying a mean value of 60% of fluorescence intensity of the center zone with a steep drop between center and border zone. Using this information, images were thresholded and two masks were created from Zinpyr1

fluorescence selecting areas above (center zone) and below 60% (border zone) of average fluorescence intensity of Zinpyr1 of the center of a plaque. These masks were used to create a selection to measure S100 signal intensity inside the respective zones of a plaque.

Protein Fractionation. To obtain P2 fractions from brain regions, the regions were dissected, and 1 g tissue was homogenized in 10 ml Buffer A containing protease inhibitor mixture (complete mini EDTA free, Roche). Cell debris and nuclei were removed by centrifugation at 3,200 rpm for 15 min resulting in supernatant S1 (soluble fraction) and pellet P1 (membrane associated fraction). Supernatants (S1) were centrifuged for 20 min at 11,400 rpm, resulting in S2 (soluble fraction) and P2 (crude synaptosomal fraction). The resulting pellet P2 was resuspended in homogenization buffer to measure protein concentration by Bradford analysis followed by western blotting.

Western Blotting. Proteins were separated by SDS-PAGE and blotted onto Nitrocellulose membranes. Immunoreactivity was visualized using HRP-conjugated secondary antibodies and the SuperSignal detection system (Pierce, Upland, United States). Evaluation of bands from Western blots was performed using ImageJ v1.52c. Three independent experiments were performed, and blots imaged using a MicroChemi Imaging System from Biostep. The individual bands were selected, and the integrated density was measured. All WB bands were normalized to β-III-Tubulin and the ratios averaged and tested for significance.

Statistics. Statistical analysis was performed using Microsoft Excel and averages tested for significance using SPSS version 20. For comparisons, analysis of variance (ANOVA) was performed followed by *post hoc* tests for within group comparisons. Data are shown as mean ± SEM. Significance levels were set at $p < 0.05$ ($<0.05^{*}$; $<0.01^{**}$; $<0.001^{***}$).

4. Results and Discussion

4.1. S100A6, S100A8 and S100B Show Brain Region and Cell Type Specific Expression

To elucidate the origin of S100 proteins in brain parenchyma, in a first set of experiments, we analyzed expression of S100A6, S100A8, and S100B in vitro using 14 days old rat hippocampal neuronal cultures. S100A8 immunoreactive signals were found in neurons and glial cells (Fig. 8A,B) revealed by co-staining with a marker for astrocytes (Glial fibrillary acidic protein, GFAP) and a marker for neurons (Microtubule-associated protein 2, MAP2). For S100A6 and S100B, we detected immunoreactive signals mostly in astrocytes, but also a weak signal in neurons (Fig. 8C).

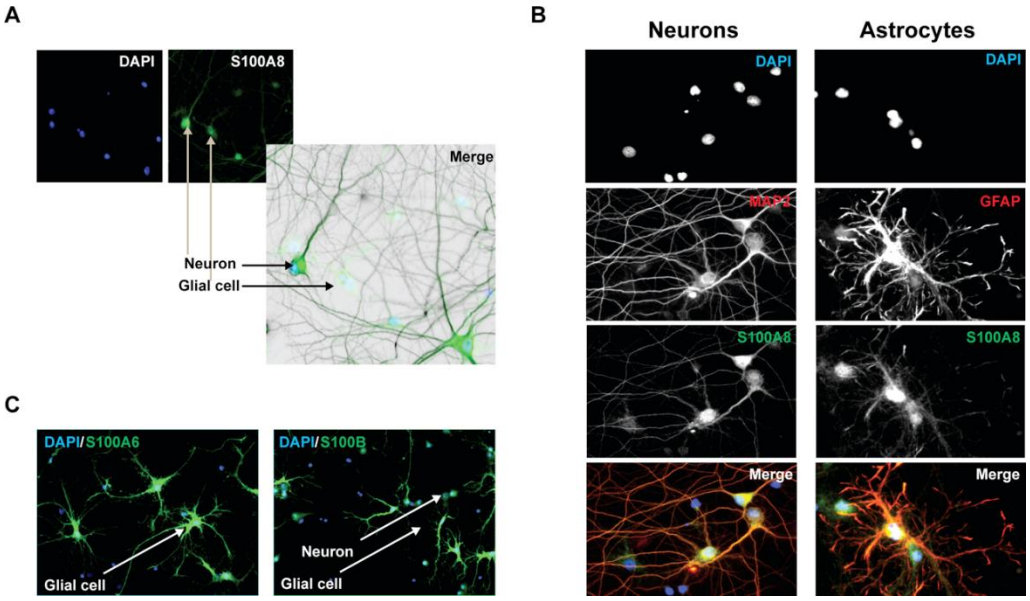

Figure 8: S100A6, S100A8, and S100B are expressed in glial cells and neurons in vitro. Rat hippocampal neuronal cultures were prepared, and immunocytochemistry performed at DIV 14. **A)** S100A8 immunoreactive signals (green) are found in neurons and glial cells. Nuclei are visualized by DAPI (blue). Merge image shows dark staining of neurons by MAP2. **B)** S100A8, accordingly, co-localizes with markers astrocytes (GFAP) and neurons (MAP2). **C)** Immunoreactive signals for S100A6 and S100B were detected in astrocytes and less in neurons.

In order to investigate whether the results obtained *in vitro* are representative for the *in vivo* situation, in the following set of experiments we analyzed RNA lysates from different brain regions (cortex, hippocampus, striatum, cerebellum) obtained from adult wildtype (WT) C57BL/6 mice. mRNA expression analysis for S100A6, S100A8, and S100B shows that the genes are expressed in all brain regions. However, S100A6 shows the highest expression in the cortex, and S100A8 in the cerebellum, and S100B in the cortex and cerebellum (Fig. 9B). mRNA expression levels were confirmed on the protein level for S100B, with the highest expression in the cerebellum (Fig. 9A).

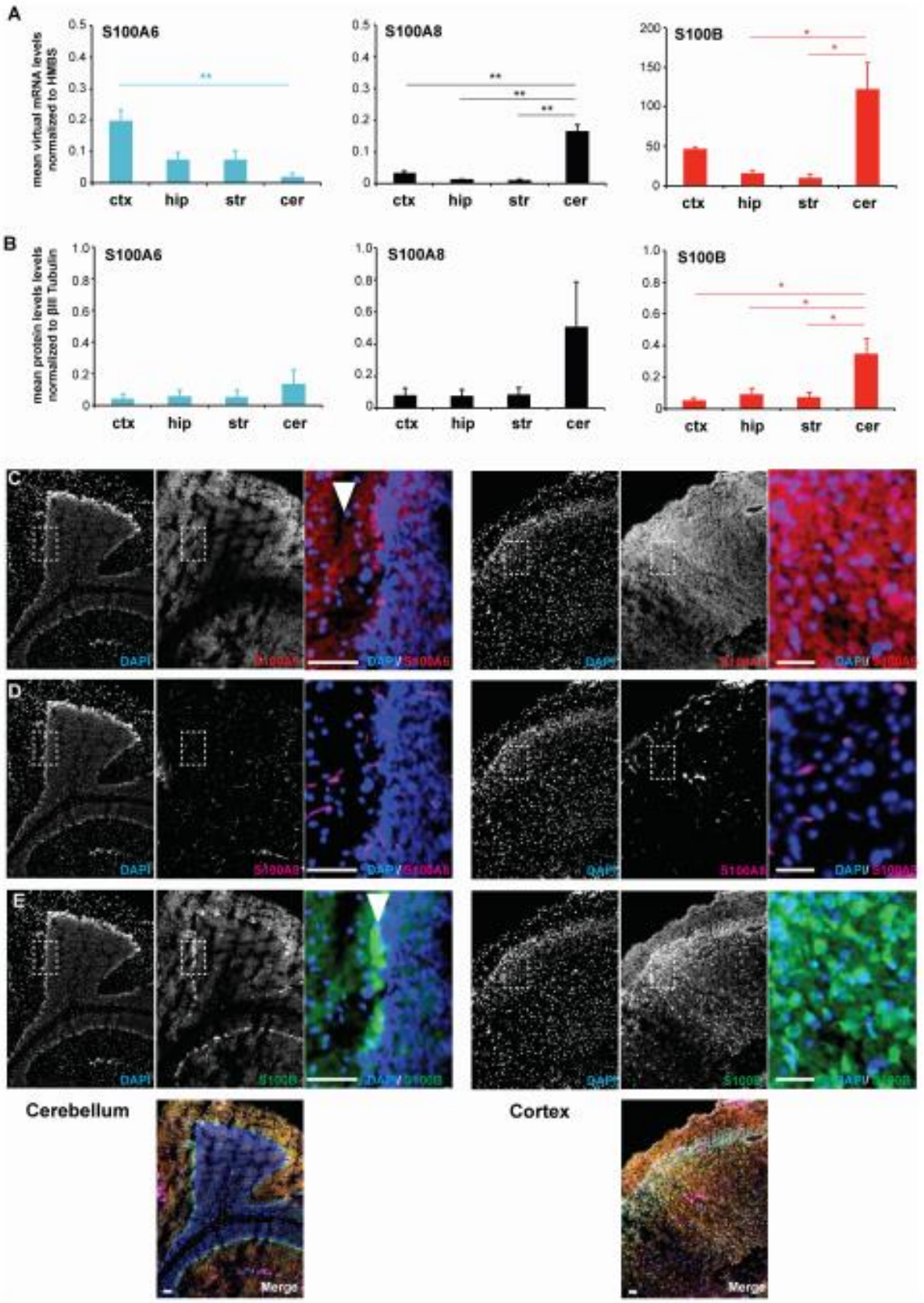

Figure 9: S100A6 and S100B show brain region specific expression in vivo. A) RNA lysate was obtained from cortex (ctx), hippocampus (hip), striatum (str) and cerebellum (cer) of wt mice. Expression analysis for S100A6, S100A8 and S100B shows that the genes are expressed in all brain regions with S100A6 showing highest expression in cortex, S100A8 in cerebellum, and S100B in cortex and cerebellum (n = 3) (one-way ANOVA,

F_{S100A6} = 8.319, p_{S100A6} = 0.008; F_{S100A8} = 40.602, p_{S100A8} = < 0.0001; F_{S100B} = 9.043, p_{S100B} = 0.006; Bonferroni Post-Hoc analysis: S100A6: a significant difference was detected between ctx and cer (p = 0.008). S100A8: a significant difference was detected between ctx and cer (p = 0.000254), hip and cer (p = 0.000857), and str and cer (p = 0.000818). S100B: a significant difference was detected between hip and cer (p = 0.014), and str and cer (p = 0.01)). **B)** The soluble protein fraction (S2) from protein lysate was obtained from cortex (ctx), hippocampus (hip), striatum (str) and cerebellum (cer) of wt mice (n = 3). No regional differences were detected on protein level for S100A6 and S100A8 (one-way ANOVA, F_{S100A6} = 0.576, p_{S100A6} = 0.647; F_{S100A8} = 2.209, p_{S100A8} = 0.165). A significant difference was detected for S100B (one-way ANOVA, F_{S100B} = 7.118, p_{S100B} = 0.012). Bonferroni post hoc analysis reveals a significant higher level of S100B in cer compared to ctx (p = 0.0228), cer compared to hip (p = 0.04934), and cer vs. str (p = 0.03557). **C)** Immunohistochemistry performed on wt brain sections shows S100A6 protein expression in cortex and cerebellum. In cerebellum, S100A6 shows high expression in the molecular layer. **D)** S100A8 expression is absent in neurons and glial in both cerebellar and cortical regions. S100A8 signals originate from blood vessels. **E)** S100B is expressed in cortex and cerebellum. In cerebellum, S100B is highly expressed specifically in Purkinje cells (arrow). (C-E) scale bars = 50µm

Based on this expression pattern, we selected the cortex and cerebellum for subsequent immunohistochemical analysis to identify protein expression and localization of S100A6, S100A8, and S100B in these brain regions. S100A6 protein expression was found in both brain regions (Fig. 9C). In the cerebellum, S100A6 seems to be enriched in the molecular layer. In contrast, S100B is very specifically expressed in the Purkinje cells of the cerebellum. Lower expression of S100B was detected in other regions of the cerebellum and in the cortex (Fig. 9E). The expression of cerebellar S100B is well established in the developing mouse cerebellum where it is proposed to be involved in interactions with vimentin, to participate in neurite extensions and to have neurotrophic activities [107]. However, S100B-deficient mice exhibit normal cerebellar development [108]. On the other hand, systematically elevated S100B levels during neurodevelopment impair cerebellar oligodendrogenesis and myelination [109]. In the cortex, S100B protein expression is the highest in layer IV. S100A8 protein expression in turn seems nearly absent in neurons and glial in both cerebellar and cortical regions. S100A8 signals almost exclusively originate from blood vessels, either from endothelial cells forming the wall of blood vessels or from protein in blood (Fig. 9D). Thus, the expression of S100A8 is different in dissociated cell culture from the *in vivo* situation. Alternatively, altered expression may be due to differences between rat used for cell culture, and mouse tissue used for *in vivo* studies.

4.2. Altered Localization of S100 Proteins in the Brain of APP23 mice S100A6, S100A8 and S100B Show Brain Region and Cell Type Specific Expression

Given that a role of S100 proteins has been proposed in AD, we next analyzed whether the expression and distribution of S100A6, S100A8, and S100B is altered in APP23 mice compared to controls before the onset of amyloid plaque pathology (3 months of age, moa) and at old age with full amyloid plaque pathology (15 moa). Pathology was confirmed by visualization of plaques in brain sections of mice. Plaques were found in the hippocampus and cortex of 15 months old APP23 mice, but in line with the literature [110], no plaques were detected in the cerebellum. The prefrontal cortex of mice was then analyzed (Fig. 10A).

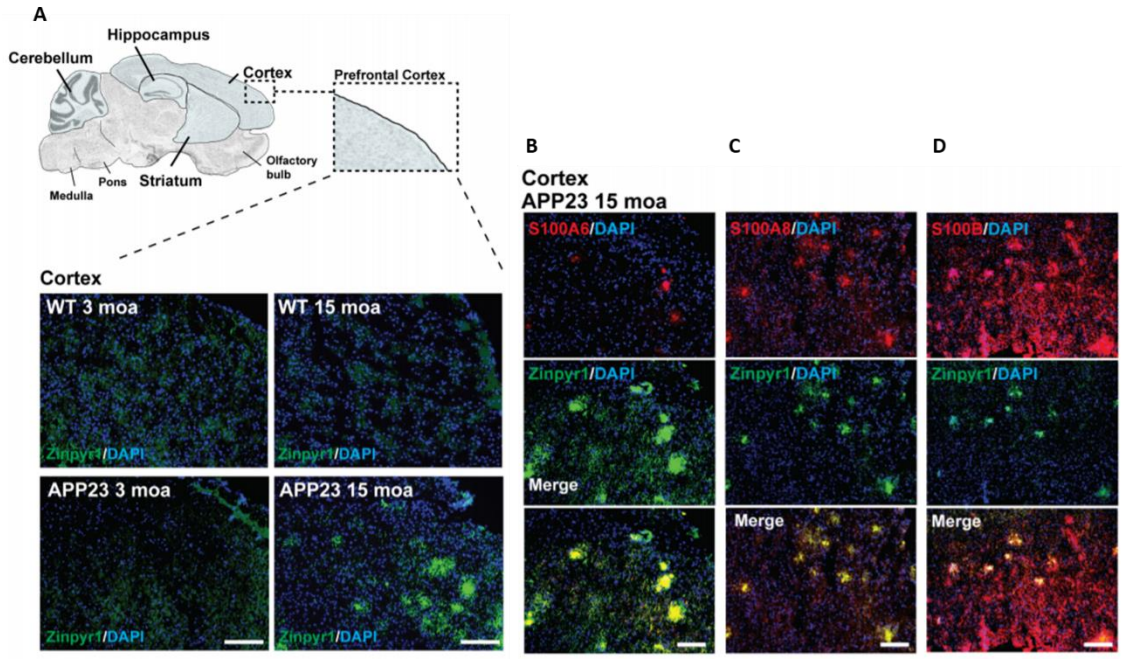

Figure 10: Altered localization of S100 proteins in the brain of APP23 mice. (A) APP23 mice were compared to controls at 3 moa and 15 moa. Representative images of mouse prefrontal cortex are shown. A severe plaque-pathology was observed in 15 moa APP23 mice in this brain region. Plaques were visualized by Zinpyr-1 staining and cell nuclei labeled using DAPI. **(B)** In 15 moa APP23 mice, S100A6 signals co-localize with Aβ plaques together with **(C)** S100A8, and **(D)** S100B. Signal intensities have been adjusted to S100 fluorescence co-localizing with plaques leading to very low fluorescent signals in the surrounding tissue. **(A–D)** scale bars = 300 µm

In APP23 mice cortex (15 moa, plaque positive), S100A8 immunoreactive signals maintain their association with blood vessels. However, in addition, S100A8 signal co-localizes with Aβ plaques (Fig. 10B). Similarly, S100A6 and S100B localize to Aβ plaques (Fig. 10C,D). Several methods exist to visualize the plaques. Among them staining with Thioflavin is commonly used. Thioflavin detects the presence of amyloid fibrils [111]. Cross-linked fibrils form the center of amyloid plaques and increasing aggregation has been hypothesized to originate from fibrils that radiate out from a center recruiting Aβ monomers and oligomers [112] that are found in the periphery of a plaque. Therefore, staining with Thioflavin results in a strong

signal in the center of plaques and weaker signals from the border zone. Like Thioflavin, Zinpyr-1, a fluorophore labeling zinc associated with Aβ aggregates results in a strong labeling of plaques. As zinc ion levels are elevated in amyloid plaques [113], and in particular in β-sheets associated with fibrillar assemblies [114], also zinc staining shows higher fluorescence in the center of plaques (Fig. 11A,B).

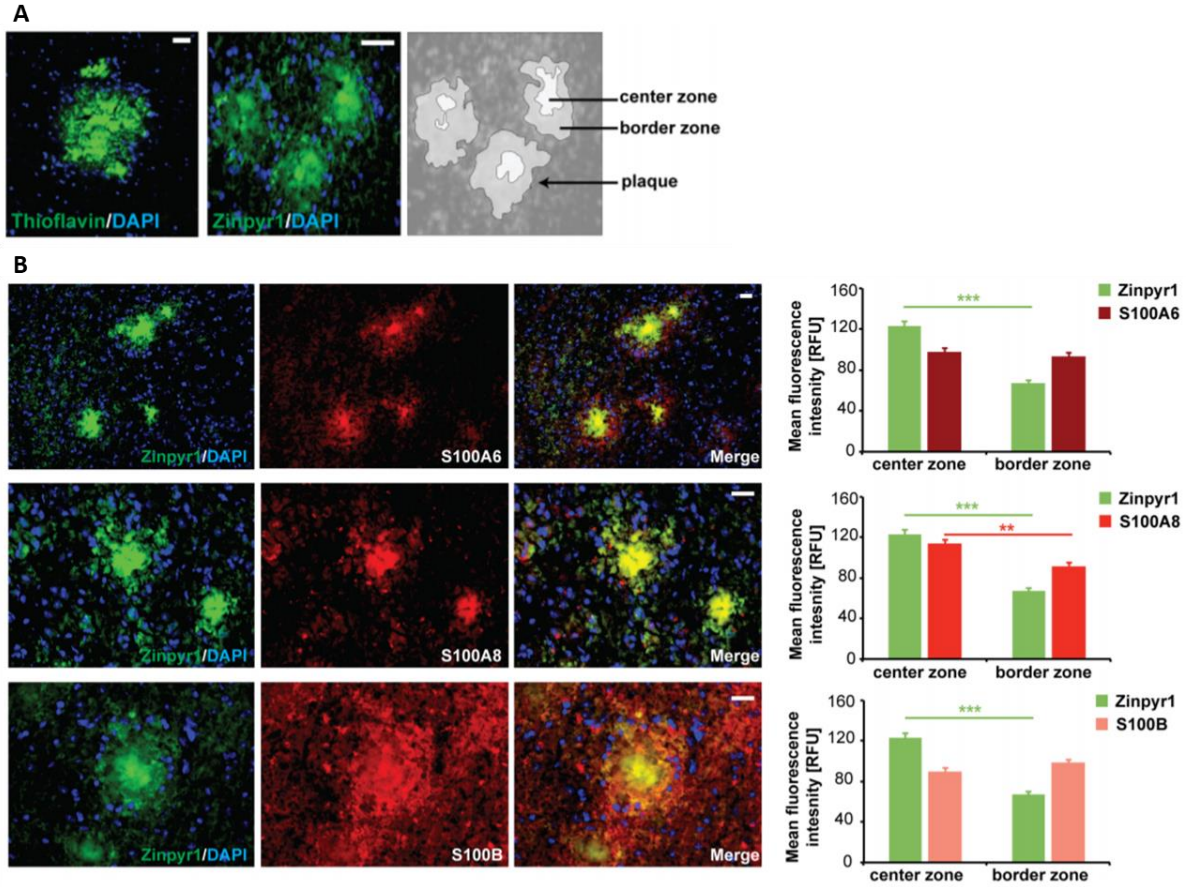

Figure 11: S100 proteins co-localized with Aβ$_{42}$ plaques in APP23 mice.(A,B) Visualization of plaques using Thioflavin or Zinpyr1 reveals strong fluorescence in the center of plaques and weaker fluorescence in the border zone corresponding to the aggregation state of Aβ. **(B)** S100A8 is significantly higher enriched in the center of Aβ aggregates (20–25 plaques each from n = 3 mice, t test, p = 0.0077). S100A6 is found in the center and periphery of Aβ plaques (pS100A6 = 0.3896). In contrast, S100B is found in the center zone and is slightly enriched in the border zone (pS100B = 0.1217). **(A,B)** = 50 µm.

Analysis of the distribution of S100 proteins within the center and border zone of plaques revealed that S100A8 is significantly enriched in the center of Aβ plaques. In contrast, S100B localizes to the center, but more so in the border zone of plaques (Fig. 11B). S100A6 is found both in the center and border zone of plaques (Fig. 11B).

4.3. Altered Concentrations of S100A8 and S100B Protein in the Brain of APP23 Mice

Given that changes in the expression of S100 family members have been reported during aging in humans and WT mice [115], we next investigated if alterations on protein level also occur for S100A8 and S100B, and whether the differences found in WT animals are also observed in APP23 mice. To that end, brain lysates were prepared and sub-fractionated. To exclude the influence from blood vessels, P2 (synaptosomal fractions) were used for the analysis. The results show that aged WT mice have decreased protein levels of S100A8 in the P2 fraction both from the cortex and cerebellum (Fig. 12A,B). However, this is not the case in the APP23 mice. A significantly higher level of S100A8 was found in the in the P2 fraction from the cortex of APP23 mice compared to WT at 15 moa (Fig. 12A). The increased S100A8 levels in the cortex of APP23 mice after development of AD pathology are in line with the previous observed shift from S100A8 signals mainly associated with blood vessels to the center of Aβ plaques. S100B levels, on average, are higher in APP23 mice compared to controls in both brain regions as early as 3 moa, with a significant higher S100B level in the cortex of APP23 mice at 15 moa (Fig. 12A).

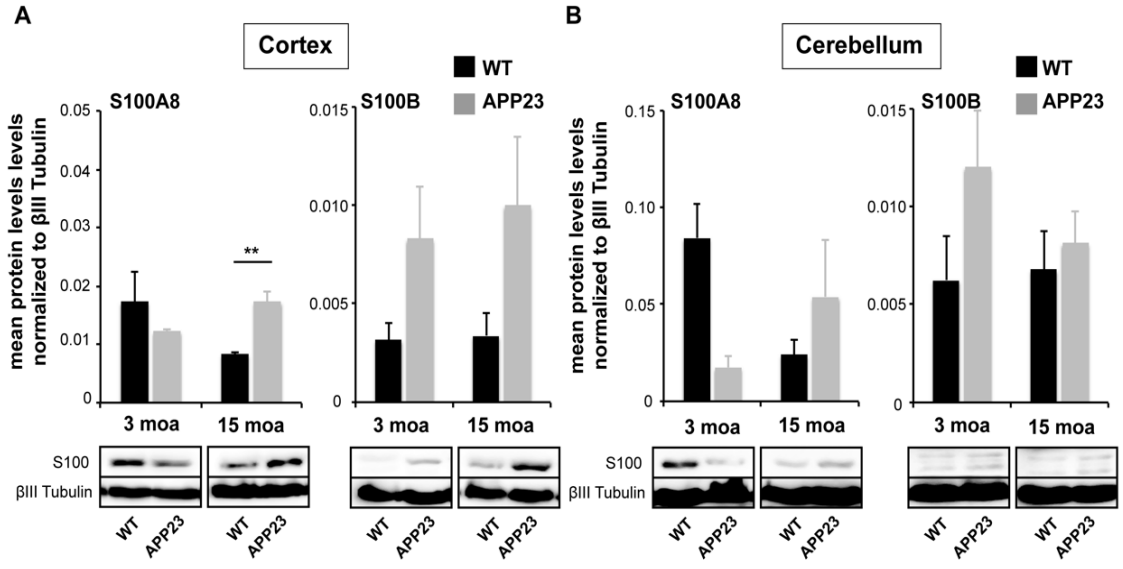

Figure 12: Altered concentrations of S100A8 and S100B proteins in the brain of APP23 mice. Brain lysate was obtained from cortex and cerebellum of control and APP23 mice at 3 and 18 moa. P2 fractions were used for analysis (n = 3). **A)** Left panel: In Cortex, a statistically significant difference was found between APP and WT mice at 15 moa, but not a 3 moa (two-way ANOVA). S100A8 levels were significantly higher in APP23 mice at 15 moa (Bonferroni test, p = 0.0091) compared to WT mice. Right panel: S100B levels were slightly higher in APP23 mice at each time-point but did no significant difference between WT and APP23 and no significant change during aging in WT and APP23 mice was found (two-way ANOVA). **B)** Left panel: In cerebellum, protein levels of S100A8 decrease during aging as observed in cortex (as trend). Pairwise comparison reveals a significant difference between WT and APP23 mice at 3 moa, and in WT mice between 3 moa and 15 moa. However, two-way ANOVA analysis does not reveal significant differences. Right panel: No significant time or genotype dependent differences were observed for S100B in cerebellum (two-way ANOVA).

5. Conclusions

S100B, S100A8, and S100A6 are among the most prominent brain expressed S100 proteins and are all upregulated upon traumatic brain injury, aging, and neuronal damage. Understanding the physiology of S100 proteins in the brain through a systematic assessment of their relative distribution and expression levels in healthy, aged, and diseased states is a critical first step to establish the molecular mechanisms through which these important signaling molecules act on AD neurodegeneration. Neuroinflammation is a well-established hallmark in AD, and glia-neuronal interactions mediated through the chronic release of glia-derived cytokines including Interleukin-1 and S100B are postulated to be key for the neurodegeneration process [116]. It is also emerging that early inflammation stages, prior to plaque formation, encompass a number of released glial mediators with the potential to regulate AD processes [71]. It is our contention that S100 proteins may play important roles in the early AD stages, and we have therefore in this work interrogated about their location and distribution in the brain, focusing on S100A8, S100A6, and S100B.

Ethics Statement

For primary neutrons from rat: Animal experiments were performed in compliance with the guidelines for the welfare of experimental animals issued by the Federal Government of Germany and approved by the Regierungspräsidium Tübingen and the local ethics committee at Ulm University (Ulm University, ID: O.103). For APP23 mice: Animal experiments were performed in compliance with the guidelines for the welfare of experimental animals issued by the Federal Government and approved by the local ethics committee of the University of Modena and Reggio Emilia.

6. References

1. https://www.alz.org/alzheimers-dementia/facts-figures. *Alzheimer's Disease Facts and Figures*. 2022.
2. https://alzheimersnewstoday.com/alzheimers-disease-statistics/. *Alzheimer's Disease Statistics*. September 2021.
3. https://www.cdc.gov/aging/aginginfo/alzheimers.htm. Out, 2021.
4. *2021 Alzheimer's disease facts and figures.* Alzheimers Dement, 2021. **17**(3): p. 327-406.
5. Iqbal, K., F. Liu, and C.X. Gong, *Alzheimer disease therapeutics: focus on the disease and not just plaques and tangles.* Biochem Pharmacol, 2014. **88**(4): p. 631-9.
6. Hyman BT, P.C., Beach TG, Bigio EH, Cairns NJ, Carrillo MC, Dickson DW, Duyckaerts C, Frosch MP, Masliah E et al *National Institute on Aging-Alzheimer's Association guidelines for the neuropathologic assessment of Alzheimer's disease. .* Alzheimers Dement 2012. **8**: p. 1–13.
7. De Strooper, B. and E. Karran, *The Cellular Phase of Alzheimer's Disease.* Cell, 2016. **164**(4): p. 603-15.
8. Karch, C.M., C. Cruchaga, and A.M. Goate, *Alzheimer's disease genetics: from the bench to the clinic.* Neuron, 2014. **83**(1): p. 11-26.
9. Piaceri, I., B. Nacmias, and S. Sorbi, *Genetics of familial and sporadic Alzheimer's disease.* Front Biosci (Elite Ed), 2013. **5**: p. 167-77.
10. Strittmatter, W.J., et al., *Binding of human apolipoprotein E to synthetic amyloid beta peptide: isoform-specific effects and implications for late-onset Alzheimer disease.* Proc Natl Acad Sci U S A, 1993. **90**(17): p. 8098-102.
11. Levy-Lahad, E., et al., *Candidate gene for the chromosome 1 familial Alzheimer's disease locus.* Science, 1995. **269**(5226): p. 973-7.
12. Goate, A., et al., *Segregation of a missense mutation in the amyloid precursor protein gene with familial Alzheimer's disease.* Nature, 1991. **349**(6311): p. 704-6.
13. Chen, G.F., et al., *Amyloid beta: structure, biology and structure-based therapeutic development.* Acta Pharmacol Sin, 2017. **38**(9): p. 1205-1235.
14. Nicolas, M. and B.A. Hassan, *Amyloid precursor protein and neural development.* Development, 2014. **141**(13): p. 2543-8.
15. Bachurin, S.O., Bovina, E.V., Ustyugov, A.A., *Current Trends in the Development of Drugs for the Treatment of Alzheimer's Disease and their Clinical Trials.* Biomedical Chemistry: Research and Methods, 2018. **1**(Special Issue).
16. Steiner, H., et al., *Making the final cut: pathogenic amyloid-beta peptide generation by gamma-secretase.* Cell Stress, 2018. **2**(11): p. 292-310.
17. Nalivaeva, N.N., et al., *Are amyloid-degrading enzymes viable therapeutic targets in Alzheimer's disease?* J Neurochem, 2012. **120 Suppl 1**: p. 167-185.
18. Chavez-Gutierrez, L., et al., *The mechanism of gamma-Secretase dysfunction in familial Alzheimer disease.* EMBO J, 2012. **31**(10): p. 2261-74.
19. Fandos, N., et al., *Plasma amyloid beta 42/40 ratios as biomarkers for amyloid beta cerebral deposition in cognitively normal individuals.* Alzheimers Dement (Amst), 2017. **8**: p. 179-187.
20. Yaffe, K., et al., *Association of plasma beta-amyloid level and cognitive reserve with subsequent cognitive decline.* JAMA, 2011. **305**(3): p. 261-6.
21. Doecke, J.D., et al., *Total Abeta42/Abeta40 ratio in plasma predicts amyloid-PET status, independent of clinical AD diagnosis.* Neurology, 2020. **94**(15): p. e1580-e1591.
22. Shankar, G.M., et al., *Amyloid-beta protein dimers isolated directly from Alzheimer's brains impair synaptic plasticity and memory.* Nat Med, 2008. **14**(8): p. 837-42.
23. Mucke, L. and D.J. Selkoe, *Neurotoxicity of amyloid beta-protein: synaptic and network dysfunction.* Cold Spring Harb Perspect Med, 2012. **2**(7): p. a006338.
24. Braak, H. and E. Braak, *Neuropathological stageing of Alzheimer-related changes.* Acta Neuropathol, 1991. **82**(4): p. 239-59.
25. Binder, L.I., et al., *Tau, tangles, and Alzheimer's disease.* Biochim Biophys Acta, 2005. **1739**(2-3): p. 216-23.
26. Dujardin, S., et al., *Tau molecular diversity contributes to clinical heterogeneity in Alzheimer's disease.* Nat Med, 2020. **26**(8): p. 1256-1263.
27. https://www.qps.com/2020/08/31/tau-propagation-influences-the-pace-of-alzheimers-disease-progression/. *QPS - preclinical and clinical research*. 2020.

28. Hardy, J., et al., *Genetic dissection of Alzheimer's disease and related dementias: amyloid and its relationship to tau.* Nat Neurosci, 1998. **1**(5): p. 355-8.
29. Thal, D.R., et al., *Phases of A beta-deposition in the human brain and its relevance for the development of AD.* Neurology, 2002. **58**(12): p. 1791-800.
30. Castellani, R.J. and G. Perry, *The complexities of the pathology-pathogenesis relationship in Alzheimer disease.* Biochem Pharmacol, 2014. **88**(4): p. 671-6.
31. Bateman, R.J., et al., *Clinical and biomarker changes in dominantly inherited Alzheimer's disease.* N Engl J Med, 2012. **367**(9): p. 795-804.
32. Maruyama, M., et al., *Imaging of tau pathology in a tauopathy mouse model and in Alzheimer patients compared to normal controls.* Neuron, 2013. **79**(6): p. 1094-108.
33. Venegas, C. and M.T. Heneka, *Danger-associated molecular patterns in Alzheimer's disease.* J Leukoc Biol, 2017. **101**(1): p. 87-98.
34. Heizmann, C.W., G. Fritz, and B.W. Schafer, *S100 proteins: structure, functions and pathology.* Front Biosci, 2002. **7**: p. d1356-68.
35. Donato, R., et al., *S100B's double life: intracellular regulator and extracellular signal.* Biochim Biophys Acta, 2009. **1793**(6): p. 1008-22.
36. Donato, R., et al., *Functions of S100 proteins.* Curr Mol Med, 2013. **13**(1): p. 24-57.
37. Cristóvão, J.S., and Gomes, C. M. , *S100 proteins in Alzheimer's Disease.* Front. Neurosci., 2019. **13:463**.
38. Leclerc, E., E. Sturchler, and S.W. Vetter, *The S100B/RAGE Axis in Alzheimer's Disease.* Cardiovasc Psychiatry Neurol, 2010. **2010**: p. 539581.
39. Sheng, J.G., R.E. Mrak, and W.S. Griffin, *S100 beta protein expression in Alzheimer disease: potential role in the pathogenesis of neuritic plaques.* J Neurosci Res, 1994. **39**(4): p. 398-404.
40. Van Eldik, L.J. and W.S. Griffin, *S100 beta expression in Alzheimer's disease: relation to neuropathology in brain regions.* Biochim Biophys Acta, 1994. **1223**(3): p. 398-403.
41. Peskind ER, G.W., Akama KT, Raskind MA, Van Eldik LJ, *Cerebrospinal fluid S100B is elevated in the earlier stages of Alzheimer's disease.* Neurochem Int. , 2001. **39(5-6):409-13**.
42. Sheng, J.G., et al., *Overexpression of the neuritotrophic cytokine S100beta precedes the appearance of neuritic beta-amyloid plaques in APPV717F mice.* J Neurochem, 2000. **74**(1): p. 295-301.
43. Roltsch E, H.L., Young KA, Marks A, Zimmer DB., *PSAPP mice exhibit regionally selective reductions in gliosis and plaque deposition in response to S100B ablation.* J Neuroinflammation 2010. **16;7:78**.
44. Mori, T., et al., *Overexpression of human S100B exacerbates cerebral amyloidosis and gliosis in the Tg2576 mouse model of Alzheimer's disease.* Glia, 2010. **58**(3): p. 300-14.
45. Hagmeyer, S., et al., *Zinc Binding to S100B Affords Regulation of Trace Metal Homeostasis and Excitotoxicity in the Brain.* Front Mol Neurosci, 2017. **10**: p. 456.
46. Cristóvão, J.S., Morris, V. K., Cardoso, I., Leal, S. S., Martinez, J., Botelho, H. M., et al. , *The neuronal S100B protein is a calcium-tuned suppressor of amyloid-beta aggregation. .* Sci. Adv. , 2018. **4:eaaq1702.**
47. Boom, A., et al., *Astrocytic calcium/zinc binding protein S100A6 over expression in Alzheimer's disease and in PS1/APP transgenic mice models.* Biochim Biophys Acta, 2004. **1742**(1-3): p. 161-8.
48. Wirths, O., et al., *Inflammatory changes are tightly associated with neurodegeneration in the brain and spinal cord of the APP/PS1KI mouse model of Alzheimer's disease.* Neurobiol Aging, 2010. **31**(5): p. 747-57.
49. Weissmann, R., et al., *Gene Expression Profiling in the APP/PS1KI Mouse Model of Familial Alzheimer's Disease.* J Alzheimers Dis, 2016. **50**(2): p. 397-409.
50. Zhi-Ying, T., Wang CY, Wang T, Yan-Chun, Li, Zhan-You, Wang, *Glial S100A6 Degrades β-amyloid Aggregation through Targeting Competition with Zinc Ions.* Aging Dis. , 2019. **10(4):756-769**.
51. Lodeiro, M., et al., *Aggregation of the Inflammatory S100A8 Precedes Abeta Plaque Formation in Transgenic APP Mice: Positive Feedback for S100A8 and Abeta Productions.* J Gerontol A Biol Sci Med Sci, 2017. **72**(3): p. 319-328.
52. Fritz, G., et al., *Natural and amyloid self-assembly of S100 proteins: structural basis of functional diversity.* FEBS J, 2010. **277**(22): p. 4578-90.
53. Carvalho, S.B., et al., *Intrinsically disordered and aggregation prone regions underlie beta-aggregation in S100 proteins.* PLoS One, 2013. **8**(10): p. e76629.

54. Carvalho, S.B.C., I.; Botelho, H. M.; Yanamandra, K.; Fritz, G.; Gomes, C. M.; Morozova-Roche, L. A., *Structural Heterogeneity and Bioimaging of S100 Amyloid Assemblies*, in *Bionanoimaging: Protein Misfolding and Aggregation*. 2013.
55. Björk P, B.A., Vogl T, Stenström M, Liberg D, Olsson A, et al., *Identification of Human S100A9 as a Novel Target for Treatment of Autoimmune Disease via Binding to Quinoline-3-Carboxamides.* PlOS Biology, 2009. **7**(4): p. e1000097.
56. Horvath, I., et al., *Pro-inflammatory S100A9 Protein as a Robust Biomarker Differentiating Early Stages of Cognitive Impairment in Alzheimer's Disease.* ACS Chem Neurosci, 2016. **7**(1): p. 34-9.
57. Gruden, M.A., et al., *The misfolded pro-inflammatory protein S100A9 disrupts memory via neurochemical remodelling instigating an Alzheimer's disease-like cognitive deficit.* Behav Brain Res, 2016. **306**: p. 106-16.
58. Chang, K.-A., Ha, T.-Y., Kim, J. and Suh, Y.-H. , *The role of S100a9 in the neuroinflammation of Alzheimer's disease transgenic mouse model, Tg2576.* Alzheimer's & Dementia: The Journal of the Alzheimer's Association 2009. **5, P481**.
59. Horvath, I., Iashchishyn, I.A., Moskalenko, R.A., Wang, C., Warmlander, S., Wallin, C., Graslund, A., Kovacs, G.G. and Morozova-Roche, L.A. , *Co-aggregation of proinflammatory S100A9 with alpha-synuclein in Parkinson's disease: ex vivo and in vitro studies.* J Neuroinflammation 2018. **15, 172.**
60. Chang, K.A., H.J. Kim, and Y.H. Suh, *The role of S100a9 in the pathogenesis of Alzheimer's disease: the therapeutic effects of S100a9 knockdown or knockout.* Neurodegener Dis, 2012. **10**(1-4): p. 27-9.
61. Kummer, M.P., et al., *Mrp14 deficiency ameliorates amyloid beta burden by increasing microglial phagocytosis and modulation of amyloid precursor protein processing.* J Neurosci, 2012. **32**(49): p. 17824-9.
62. Shepherd, C.E., et al., *Inflammatory S100A9 and S100A12 proteins in Alzheimer's disease.* Neurobiol Aging, 2006. **27**(11): p. 1554-63.
63. Wang, C., et al., *The role of pro-inflammatory S100A9 in Alzheimer's disease amyloid-neuroinflammatory cascade.* Acta Neuropathol, 2014. **127**(4): p. 507-22.
64. Wang, C., et al., *S100A9-Driven Amyloid-Neuroinflammatory Cascade in Traumatic Brain Injury as a Precursor State for Alzheimer's Disease.* Sci Rep, 2018. **8**(1): p. 12836.
65. Zhang, C., et al., *MRP14 (S100A9) protein interacts with Alzheimer beta-amyloid peptide and induces its fibrillization.* PLoS One, 2012. **7**(3): p. e32953.
66. Ha, T.Y., et al., *S100a9 knockdown decreases the memory impairment and the neuropathology in Tg2576 mice, AD animal model.* PLoS One, 2010. **5**(1): p. e8840.
67. Shen, L., et al., *Proteomics Analysis of Blood Serums from Alzheimer's Disease Patients Using iTRAQ Labeling Technology.* J Alzheimers Dis, 2017. **56**(1): p. 361-378.
68. Afanador, L., et al., *The Ca2+ sensor S100A1 modulates neuroinflammation, histopathology and Akt activity in the PSAPP Alzheimer's disease mouse model.* Cell Calcium, 2014. **56**(2): p. 68-80.
69. Qiu, X., et al., *S100a9 knockout contributes to neuroprotection and functional improvement after traumatic brain injury.* J Neurotrauma, 2019.
70. Wang, C., et al., *Proinflammatory and amyloidogenic S100A9 induced by traumatic brain injury in mouse model.* Neurosci Lett, 2019. **699**: p. 199-205.
71. Cuello, A.C., *Early and Late CNS Inflammation in Alzheimer's Disease: Two Extremes of a Continuum?* Trends Pharmacol Sci, 2017. **38**(11): p. 956-966.
72. Cristovao, J.S. and C.M. Gomes, *S100 Proteins in Alzheimer's Disease.* Front Neurosci, 2019. **13**: p. 463.
73. Cristóvão, J.S.F., A.J.; Carapeto, A.; Rodrigues, M.S.; Cardoso, I.; Gomes, C.M., *The S100B alarmin is a dual-function chaperone suppressing Aβ oligomerization through combined zinc chelation and inhibition of protein aggregation.* ACS Chem. Neurosci., 2020. **11**: p. 2753-2760.
74. Moreira, G.G., et al., *Dynamic interactions and Ca(2+)-binding modulate the holdase-type chaperone activity of S100B preventing tau aggregation and seeding.* Nat Commun, 2021. **12**(1): p. 6292.
75. Barre-Sinoussi, F. and X. Montagutelli, *Animal models are essential to biological research: issues and perspectives.* Future Sci OA, 2015. **1**(4): p. FSO63.
76. Kathleen R Zahs, K.H.A., *'Too much good news' - are Alzheimer mouse models trying to tell us how to prevent, not cure, Alzheimer's disease?* Trends Neurosci 2010. **33(8)**: p. 381-9.
77. Onos, K.D., et al., *Toward more predictive genetic mouse models of Alzheimer's disease.* Brain Res Bull, 2016. **122**: p. 1-11.

78. Eleanor Drummond, T.W., *Alzheimer's disease: experimental models and reality.* Acta Neuropathol, 2017. **133(2)**: p. 155-175.
79. Drummond, E. and T. Wisniewski, *Alzheimer's disease: experimental models and reality.* Acta Neuropathol, 2017. **133**(2): p. 155-175.
80. Tellechea, P., et al., *Early- and late-onset Alzheimer disease: Are they the same entity?* Neurologia (Engl Ed), 2018. **33**(4): p. 244-253.
81. Shinohara, M., et al., *Regional distribution of synaptic markers and APP correlate with distinct clinicopathological features in sporadic and familial Alzheimer's disease.* Brain, 2014. **137**(Pt 5): p. 1533-49.
82. Hiroki Sasaguri, c.a., Per Nilsson, Shoko Hashimoto, Kenichi Nagata, Takashi Saito, Bart De Strooper, John Hardy, Robert Vassar, Bengt Winblad, and Takaomi C Saido, *APP mouse models for Alzheimer's disease preclinical studies.* EMBO J., 2017. **36(17)**: p. 2473–2487.
83. Xu, G., et al., *Murine Abeta over-production produces diffuse and compact Alzheimer-type amyloid deposits.* Acta Neuropathol Commun, 2015. **3**: p. 72.
84. Dujardin S, C.M., Buee L, *Invited review: animal models of tauopathies and their implications for research/translation into the clinic. .* Neuropathol Appl Neurobiol 2015. **41**: p. 59–80.
85. Selkoe DJ, H.J., *The amyloid hypothesis of Alzheimer's disease at 25 years* EMBO Mol Med 2016 **8**: p. 595–608.
86. C Sturchler-Pierrat, M.S., *Pathogenic mechanisms of Alzheimer's disease analyzed in the APP23 transgenic mouse model.* Ann N Y Acad Sci, 2000. **920**: p. 134-9.
87. Karch, C.M. and A.M. Goate, *Alzheimer's disease risk genes and mechanisms of disease pathogenesis.* Biol Psychiatry, 2015. **77**(1): p. 43-51.
88. Jankowsky, J.L. and H. Zheng, *Practical considerations for choosing a mouse model of Alzheimer's disease.* Mol Neurodegener, 2017. **12**(1): p. 89.
89. Blessed G, T.B., *The association between quantitative measures of dementia and senile change in the gray matter of elderly subjects. .* Br J Psychiatry 1968. **114:**: p. 797–811.
90. Blennow K, M.N., Scholl M, Hansson O, Zetterberg H, *Amyloid biomarkers in Alzheimer's disease.* Trends Pharmacol Sci 2015. **36:**: p. 297–309.
91. Kim, D.H., et al., *Genetic markers for diagnosis and pathogenesis of Alzheimer's disease.* Gene, 2014. **545**(2): p. 185-93.
92. Elfenbein, H.A., et al., *Cerebral beta-amyloid angiopathy in aged squirrel monkeys.* Histol Histopathol, 2007. **22**(2): p. 155-67.
93. Ghosal, K., et al., *Alzheimer's disease-like pathological features in transgenic mice expressing the APP intracellular domain.* Proc Natl Acad Sci U S A, 2009. **106**(43): p. 18367-72.
94. Fryer, J.D., et al., *Apolipoprotein E markedly facilitates age-dependent cerebral amyloid angiopathy and spontaneous hemorrhage in amyloid precursor protein transgenic mice.* J Neurosci, 2003. **23**(21): p. 7889-96.
95. Fernandez-Funez, P., L. de Mena, and D.E. Rincon-Limas, *Modeling the complex pathology of Alzheimer's disease in Drosophila.* Exp Neurol, 2015. **274**(Pt A): p. 58-71.
96. Bales KR, V.T., Cummins DJ, Du Y, Dodel RC, Saura J, Fishman CE, DeLong CA, Piccardo P, Petegnief V et al *Apolipoprotein E is essential for amyloid deposition in the APPV717F transgenic mouse model of Alzheimer's disease. .* PNAS 1999. **96**: p. 15233–15238.
97. Cash DM, R.G., Liang Y, Ryan NS, Kinnunen KM, Yeatman T, Malone IB, Benzinger TL, Jack CR Jr, Thompson PM et al *The pattern of atrophy in familial Alzheimer disease: volumetric MRI results from the DIAN study.* Neurology 2013. **81**: p. 1425–1433.
98. Hunter, J.M., et al., *Biochemical and morphological characterization of the AbetaPP/PS/tau triple transgenic mouse model and its relevance to sporadic Alzheimer's disease.* J Alzheimers Dis, 2011. **27**(2): p. 361-76.
99. Holtzman, D.M., et al., *Apolipoprotein E facilitates neuritic and cerebrovascular plaque formation in an Alzheimer's disease model.* Ann Neurol, 2000. **47**(6): p. 739-47.
100. Holcomb L, G.M., McGowan E, Yu X, Benkovic S, Jantzen P, Saad WK, Mueller R, Morgan D, Sanders S et al *Accelerated Alzheimer-type phenotype in transgenic mice carrying both mutant amyloid precursor protein and presenilin 1 transgenes. .* Nat Med 1998. **4**: p. 97–100.
101. Knopman DS, J.C.J., Lundt ES, Weigand SD, Vemuri P, Lowe VJ, Kantarci K, Gunter JL, Senjem ML, Mielke MM et al *Evolution of neurodegeneration-imaging biomarkers from clinically normal to dementia in the Alzheimer disease spectrum. .* Neurobiol Aging, 2016. **46**: p. 32–42.
102. Bolmont, T., et al., *Induction of tau pathology by intracerebral infusion of amyloid-beta -containing brain extract and by amyloid-beta deposition in APP x Tau transgenic mice.* Am J Pathol, 2007. **171**(6): p. 2012-20.

103. Heuer, E., et al., *Nonhuman primate models of Alzheimer-like cerebral proteopathy.* Curr Pharm Des, 2012. **18**(8): p. 1159-69.
104. Botelho, H.M., G. Fritz, and C.M. Gomes, *Analysis of S100 oligomers and amyloids.* Methods Mol Biol, 2012. **849**: p. 373-86.
105. Brophy, M.B., J.A. Hayden, and E.M. Nolan, *Calcium ion gradients modulate the zinc affinity and antibacterial activity of human calprotectin.* J Am Chem Soc, 2012. **134**(43): p. 18089-100.
106. Grabrucker, A., et al., *Synaptogenesis of hippocampal neurons in primary cell culture.* Cell Tissue Res, 2009. **338**(3): p. 333-41.
107. Hachem, S., et al., *Expression of S100B during embryonic development of the mouse cerebellum.* BMC Dev Biol, 2007. **7**: p. 17.
108. Bluhm, B., et al., *Normal cerebellar development in S100B-deficient mice.* Cerebellum, 2015. **14**(2): p. 119-27.
109. Santos, G., et al., *Impaired oligodendrogenesis and myelination by elevated S100B levels during neurodevelopment.* Neuropharmacology, 2018. **129**: p. 69-83.
110. Maier, F.C., et al., *Quantification of beta-Amyloidosis and rCBF with Dedicated PET, 7 T MR Imaging, and High-Resolution Microscopic MR Imaging at 16.4 T in APP23 Mice.* J Nucl Med, 2015. **56**(10): p. 1593-9.
111. Xue, C., Lin, T. Y., Chang, D., and Guo, Z. , *Thioflavin T as an amyloid dye: fibril quantification, optimal concentration and effect on aggregation. .* R Soc. Open Sci., 2017. **4:160696**.
112. Drolle, E., et al., *Atomic force microscopy to study molecular mechanisms of amyloid fibril formation and toxicity in Alzheimer's disease.* Drug Metab Rev, 2014. **46**(2): p. 207-23.
113. Stewart, K.L. and S.E. Radford, *Amyloid plaques beyond Abeta: a survey of the diverse modulators of amyloid aggregation.* Biophys Rev, 2017. **9**(4): p. 405-419.
114. Rambaran, R.N. and L.C. Serpell, *Amyloid fibrils: abnormal protein assembly.* Prion, 2008. **2**(3): p. 112-7.
115. Swindell, W.R., et al., *Robust shifts in S100a9 expression with aging: a novel mechanism for chronic inflammation.* Sci Rep, 2013. **3**: p. 1215.
116. Sheng, J.G., R.E. Mrak, and W.S. Griffin, *Glial-neuronal interactions in Alzheimer disease: progressive association of IL-1alpha+ microglia and S100beta+ astrocytes with neurofibrillary tangle stages.* J Neuropathol Exp Neurol, 1997. **56**(3): p. 285-90.

Chapter IV: Neuronal S100 proteins as modulators of Aβ42 aggregation

Part of this chapter will be included in Figueira, A., **Romão**, M.A., Cristóvão, J.S., Gomes, C.M. (2022) Brain expressed S100 proteins act concertedly to suppress amyloid-β aggregation by targeting diverse microscopic mechanisms (in preparation)

1. Abstract

Alzheimer's disease is commonly accompanied by neuroinflammation and Aβ peptide aggregation, which are key features for the initiation of neurodegeneration. Some cytokines, including S100 proteins, are increased in the brain during neuroinflammation; in particular, S100B, which is augmented and is secreted to the synaptic space by astrocytes, has been recently implicated in the inhibition of Aβ and tau aggregation. In the last chapter we have shown that several S100 proteins co-localize with Aβ plaques in the brain and our preliminary experiments showed that S100A6 and S100A8 delay Aβ aggregation similarly to S100B. Here we explore the possibility that other neuronal S100 proteins - S100A6, S100A8, S100A9 and the heterodimer S100A8/A9, may also suppress amyloid-β oligomerization. For this we followed the kinetics of Aβ aggregation in the absence and in the presence of selected S100 proteins, monitoring ThT fluorescence. Mechanistic analysis through global fitting was performed to determine how these distinct S100 proteins influence the aggregation mechanism of Aβ$_{42}$. Taken together, our findings suggest that several S100s proteins delay Aβ$_{42}$ aggregation in a Ca^{2+}-dependent fashion, inhibiting microscopic steps. However, the dominant aggregation mechanism of Aβ$_{42}$, with dominant secondary nucleation, is not altered by chaperones. Altogether, these initial results open new avenues for the potential use of these proteins as therapeutic modulators of Aβ$_{42}$ fibril formation.

2. Introduction

The Mechanisms of Amyloid β aggregation

The aggregation of protein molecules into filaments is a common form of self-assembly. The elucidation of the molecular mechanisms by which soluble proteins convert into their amyloid forms is a fundamental prerequisite for understanding and controlling disorders that are linked to protein aggregation, such as Alzheimer's and Parkinson's diseases. The major aggregation pathways include physical aggregation through unfolding intermediates and unfolded states, aggregation through protein self-association or chemical linkages, or aggregation through chemical degradation. The extent of aggregation is dependent on many factors: intrinsic – protein sequence or mutations; primary, secondary, tertiary, or quaternary structure – or extrinsic – linked to the environmental conditions in which protein is present, such as temperature, stress, or pH [1, 2]. Protein aggregates and amyloids are dysfunctional protein forms as they have reduced or no biological activity, potential for immunogenicity or to trigger cellular toxicity. The basic mechanism of self-assembly leading to amyloid fibril

formation which has commonalties across different amyloid diseases, is schematically represented in Fig. 1.

According to the fibril formation model, amyloid is formed by the aggregation of monomeric precursors into fibrils by a common nucleation growth mechanism. Aggregation is initiated by unfolded (e.g., intrinsically disordered) or partially unfolded monomeric precursors (this last group refers to transient unfolded forms of a native protein, or transient folding of an unfolded protein). So, native proteins misfold and undergo conformational changes exposing aggregation prone regions. When these misfolded proteins reach a critical concentration, oligomers are formed that result in protofibrils that mature into fibrils. Misfolded proteins can also form off-pathway oligomers and amorphous aggregates that may nevertheless be toxic and important in pathological states. Mature fibrils are able to shear or fragmentate to form fibrillar oligomers to again aggregate and form new mature fibrils, or to act as a template for secondary nucleation oligomerization [2, 3].

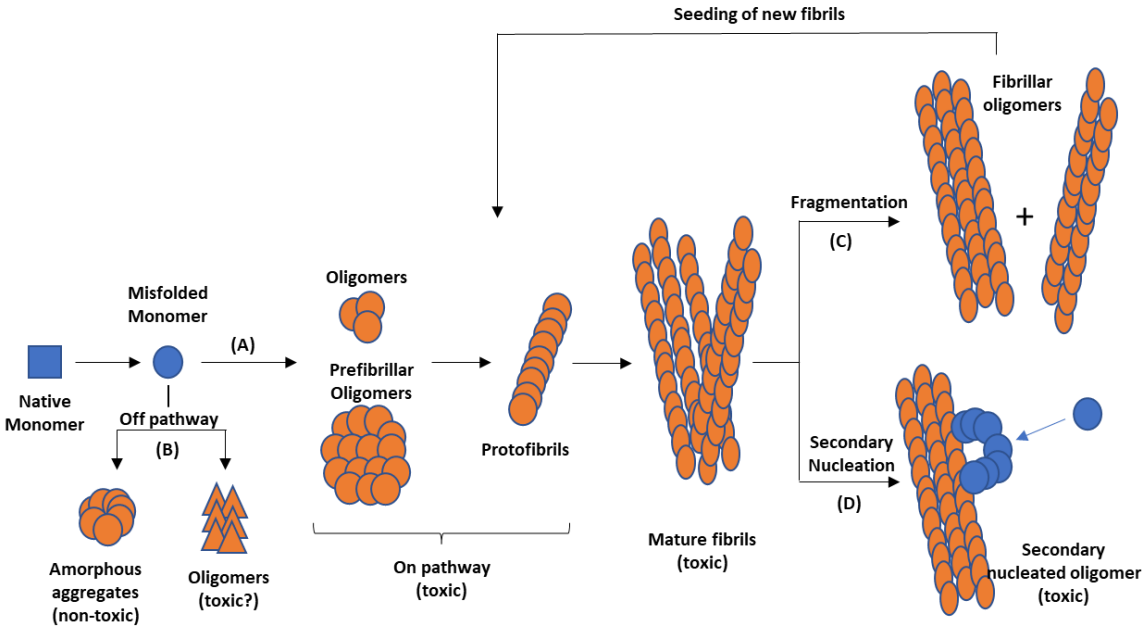

Figure 1 – **Schematic illustration of protein aggregation and amyloid formation in disease states.** The self- assembly of a protein into amyloid involves a multitude of species with different properties, and multiple concurring pathways. (A) Native proteins misfold and undergo conformational change to form protofibrils and mature fibrils; (B) misfolded monomers may form off-pathway oligomers which do not end up in fibrils; (C) mature fibrils undergo shearing or fragmentation to form fibrillar oligomers (originated from fibrils) that again aggregate to form mature fibrils; (D) mature fibrils act as a template for oligomerization and catalysis the secondary nucleation reactions, forming diffusible oligomers from monomers, amplifying the self-assembly reaction.

Macroscopically, a typical aggregation curve depicting the kinetics of amyloid formation displays a characteristic sigmoidal shape (Fig. 2). The shape of the aggregation curve can be divided into three phases: lag phase, in the beginning, followed by a growth or elongation phase, reaching a final plateau. As the reaction completes, the slope of the kinetic curve decreases due to monomer consumption. During the growth phase we observe the greatest conversion rate of peptides/proteins into oligomers and amyloid, while the plateau stage represents a steady state where the monomer concentration has reached its equilibrium value [30]. On the other hand, it is in the lag phase that the underlying microscopic aggregation steps dominate.

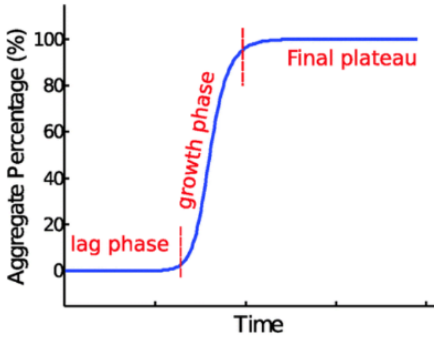

Figure 2 – Macroscopic aggregation sigmoidal curve for amyloid formation. Sigmoidal curve represented by concentration of aggregates formed during time. Curve is divided into three phases: lag phase, growth phase and final plateau. From [30]

The initial increase shape curve and the approach to the plateau is more or less sharp and have characteristic symmetries and asymmetries, depending on the dominant underlying mechanism of fibril formation [4]. During the lag phase, where monomers are the prevalent species, the process is initiated by, at least, two microscopic steps: primary nucleation from monomers in solution and elongation of fibrils (Fig. 3a and 3b). Primary nucleation is the most important process at the beginning of the reaction and refers to formation of aggregates or amyloid oligomers/protofibrils in a reaction involving stacking of monomers [5]. It is treated as a process with single step kinetics with a constant rate k_n and reaction order n_c in monomer. Elongation refers to the process by which monomers are added to the ends of existing aggregates/protofibrils leading to their growth in length. In this case, elongation is modelled either as a single step reaction with rate constant k_+ or more generally as a 2-step reaction. Secondary processes summarize mechanisms in which new fibrils are produced and are dependent on the number of present fibrils. They can have a very significant effect on a protein aggregation behavior, due to their auto-catalytic nature, and lead to near exponential increase in fibril mass over time, very characteristic of proteins involved in disease-states. In these secondary processes are included secondary nucleation and fragmentation. Secondary nucleation can be monomer-dependent, which is defined as a process whereby nucleus

formation from monomers is catalyzed by aggregates composed of the same type of monomeric building blocks (Fig.3c) or monomer-independent, known as fragmentation, in which the surface of growing fibrillar aggregates break into smaller pieces catalyzing the formation of new clusters that act as aggregation nuclei (Fig. 3d) [6]. In the case of monomer dependent secondary nucleation, this process is modelled either as a single process with rate constant k_2 and reaction order n2 in monomer, or more generally as a 2-step process with an initial step in which monomers attach to the fibril surface. As it is monomer-independent, the modulation assumes an equal probability of fragmentation at each monomer in a fibril, given by the rate constant k_-. The molecular mechanisms of the two nucleation processes and the catalytic roles of the surfaces are probably different. Both surfaces may provide “binding sites”, or merely surface accumulation of monomers, whereby increased local concentration of monomers may govern nucleation [7].

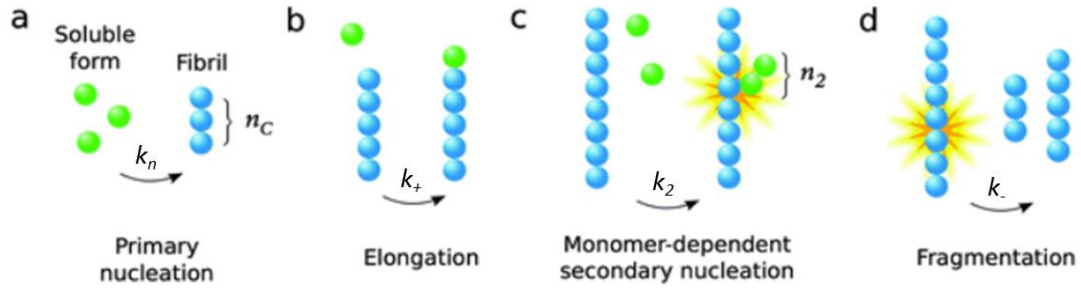

Figure 3 – Amyloid formation microscopic mechanisms and associated rate constants. (a) Primary nucleation from monomers in solution, (b) elongation (growth) by monomers addition to existing aggregates, (c) monomer-dependent nucleation in which surface catalyze secondary nucleation from monomers on fibril surface and (d) fragmentation in a monomer-independent nucleation (d). Rate constants are labelled as k_n to primary nucleation rate, k_+ to elongation, k_2 to secondary nucleation rate and k_- to fragmentation rate. n_c and n_2 refers to the nucleation reactions order. From [6].

The lag phase is generally described as the time needed for the primary nucleation. But, during all phases of the sigmoidal curve, an interconversion between different species operates at the same time. Modifications of each microscopic process influence the overall growth curve in different characteristic manners and to different extents. By analyzing the shape of the aggregation curves it is possible infer on the effects on macroscopic parameters, as the lag time (duration of the lag phase), half-time (time-point where the signal relative to the pre-transition base line has reached 50%), maximal growth rate, endpoint, and they depend on the combination of multiple microscopic rate constants [6].

An aggregation reaction which starts solely with monomeric species in solution will have a growth phase less steep than a reaction which starts with a number of preformed seeds, as shown in Fig.4. In this last case, the curve translates a process dominated by secondary processes, where seeds dominates the growth rate; even if primary nucleation occurs, is not as high as the main growth rate [4]. In this way, is possible, within an aggregation process, to determine the reaction order of the dominant nucleation process (n_c or n_2 for primary and secondary nucleation, respectively). This parameter is called scaling exponent, γ, which relates the time where half of the monomeric protein has been sequestered into aggregates with the total initial monomer concentration [4] (Fig. 4c). The scaling exponent, which is the slope of aggregation curve, depends not only on the elongation rate of the aggregates in solution but also on growth and nucleation processes, depicted in Fig. 4b.

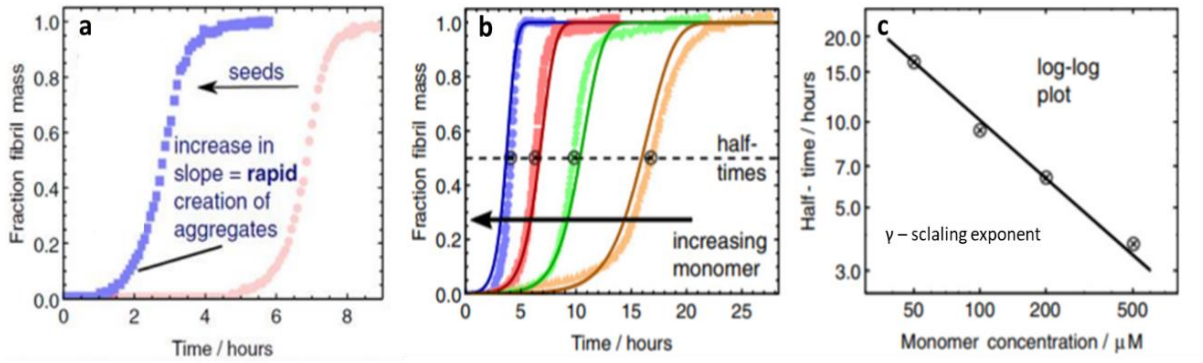

Figure 4 – Elucidation of the halftime scaling and global fitting of data. (a) example pf a sigmoidal curve of aggregation reaction In vitro from a solution with only monomers, in red, and when seeds are added at the beginning of the reaction. (b) Data for increasing initial monomer concentration. Based on the analysis of the half-times in (c), the data are fitted globally with the integrated rate law for fragmenting filaments. From [4]

The scaling exponent γ of $t_{1/2}$ in amyloid aggregation provides a convenient way of determining the reaction order of the dominant nucleation mechanism. The exponent for processes where a classical homogeneous nucleation step is the major source of aggregates is given by $\gamma = - n_c /2$ and for processes where secondary nucleation dominates, is given by $\gamma = -(n_2 +1) /2$ [5]. If γ = -1/2, implies that $n_2=0$, which corresponds to a monomer-independent secondary pathway, whereas $n_2>0$ corresponds to a monomer-dependent process. The importance of defining these parameters, is that it allows better characterization of a specific molecular mechanism of protein aggregation, as well determination of microscopic rates which can give us important information about how some proteins/peptides/drugs can affect Aβ$_{42}$ aggregation. Quantitative kinetic analysis and global fitting can nowadays be performed using AmyloidFit [8], a robust web-based free server that allows to verify which mechanism better describes a given aggregation reaction.

Types of Amyloid β oligomers

During amyloid aggregation (Fig.1) many and different species are formed, and identifying the toxic species formed during amyloid formation remains a challenge. To reach fibril assembly, formation of oligomers is necessary and they are very dynamic, transient, heterogeneous and of unknow and possibly varied structure [9]. Oligomers can then further associate to produce higher-order species, which can be either essential precursors of amyloid fibrils (on-pathway) or dead-end assemblies that do not produce fibrils (off-pathway). Besides off-pathway oligomers do not enter the route to form fibrils, they may be cytotoxic and relevant to diseases. The molecular structure of these transient species is not clearly defined but they tend to exhibit spherical or annular morphologies, where annular oligomers are doughnut or ring shaped assemblies [2]. FTIR and NMR studies showed that oligomers lack the parallel in-register β-sheet structure present in fibrillar forms, but they contain the β-loop-β secondary and tertiary folds as in fibrils [10]. However, it becomes very difficult to distinguish off-pathway and on-pathway oligomers, once they have common immunological epitopes that are recognized by conformational antibodies, A11 (spherical) and αAPF (annular). Interestingly, A11 and αAPF antibodies do not bind to mature fibrils or oligomers formed by fragmentation of fibrils/protofibrils (fibrillar oligomers) [2, 10, 11]. The mature fibrils and the fibrillar oligomers share generic epitopes that are recognized by another conformational antibody, called OC. The OC antibody does not bind prefibrillar oligomers suggesting that prefibrillar and fibrillar oligomers are structurally different [12].

Initially, neurotoxicity was attributed to the presence of amyloid plaque rich in Aβ fibrils in brains of AD and was linked to be the primary cause of cell death and disease pathogenesis [2]. However, more recent evidences in AD suggest that smaller, soluble and misfolded oligomers, appear to be implied in neurodegeneration [13]. It was shown that the severity of cognitive decline arises from pre-amyloid aggregates, instead of the correlation with Aβ plaque formation [14-16]. Earlier transgenic AD mice models exhibited plaque formation as the dominant feature in AD pathology with little neurotoxicity, but very recent studies on AD transgenic mice support that neurotoxicity is due to Aβ oligomers [17]. In this study, Aβ oligomers accumulated in neurons, causing memory loss, synaptic dysfunction and tau hyperphosphorylation, with no extracellular amyloid plaques [17]. Consistently, other *in vitro* experiments have also demonstrated the cytotoxicity of oligomeric species, including their ability to disrupt membranes, suggesting that they can be the causative agents of amyloid-associated cellular dysfunction [18, 19]. Oligomers formed from disease-related precursors have also been shown to impair memory and long-term potentiation, again supporting their role in disease [20].

Structural arrangements may be the reason for differential toxicity of amyloid oligomers and fibrils: oligomers are highly unstable structures whereas fibrils are stable and organized; oligomers expose hydrophobic surfaces in β-sheets while they are hidden inside the interacting stacks in fibrils [21]; oligomers are smaller in size, allowing the easily diffusion in tissues as compared to longer fibrils [22]; oligomers have more open active ends than fibrils, allowing improved interaction with more cellular targets. In the future, it will be very important to develop *in vivo* techniques able to distinguish between functional proteins, oligomeric intermediates, and mature fibrils to dissect the process of protein aggregation in relation with disease state or severity.

Kinetics and analysis of Aβ$_{42}$ aggregation mechanisms

The kinetics of amyloid fibril formation are normally monitored by tracking the increase in total aggregate mass concentration M (t) as a function of time. We can use methods which follow the decreasing concentration of monomeric species or the appearance of aggregates. For several decades the detection of these species relied on small hydrophobic dyes, such as derivatives and Congo Red (CR) and Thioflavin T (ThT). These ligands do not bind to specific proteins but are rather selective towards protein aggregates having an extensive cross β-pleated sheet conformation and a structural regularity, the typical molecular characteristics of presumably all amyloid fibrils [23]. ThT fluorescence was historically one of the first assays to be used to probe the kinetics of protein aggregation and remains one of the most widely used experimental approaches for this purpose [24, 25].Thus, it remains challenging the usage of ThT, due to the fact that the molecular details of the binding of ThT to amyloid fibrils are not fully known and that the resulting fluorescence intensity is susceptible to perturbations from the presence of impurities or amorphous protein aggregates in the system.

In kinetic analysis of fibril mass formation, the first step usually involves the selection of a set of suitable mechanisms for global fitting to the experimental data. The determination of scaling exponent (discussed above) of the reaction half-times in respect to the initial monomer concentration can be useful to access the mechanisms that underlies aggregation. As an example of the application of this approach, we have the elucidation of the microscopic mechanisms of aggregation of the Aβ$_{42}$ peptide of Alzheimer's disease [5], Fig. 5. This strategy revealed that the aggregation of Aβ into fibrils is controlled by secondary nucleation processes in the form of aggregate-surface catalysis, a finding that could have important implications in the context of Alzheimer's disease [5, 26]. This type of analysis can be applied to other self-assembling systems, from prions to amyloidogenic proteins, as a tool to interpreting and

comparing the specific fibril formation mechanisms that underlies that proliferation of amyloid fibrils.

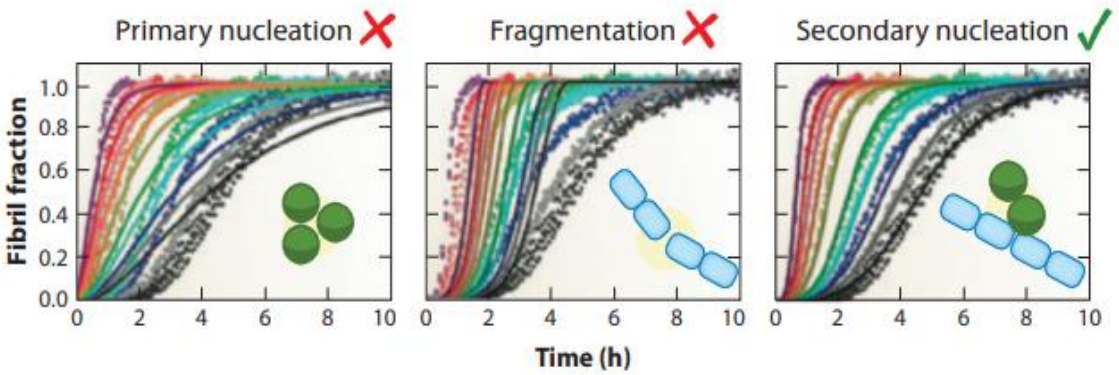

Figure 5 – Scheme of global fits of the three models to kinetic data of Aβ$_{42}$ peptide aggregation in various concentrations. Both a model lacking any processes of self-replication (primary nucleation) and a model assuming that self-replication occurs via fragmentation fail to reproduce the experimental data. A model assuming that self-replication occurs through surface-catalyzed nucleation of monomers, by contrast, matches the data well at all monomer concentrations, with only three free global fitting parameters in total. From [27]

Besides ThT, other fluorescent dyes have been used to detect amyloid fibrils and protein aggregates, such as ANS and Bis-ANS and, more recently, luminescent conjugated oligothiophenes (LCOs), as h-FTAA (heptamer formyl thiophene acetic acid) or p-FTAA among many others [23, 28]. Those are used to detect early non thioflavinophilic protein assemblies that precede formation of amyloid fibrils and also for obtaining distinct spectral signatures of the same fibrils. Such LCOs can be highly useful for studying the underlying molecular events of protein aggregation diseases due to its ability to recognize multiple types of β-aggregates and could also be utilized for the development of novel diagnostic tools for these diseases.

It is also possible study amyloid formation using more direct experimental methods such as nuclear magnetic resonance (NMR) and circular dichroism spectroscopy (CD), in order to observe β-sheet formation along time [29]. These biophysical techniques need to be performed in relatively highly concentrated protein samples. Due to the very low protein concentration (nanomolar or micromolar) at the beginning of aggregation events and due to complex, heterogeneous and transient nature of the involved species, it is hard to study aggregation mechanisms with NMR neither CD. However, they are good tools to confirm secondary structures of intermediates or fibrils.

How Molecular chaperones suppress amyloid formation

As discussed in chapter 1, molecular chaperones are vital components for maintaining protein quality control, and are able to assist in the synthesis, folding, trafficking and degradation of proteins [30]. In addition to these functions, increasing evidence from *in vitro* and *in vivo* studies have demonstrated that molecular chaperones play a role in modulating the formation of amyloid fibrils, namely suppressing their formation and toxicity [31, 32]. Understanding the mechanism by which molecular chaperones suppress amyloid formation is very challenging because of the great complexity of protein aggregation processes. Several mechanisms of action have been proposed, but the big challenge lies in the identification of a specific molecular event associated with a given protein- chaperone system. There is a large variety of potential interactions between a molecular chaperone and the different protein species that can be present during aggregation process, Fig. 6.

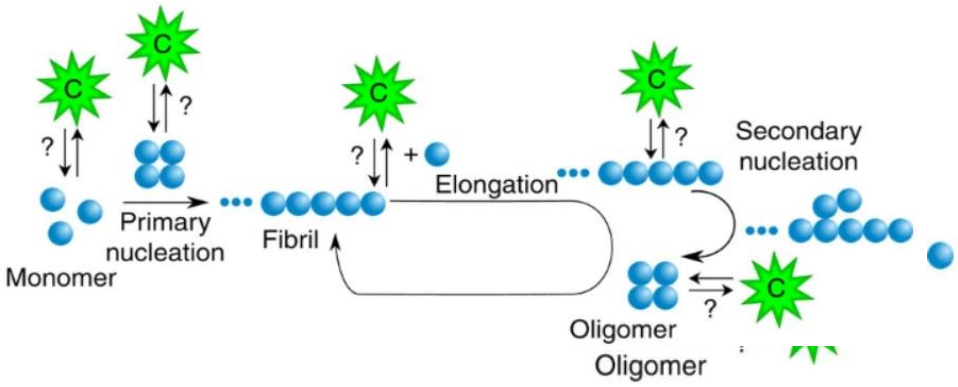

Figure 6 – Schematic illustration of possible interactions of molecular chaperones in the aggregation mechanism. Aggregation reaction network made by microscopic steps in aggregation of an amyloidogenic protein (blue) and possible interactions between chaperones (green) and different protein species present in the system. Some chaperones implicated in these steps are DNAJB6 (DnaJ Heat Shock Protein Family (Hsp40) Member B6), Ssa1 (a member of the Hsp70 family) and proSP-C Brichos (a molecular chaperone belonging to the Brichos family). From [33]

Molecular chaperones can interact with monomeric misfolded or unfolded forms of proteins and also with a variety of aggregated species [34, 35]. As a consequence, any microscopic events that make up the macroscopic protein aggregation process can be influenced by chaperone binding. Is complicated to identify the specific step perturbed by an individual molecular chaperone due to the heterogeneity of species and the different nature of the protein aggregation kinetics, which are a result of numerous combinations of microscopic reactions involving primary and secondary nucleation, elongation, and fragmentation [5, 33, 36]. If the target specie is monomer, the inhibited microscopic event is primary and secondary nucleation and elongation; if it is oligomers, is primary and secondary nucleation; if it is the

fibril ends, elongation is inhibited; and if it is the fibril surface, is the secondary nucleation that is affected [33], Fig. 7.

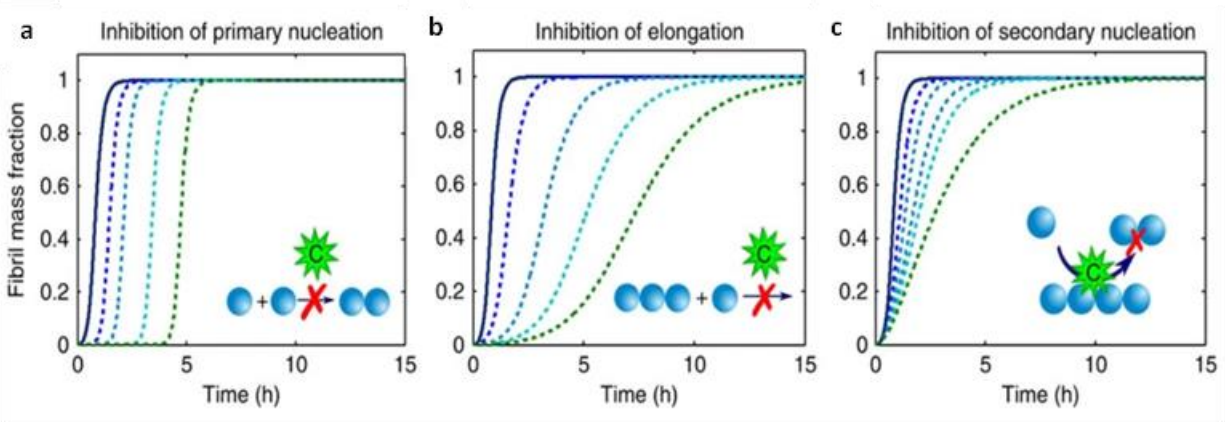

Figure 7 – Molecular chaperones can affect individual microscopic steps in the aggregation process. a-c integration of master equations illustrates how perturbations of specific microscopic aggregation events modify characteristic ways the global kinetic profiles. The analysis of the changes in the macroscopic profiles provides quantitative information on the microscopic events altered by the interaction with molecular chaperones. From [33]

It has been proposed that molecular chaperones are neuroprotective because of their ability to modulate the earliest aberrant protein interactions that trigger pathogenic cascades, such as in Alzheimer's disease, amyotrophic lateral sclerosis and Parkinson's disease [37]. In fact, S100 proteins conjugate some characteristics which suggested that they can act as chaperones: (i) are low molecular weight proteins; (ii) occur in different conformational states, including high molecular mass oligomers; (iii) have a secondary structure that is conserved at non-physiological temperatures; (iv) are highly resistant to thermal denaturation; (v) have expression levels correlated with stress conditions; and (vi) interact with aggregation prone proteins. Indeed, as reported in [38] and already mentioned, S100B was introduced as a dual function chaperone that in low concentrations are capable of suppress the formation of toxic Aβ oligomers and inhibit of protein aggregation. Also S100A1, was reported to act as a potent chaperone and a new member of the multichaperone complex Hsp70/Hsp90 [39].

The way to define the reactional mechanisms by which molecular chaperones are acting consists of perform kinetic experiments and compare the results o rate laws derived from canonical molecular mechanisms [4, 27]. A detailed understanding of the molecular basis of chaperone-mediated protection against neurodegeneration might lead to development of therapies for neurodegenerative disorders that are associated with protein misfolding and aggregation.

.

3. Materials and methods

Materials. All reagents were of the highest grade commercially available. Thioflavin T (ThT) was obtained from Sigma. A Chelex resin (Bio-Rad) was used to remove contaminant trace metals from all solutions.

Protein Expression and Purification. Human S100A6, S100A8, S100A9, S100A8/A9 and S100B were expressed in *Escherichia coli* and purified to homogeneity using a previously established protocol. Apo S100 protein family was prepared by incubation at 37°C for 2h with a 300-fold excess of Dithiothreitol (DTT) and 0.5 mM ethylenediamine tetraacetic acid (EDTA) and eluted in a Superdex S75 (GE Healthcare). Human recombinant Aβ$_{42}$ was expressed in Escherichia coli and purified as described previously [40]. The human Aβ$_{42}$ expression plasmid was a gift from J. Presto (Karolinska Institute, Sweden). To obtain the monomeric form, 1 mg of Aβ$_{42}$ was dissolved in 7 M guanidine hydrochloride and eluted in a Superdex S75 (GE Healthcare) with 50 mM HEPES (pH 7.4). Low-bind tubes (Axygen Scientific, Corning) were used in all procedures employing Aβ$_{42}$.

Aβ$_{42}$ Aggregation Kinetics. Aβ$_{42}$ aggregation kinetics was investigated by monitoring the fluorescence increase of the amyloid-sensitive dye Thioflavin-T (ThT) [24, 41] as a function of time in a plate reader (FLUOstar OPTIMA, BMG Labtech) using a 440nm excitation filter and a 480nm emission filter. Fluorescence was recorded using bottom optics in 96-well polyethylene glycol-coated black polystyrene plates with a clear bottom (Corning, 3881). Briefly, Aβ42 monomer was isolated by gel filtration (Tricorn Superdex75 column, GE Healthcare) in 50 mM HEPES (pH 7.4) immediately prior to experiments and diluted in the same buffer with 1.1 mM CaCl2. ThT (10 μM) was added to each condition. Monomeric Aβ$_{42}$ (5 μM) was used in aggregation assays at 37°C, without agitation with fluorescence read every 400s. For testing the effects of 15-times fold S100A6, S100A8, S100A9 and S100A8/A9 the proteins were added to the reaction media. S100B, whose effects on Aβ42 aggregation had been previously reported [42], was tested under identical assay conditions as a comparison and control. Appropriate controls in the absence of Aβ$_{42}$ did not reveal significant variations on ThT intensity due to S100 proteins alone. Triplicates were routinely performed for all assays. Data analysis was carried out using the *AmyloFit* platform, which implements the master equations derived from basin-hopping algorithm that describe the evolution of total fibril mass in the presence of primary and secondary nucleation events, and from which microscopic processes and reaction rates can be determined from global fitting [8]. The kinetic traces were fitted using the secondary nucleation model. The normalized intensity curves and corresponding fits were extracted from the platform and presented as normalized intensities representing fibrillar mass fraction, from which the reaction half times ($t_{1/2}$) were estimated [6].

4. Results and Discussion

4.1 S100 proteins delay half-time of Aβ42 aggregation

Considering the recent finding that S100B is a calcium-tuned suppressor of $A\beta_{42}$ aggregation [42], and that several S100 proteins are present in AD brains and co-localized with amyloid plaques [43], we sought to understand if they play similar roles, to gain further mechanistic insights into the yet unclear roles of S100 proteins in AD brain. To access that, 5 µM monomeric $A\beta_{42}$ peptide was incubated in the absence and presence of each S100 protein, namely S100A6, S100A8, S100A9, S100A8/A9, individually, in a range of S100 concentrations between 10-75 µM in the presence of Ca^{2+}. Aggregation was monitored by ThT fluorescence signal, following the evolution of fibril formation, Fig. 8.

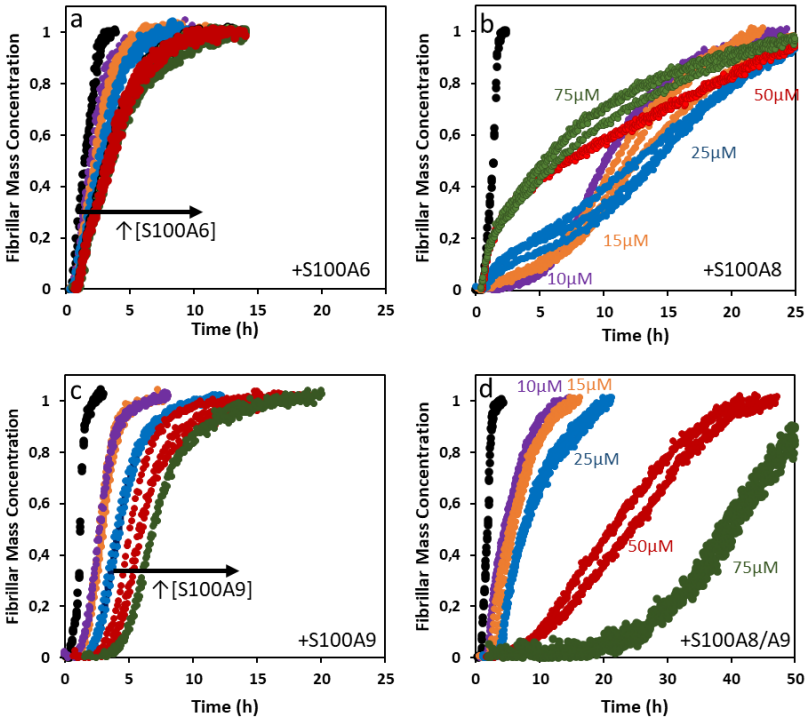

Figure 8 –Impact of S100 proteins on $A\beta_{42}$ aggregation. Fibril formation of 5 µM $A\beta_{42}$ (black, $t_{1/2}$= 1.3h) in 50 mM HEPES (pH 7.4), 1.1 mM $CaCl_2$, at 37°C under quiescent conditions, in the presence of a range of S100 protein concentrations between 10-75µM of S100A6 (a), S100A8 (b), S100A9 (c), and S100A8/A9 (d). 10 µM represented in purple, 15 µM in orange, 25 µM in blue, 50 µM in red and 75 µM in green. Plots represent average normalized intensity curves, obtained from three independent experiments.

Calcium-binding-S100 proteins, S100A6, S100A8, S100A9 and S100A8/A9, can delay fibril formation even at the lower concentration (10µM), shown in purple in Fig.8. This inhibitory effect is proportional to S100 concentration. For S100A6, Fig. 8a, an increase in half-time with increasing concentration was noted, suggesting that secondary nucleation is being inhibited. The impact of S100A8 is different: while for lower concentrations there is an increased lag phase, as concentration increases there is no impact in the lag phase, but on the half-times of

fibril formation (which increase), Fig. 8b. S100A8 seems to inhibit different microscopic events depending on concentration: for low concentrations inhibits elongation, and as concentrations increases there is more inhibition on secondary nucleation. In the case of S100A9, Fig. 8c, with increased concentrations, there is an increased lag phase and half-time, in a concentration dependent manner. This effect on the aggregation kinetics is suggestive of primary nucleation inhibition. For calprotectin (S100A8/A9), Fig. 8d, the impact is opposite than the one observed for S100A8 alone: in low concentrations, secondary nucleation may be inhibited, while at high concentrations, a large impact in lag-phase in observed, inhibiting mainly elongation and primary nucleation events. S100A6, S100A8, S100A9 and S100A8/A9 induces alterations on Aβ$_{42}$ aggregation mechanism, altering it in different microscopic events. I.e., different nucleation types are being inhibited. In Fig.9 is plotted the effect of each S100 on Aβ$_{42}$ aggregation at the fixed ratio Aβ$_{42}$:S100 of 1:3.

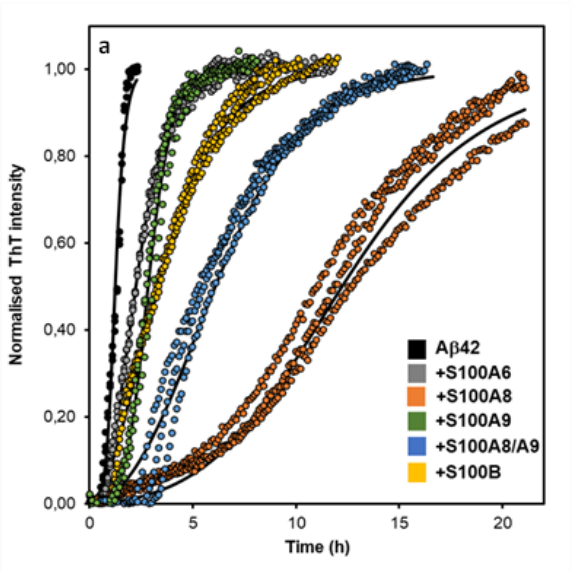

b

	half-time (h)
Aβ$_{42}$	1.32
Aβ$_{42}$: S100A6	2.23
Aβ$_{42}$:S100A8	12.27
Aβ$_{42}$:S100A9	2.84
Aβ$_{42}$:S100A8/A9	5.88
Aβ$_{42}$:S100B	3.49

Figure 9 – S100 protein family modulates Aβ$_{42}$ aggregation. a) Fibril formation of 5μM Aβ$_{42}$ (black, $t_{1/2}$= 1.3h) in 50mM HEPES (pH 7.4), 1.1mM $CaCl_2$, at 37°C under quiescent conditions, in the presence of 15μM of S100A6 (grey, $t_{1/2}$= 2.2h), S100A8 (orange, $t_{1/2}$= 12.3h), S100A9 (green, $t_{1/2}$= 2.8h), S100A8/A9 (blue, $t_{1/2}$= 5.9h) and S100B (yellow, $t_{1/2}$= 3.5h). Plots represent average normalized intensity curves (a), fitted to a secondary nucleation model, obtained from three independent replicates for each of the tested conditions. $t_{1/2}$= reaction half-times. Table with half-times for each reaction is shown in (b).

S100s have different effects on Aβ$_{42}$ aggregation. At the same ratio, S100A6, S100A9 and S100B inhibit secondary nucleation, while S100A8 inhibit elongation and S100A8/A9 inhibit primary nucleation. Focusing on half-times ($t_{1/2}$) of the Aβ$_{42}$ aggregation in the presence of S100s reveal that S100A8 has the strongest effect (~15 × increase) in delaying fibril formation, under the tested conditions. The effect of S100A6 and S100A9 is not so pronounced, but the presence of the heterodimer S100A8/A9 also increases half-time. The effect of S100A8/A9 seems to be an intermediate effect between S100A8 and S100A9 alone. In the case of S100B, the inhibitory effect has been shown to result from a direct physical

interaction with Aβ42 [42]. These results suggest that these S100 proteins influence Aβ42 aggregation possibly through physical interactions like those described for S100B. In support of this possibility interaction is the evidence that the S100A8-containing heterodimer calprotectin interacts with Aβ40, also influencing its aggregation [44]. Although this study gave us clues about the impact of S100s on Aβ42 aggregation, other approaches are necessary to study the influence of that interaction on the mechanism of self-assembly.

4.2. Scaling exponent of Aβ42 aggregation kinetic dominant mechanism is not altered upon interaction with S100 proteins

For Aβ42 aggregation, the secondary nucleation mechanism under the studied *in vitro* conditions has emerged as the most important type of micro-step and a source of toxic oligomeric species [5]. Understanding how S100 proteins can mechanistically affect Aβ42 aggregation in fundamental to understand the impact that this protein family can have, namely in Alzheimer's disease. To explore the dependence of the various microscopic steps in the Aβ42 aggregation in the presence of S100 proteins, we carried out a series of kinetic experiments at different concentrations of Aβ42, maintaining a fixed ration of Aβ42: S100 [45]. To determine this molar ratio, we first studied the impact of a S100 on Aβ42 aggregation, individually, Fig. 10. The goal was to choose the lowest molar ratio at which a given S100 protein starts to influence the macroscopic parameters of Aβ42 aggregation.

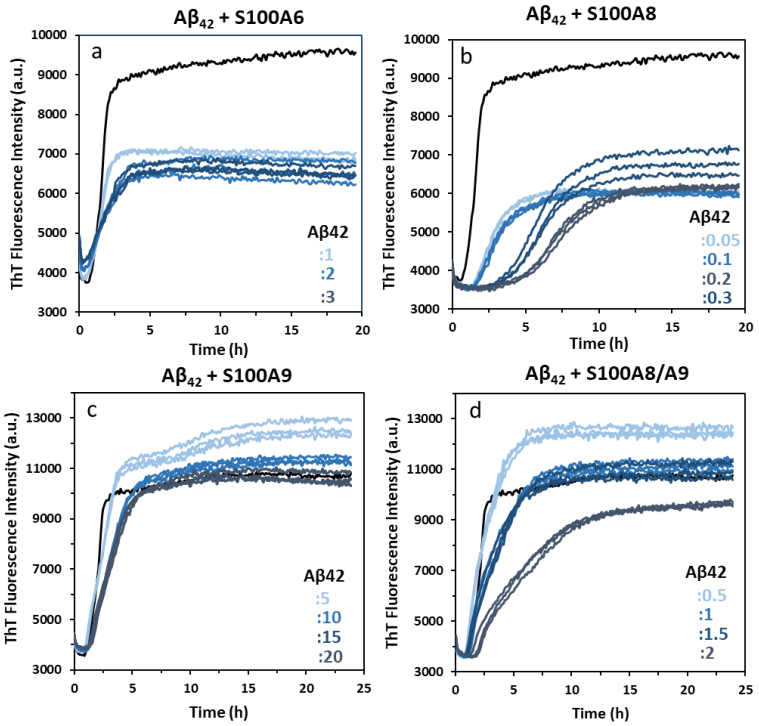

Figure 10 – Aβ42 aggregation in the presence of different ratios of S100 proteins. Aβ42 peptide were incubated in 5μM concentration in different ratios Aβ42: S100 protein. In (A) S100A6 were studied from 1-3-fold

excess, in (B) S100A8 was studied from 0.05-0.3-fold excess, in (C) S100A9 was studied from 5-20-fold excess and in (D) S100A8/A9 was studied from 0.5-2-fold excess. Plots represent average normalized intensity curves, obtained from three independent

Different Aβ$_{42}$: S100 molar ratios were used for each studied S100 protein because different effects for different concentrations are observed. Ratios of 1:3, 1:0.05, 1:15 and 1:2 were chosen for S100A6, S100A8, S100A9 and S100A8/A9, respectively. Using these selected molar ratios, we sought to understand if S100s are capable of changing the dominant aggregation mechanism of Aβ$_{42}$. Processing and global analysis of protein aggregation kinetic data were performed suing AmyloFit (http://www.amylofit.ch.cam.ac.uk, [8]). This fitting platform is freely accessible online, and it enables robust global data analysis without the need for programming or detailed mathematical knowledge. Fig. 11 represents the fitted data obtained for Aβ$_{42}$ aggregation in the presence of S100A6, S100A8, S100A9 and S100A8/A9.

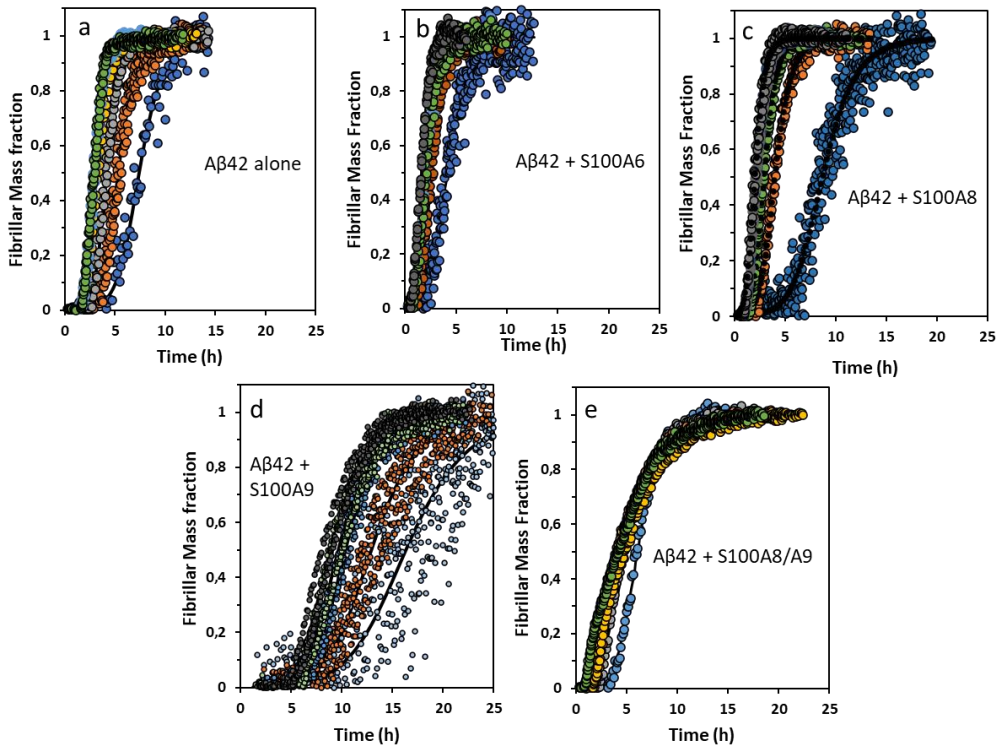

Figure 11 – Analysis of the effect of S100 proteins on the aggregation kinetics of Aβ$_{42}$. Fibril formation of a concentration range of Aβ$_{42}$ peptide from 1 to 6μM alone **(a)** and in the presence of 3-fold excess of S100A6 **(b)**, 0.05-fold excess for S100A8 **(c)**, 15-fold excess for S100A9 **(d)** and 2-fold excess for S100A8/A9 **(e)**. Curves fitted by AmyloidFit online platform. Plots represent average normalized intensity curves obtained from three independent replicates for each of the tested conditions.

To infer on the impact of each S100 protein on the dominant reaction mechanism of Aβ$_{42}$ it is necessary to determine scaling exponent (γ), which describes how the lag time or half-time of the reaction scales with the initial Aβ$_{42}$ concentration of monomer, by double-logarithmic plots [8], represented in Fig. 12. Scaling exponent will give us some guidance regarding a possible alteration in the dominant aggregation mechanisms [8].

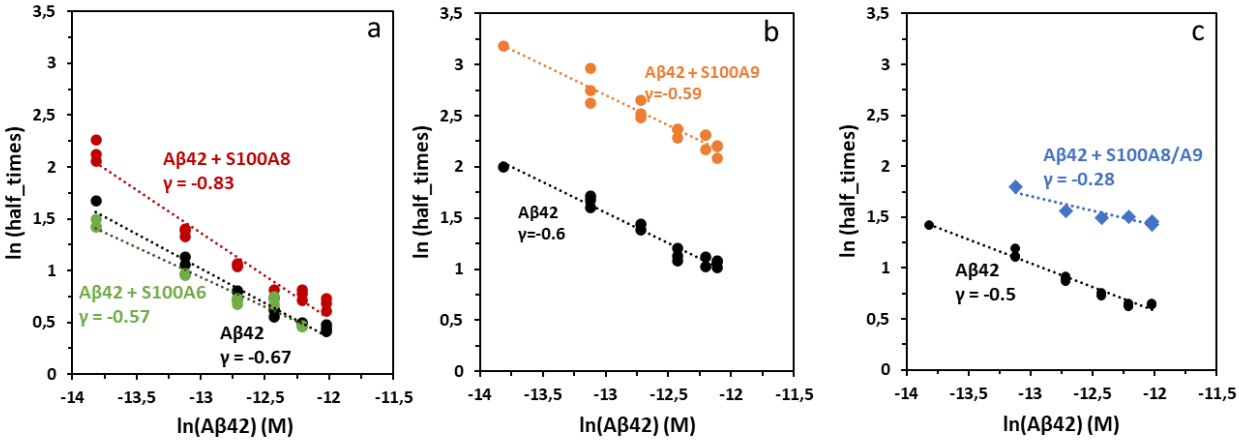

Figure 12 – Scaling exponent of S100 in modulation of Aβ$_{42}$ aggregation. Double log plot of time to half-completion of Aβ$_{42}$ aggregation as function of Aβ$_{42}$ initial monomer concentration, in the presence of 1.1mM $CaCl_2$, in interaction with 15xfold excess of (a) S100A8 (red) and S100A6 (green), (b) S100A9 (orange) and (c) S100A8/A9 (blue).

This approach allowed us to determine a scaling exponent ≈-0.6 for Aβ$_{42}$ aggregation alone, following a linearity, confirming that Aβ$_{42}$ aggregation pathway proceeds *via* a mechanism where secondary events dominate the generation of new fibrils, consistent with previously reported ranges of scaling exponents obtained under identical experimental conditions [5, 8]. Analyzing scaling exponent data for Aβ$_{42}$ in presence of S100s, we observe a straight line for all conditions. Linear plots indicate that the dominant mechanism does not change at different monomer concentrations. The presence of S100A8 is the one that shows the major effect, showing a smooth negative curvature (which may indicate that competition of several processes in parallel are present) but the difference is not significative. Overall, we observe that studied S100 proteins does not change the dominant mechanism of Aβ$_{42}$ aggregation, which is secondary nucleation process. S100 proteins inhibit some Aβ$_{42}$ aggregation microscopic events, but, overall, do not change Aβ$_{42}$ aggregation mechanism, in these conditions. S100s are able to inhibit secondary nucleation, but not to the point of changing the dominant aggregation mechanism.

Altogether, these results corroborate that several proteins of S100 family can interfere with the aggregation of Aβ$_{42}$, by delaying half-times and lag-phases and inhibiting the microscopic events, presumably through direct interactions.

5. Conclusions

Alzheimer's disease is a the most common progressive neurological disorder which affects millions of people worldwide. One of the major hallmarks of the disease is the deposition of amyloid-β peptide in the brain forming plaques and amyloids. During neuroinflammation, several S100 proteins are released, augmenting their levels in the brain and co-localizing with Aβ plaques in AD models. Recent work has shown that S100B has novel chaperone-like functions, interacting physically with Aβ$_{42}$ affecting its aggregation mechanisms. Here, we provide evidence that other S100 proteins, namely S100A6, S100A8, S100A9 and S100A8/A9 also affect Aβ$_{42}$ aggregation presumably through physical interactions as with S100B. By studying the impact of increasing concentrations of S100 proteins on Aβ$_{42}$ aggregation, we can infer in a preliminary basis which micro steps are being inhibited. Different S100s inhibit Aβ$_{42}$ aggregation differently: S100A6 inhibits mostly secondary nucleation; S100A8, at low concentrations, inhibits elongation and at high concentrations inhibit secondary nucleation; S100A9 inhibits primary nucleation; and S100A8/A9 inhibit secondary nucleation at low concentrations and elongation and primary nucleation at high concentrations. Using the scaling exponent approach, we could access which is the dominant aggregation mechanism; We observed that the presence of any of the S100 proteins influenced the predominant mechanism of Aβ$_{42}$ aggregation. These findings suggest that prior to pro-inflammatory and disease-aggravating roles in later disease stages, S100 proteins may engage in new protective activities related to amyloid aggregation processes, which might be amenable to future pharmacological intervention to mitigate AD progression. Understanding the roles that S100 proteins play in the early AD aggregation and how they interact with Aβ$_{42}$ can open new clues and approaches to better understand the biology of AD regulation.

6. References

1.Wang, W., S. Nema, and D. Teagarden, *Protein aggregation--pathways and influencing factors.* Int J Pharm, 2010. **390**(2): p. 89-99.
2. Verma, M., A. Vats, and V. Taneja, *Toxic species in amyloid disorders: Oligomers or mature fibrils.* Ann Indian Acad Neurol, 2015. **18**(2): p. 138-45.
3. Chiti, F. and C.M. Dobson, *Protein Misfolding, Amyloid Formation, and Human Disease: A Summary of Progress Over the Last Decade.* Annu Rev Biochem, 2017. **86**: p. 27-68.
4. Cohen, S.I., et al., *From macroscopic measurements to microscopic mechanisms of protein aggregation.* J Mol Biol, 2012. **421**(2-3): p. 160-71.
5. Cohen, S.I., et al., *Proliferation of amyloid-beta42 aggregates occurs through a secondary nucleation mechanism.* Proc Natl Acad Sci U S A, 2013. **110**(24): p. 9758-63.
6. Arosio, P., T.P. Knowles, and S. Linse, *On the lag phase in amyloid fibril formation.* Phys Chem Chem Phys, 2015. **17**(12): p. 7606-18.
7. Linse, S., *Mechanism of amyloid protein aggregation and the role of inhibitors.* Pure and Applied Chemistry, 2019. **vol. 91**(2. Special issue): p. 211-229.
8. Meisl, G., et al., *Molecular mechanisms of protein aggregation from global fitting of kinetic models.* Nat Protoc, 2016. **11**(2): p. 252-72.
9. Iadanza, M.G., et al., *A new era for understanding amyloid structures and disease.* Nat Rev Mol Cell Biol, 2018. **19**(12): p. 755-773.
10. Yu, X. and J. Zheng, *Polymorphic structures of Alzheimer's beta-amyloid globulomers.* PLoS One, 2011. **6**(6): p. e20575.
11. Yu, L., et al., *Structural characterization of a soluble amyloid beta-peptide oligomer.* Biochemistry, 2009. **48**(9): p. 1870-7.
12. Kayed, R., et al., *Fibril specific, conformation dependent antibodies recognize a generic epitope common to amyloid fibrils and fibrillar oligomers that is absent in prefibrillar oligomers.* Mol Neurodegener, 2007. **2**: p. 18.
13. Soto, C. and S. Pritzkow, *Protein misfolding, aggregation, and conformational strains in neurodegenerative diseases.* Nat Neurosci, 2018. **21**(10): p. 1332-1340.
14. Nelson, P.T., et al., *Correlation of Alzheimer disease neuropathologic changes with cognitive status: a review of the literature.* J Neuropathol Exp Neurol, 2012. **71**(5): p. 362-81.
15. Baglioni, S., et al., *Prefibrillar amyloid aggregates could be generic toxins in higher organisms.* J Neurosci, 2006. **26**(31): p. 8160-7.
16. Simoneau, S., et al., *In vitro and in vivo neurotoxicity of prion protein oligomers.* PLoS Pathog, 2007. **3**(8): p. e125.
17. Zhang, Y., et al., *A lifespan observation of a novel mouse model: in vivo evidence supports abeta oligomer hypothesis.* PLoS One, 2014. **9**(1): p. e85885.
18. Serra-Batiste, M., et al., *Abeta42 assembles into specific beta-barrel pore-forming oligomers in membrane-mimicking environments.* Proc Natl Acad Sci U S A, 2016. **113**(39): p. 10866-71.
19. Evangelisti, E., et al., *Binding affinity of amyloid oligomers to cellular membranes is a generic indicator of cellular dysfunction in protein misfolding diseases.* Sci Rep, 2016. **6**: p. 32721.
20. Shankar, G.M., et al., *Amyloid-beta protein dimers isolated directly from Alzheimer's brains impair synaptic plasticity and memory.* Nat Med, 2008. **14**(8): p. 837-42.
21. Paravastu, A.K., et al., *Molecular structural basis for polymorphism in Alzheimer's beta-amyloid fibrils.* Proc Natl Acad Sci U S A, 2008. **105**(47): p. 18349-54.
22. !!! INVALID CITATION !!! {}.
23. Klingstedt, T., et al., *Synthesis of a library of oligothiophenes and their utilization as fluorescent ligands for spectral assignment of protein aggregates.* Org Biomol Chem, 2011. **9**(24): p. 8356-70.
24. Gade Malmos, K., et al., *ThT 101: a primer on the use of thioflavin T to investigate amyloid formation.* Amyloid, 2017. **24**(1): p. 1-16.
25. Biancalana, M. and S. Koide, *Molecular mechanism of Thioflavin-T binding to amyloid fibrils.* Biochim Biophys Acta, 2010. **1804**(7): p. 1405-12.
26. Meisl, G., et al., *Differences in nucleation behavior underlie the contrasting aggregation kinetics of the Abeta40 and Abeta42 peptides.* Proc Natl Acad Sci U S A, 2014. **111**(26): p. 9384-9.
27. Knowles, T.P., M. Vendruscolo, and C.M. Dobson, *The amyloid state and its association with protein misfolding diseases.* Nat Rev Mol Cell Biol, 2014. **15**(6): p. 384-96.
28. Younan, N.D. and J.H. Viles, *A Comparison of Three Fluorophores for the Detection of Amyloid Fibers and Prefibrillar Oligomeric Assemblies. ThT (Thioflavin T); ANS (1-Anilinonaphthalene-8-sulfonic*

Acid); and bisANS (4,4'-Dianilino-1,1'-binaphthyl-5,5'-disulfonic Acid). Biochemistry, 2015. **54**(28): p. 4297-306.
29. Hellstrand, E., et al., *Amyloid beta-protein aggregation produces highly reproducible kinetic data and occurs by a two-phase process.* ACS Chem Neurosci, 2010. **1**(1): p. 13-8.
30. Hartl, F.U., A. Bracher, and M. Hayer-Hartl, *Molecular chaperones in protein folding and proteostasis.* Nature, 2011. **475**(7356): p. 324-32.
31. Balch, W.E., et al., *Adapting proteostasis for disease intervention.* Science, 2008. **319**(5865): p. 916-9.
32. Mannini, B., et al., *Molecular mechanisms used by chaperones to reduce the toxicity of aberrant protein oligomers.* Proc Natl Acad Sci U S A, 2012. **109**(31): p. 12479-84.
33. Arosio, P., et al., *Kinetic analysis reveals the diversity of microscopic mechanisms through which molecular chaperones suppress amyloid formation.* Nat Commun, 2016. **7**: p. 10948.
34. Knowles, T.P., et al., *Kinetics and thermodynamics of amyloid formation from direct measurements of fluctuations in fibril mass.* Proc Natl Acad Sci U S A, 2007. **104**(24): p. 10016-21.
35. Dedmon, M.M., et al., *Heat shock protein 70 inhibits alpha-synuclein fibril formation via preferential binding to prefibrillar species.* J Biol Chem, 2005. **280**(15): p. 14733-40.
36. Knowles, T.P., et al., *An analytical solution to the kinetics of breakable filament assembly.* Science, 2009. **326**(5959): p. 1533-7.
37. Muchowski, P.J. and J.L. Wacker, *Modulation of neurodegeneration by molecular chaperones.* Nat Rev Neurosci, 2005. **6**(1): p. 11-22.
38. Cristóvão, J.S.F., A.J.; Carapeto, A.; Rodrigues, M.S.; Cardoso, I.; Gomes, C.M., *The S100B alarmin is a dual-function chaperone suppressing Aβ oligomerization through combined zinc chelation and inhibition of protein aggregation.* ACS Chem. Neurosci., 2020. **11**: p. 2753-2760.
39. Okada, M., et al., *S100A1 is a novel molecular chaperone and a member of the Hsp70/Hsp90 multichaperone complex.* J Biol Chem, 2004. **279**(6): p. 4221-33.
40. Walsh, D.M., et al., *A facile method for expression and purification of the Alzheimer's disease-associated amyloid beta-peptide.* FEBS J, 2009. **276**(5): p. 1266-81.
41. Cristovao, J.S., B.J. Henriques, and C.M. Gomes, *Biophysical and Spectroscopic Methods for Monitoring Protein Misfolding and Amyloid Aggregation.* Methods Mol Biol, 2019. **1873**: p. 3-18.
42. Cristóvão, J.S., Morris, V. K., Cardoso, I., Leal, S. S., Martinez, J., Botelho, H. M., et al. , *The neuronal S100B protein is a calcium-tuned suppressor of amyloid-beta aggregation. .* Sci. Adv. , 2018. **4:eaaq1702.**
43. Hagmeyer, S., et al., *Distribution and Relative Abundance of S100 Proteins in the Brain of the APP23 Alzheimer's Disease Model Mice.* Front Neurosci, 2019. **13**: p. 640.
44. Lee, H.J., et al., *Calprotectin influences the aggregation of metal-free and metal-bound amyloid-beta by direct interaction.* Metallomics, 2018. **10**(8): p. 1116-1127.
45. Scheidt, T., et al., *Secondary nucleation and elongation occur at different sites on Alzheimer's amyloid-beta aggregates.* Sci Adv, 2019. **5**(4): p. eaau3112.

Chapter V: Analysis of S100A9 self-assembly into pseudo-amyloid fibrils

Part of this chapter will be published in: Romão MA et al (2022) Nanoscale analysis of self-assembled worm-like fibrils formed by native globular protomers (*in preparation*)

The ATR-FTIR experiments and analysis have been performed by Guilherme M. Moreira; TEM images were made by Isabel Cardoso; AFM imaging was performed at the BioISI AFM Magnano laboratory. SAXS experiments were performed by Guenter Fritz (University Hohenheim, Germany). Luisa Corvo (FFUL) is gratefully acknowledged for granting access to a DLS instrument.

1. Abstract

S100A9 protein is an aged-related proinflammatory cytokine from the S100 family, which is found to be upregulated in neurodegenerative diseases. Recent literature suggests that increased S100A9 levels during inflammation may lead to its amyloid formation and toxic deposition, due to exposure of its aggregation prone regions in helix IV, as proposed for neurodegenerative disorders [1, 2] and the aging prostate [3]. It has also been proposed that in Traumatic Brain Injury (TBI) and Alzheimer's disease (AD) brains S100A9 co-aggregates intracellularly with the formation of fibrillar materials [4]. However, the evidence that these S100A9 fibrils are truly amyloid structures that are formed during disease states is not fully established nor is well defined from a mechanistic viewpoint.

In this work, we focused on investigating the formation of S100A9 polymeric assemblies under physiological conditions with the absence and in the presence of metal ions. We gathered evidence suggesting that these string-like polymeric structures are very stable and structurally keep the α-helical fold characteristic of native S100A9. We show that these polymers are not truly amyloid in nature and can reversibly dissociate, being composed by assembly units comprising native-like S100A9 protomers. Our data shows that formation of the S100A9 polymers is a dynamic process which nevertheless does not involve major conformational changes in the S100A9 α-helical fold, and the properties and characteristics of those polymers are discussed. We hypothesize that these structures may be a form of protein stabilization to maximize the lifetime of the protein in extracellular environments, notably in the synapse.

2. Introduction

Proteins occur in a multitude of quaternary structures among which are higher order oligomers and fibrils generated through self-assembly. The formation of protein fibrillar assemblies is critical in biology as they are implicated in important structural functions such as cytoskeleton formation. This involves mostly globular proteins that interact with each other through multiple assembly mechanisms to form fibrils [5]. In some cases, protein fibrils have amyloid or amyloid-like characteristics resulting from tight intermolecular hydrogen bonding and cross-β structure [6, 7]. Such structures are frequently associated to protein misfolding diseases as is the case of the amyloid β peptide and Tau, which are culprits in Alzheimer's disease. However, pathological self-assembly of globular protomers also occurs, as illustrated by polymerization of deoxyhemoglobin S, in sickle cell anemia [8, 9]. Amyloid fibrils are not necessarily toxic, and the so-called functional amyloids illustrate how the amyloid fold can be

implicated in diverse physiological functions in cells [10]. Therefore, protein self-association into elongated fibrils underscores multiple physiological functions as well as pathological threats to cells.

While toxic protein oligomerization is repressed from an evolutionary perspective through multiple strategies that encompass minimizing aberrant intermolecular interactions [11, 12], functional oligomerization has been positively selected as a strategy to regulate or enhance protein functions [13]. Such multimers - amyloid or not - allow proteins to form higher order oligomers, from low order quaternary assemblies to higher order filamentous structures. Examples include protein self-assembly mechanisms for concentration and natural storage such as those of the functional amyloids formed by pituitary peptide hormones in granules [14], to antagonize toxic self-aggregation as established for TDP-43, that forms physiological globular filaments in the nucleus [15], to increase local concentration and signaling activity as in the case of multi-protein signalosomes [16], or of S100 proteins whose diverse quaternary multimers allow tuneable activation of advanced glycation end products receptors (RAGE) [17].

In this respect, S100 proteins are interesting working models to investigate the molecular basis for oligomerization in both physiological and pathological contexts. S100 proteins are multifunctional signaling molecules, with intra- and extracellular functions which are implicated in multiple cellular processes, including signal transduction, cell differentiation, regulation of cell motility, proteostasis, and inflammation [18, 19]. For these reasons, S100 proteins have been implicated in several human pathologies, notably cancer, inflammatory diseases, and neurodegeneration [20-23]. This family of signaling Ca^{2+}-binding proteins comprises +20 members that are structurally conserved and occur mostly as homodimers. However, they are also found in tissues as higher order native multimers (tetramers, hexamers and octamers) [24, 25]. Under destabilizing conditions, S100 proteins form amyloid fibrils due to exposure of otherwise shielded aggregation prone regions [3, 24, 26, 27], whose eventual physiopathological relevance is still unclear. Furthermore, several S100 proteins evolved additional binding sites for Zn^{2+} and Cu^{2+} [19, 24]. Their pleiotropic functions therefore relate to expression levels, to the biochemical milieu of the expression sites (intra- or extracellular), to metal binding and quaternary structure.

S100A9 is abundant in the brain and has been found in diseased and aged tissues, in the form of punctiform histological inclusions in correlation with classical amyloid pathological hallmarks [1, 4, 28, 29], making it a robust biomarker of neurodegeneration, notably Alzheimer's Disease [30]. S100A9 has been implicated in spontaneous interconversion into amyloid due to an initial misfolding event and subsequent intermolecular β-sheet formation, with no observable lag phase [31, 32]. In the recent literature, it is described that S100A9 is able to form polymeric structures that resemble amyloid structures and bind to amyloid

fluorophores [31]. The polymerization reaction occurs through a two-step nucleation−autocatalytic growth model concentration dependent of α-helical S100A9 protein. The self-assembly demonstrates that initial misfolding and β-sheet formation, defined as "nucleation" step, spontaneously takes place within individual S100A9 molecules [31]. The impact of S100A9 oligomers or self-assemblies on memory was studied through intranasal administration of S100A9 (dimers, oligomers and fibrillar states) in aged mice. S100A9 oligomers and fibrils, but not dimers, evoked amnestic activity which is correlated with disruption of dopaminergic and glutamate neurochemistry in the prefrontal cortical and hippocampal regions [29, 33]. Additionally, intranasal administration of S1009 induces cellular stress in the frontal lobe, hippocampus, and cerebellum of aged mice, as well as impaired learning [29]. However, the underlying structural and molecular details of such processes remain enigmatic, and the characteristics of the fibrillar materials formed may differ from those of canonical amyloid fibrils. Here, we study the formation of S100A9 fibrillar self-assemblies combining chemical kinetics, nanoscopic analyses by electron and atomic force microscopies, DLS and spectroscopic approaches.

Under physiological conditions and high concentrations, we established that the natively folded S100A9 dimer self-assembles into worm-like protofibrils. We establish that S100A9 in these fibrils retains its native-like conformation, despite a slight increase in intermolecular β-sheets. We propose that this mode of self-assembly, so far unique to S100A9 among the S100 family, is related to a disordered C-terminal extension, found exclusively in this protein, which mediates self-assembly process into wormlike fibrils that lack the hallmark features of amyloid.

Functional amyloids

Amyloids are usually associated with disease state; however, in the past two decades it has become increasingly clear that amyloids can also play physiological roles. Amyloids are used by nature in multifaceted ways, occurring in bacteria, fungi, and mammals. Recent studies have deepened our understanding of the role of functional amyloids pay in these processes and the regulatory mechanisms that underlie them. Furthermore, functional amyloids may possess noncanonical supramolecular morphologies [34], being composed by relatively short peptide building blocks [35] [8], and assemble in response to environmental fluctuations [36]. There is a growing list of amyloids with functional properties which can be divided in chemical storage (such as different peptide hormones which are stored as inert amyloids inside secretary granules ready for activation), structure (includes amyloids that fulfill structural functions), information (like amyloids involved in epigenetic inheritance and

memory), loss-of-function (amyloids whose formation leads to loss of their activity in the soluble state) and signaling/gain-of-functions (activated on amyloid formation in different ways) [10]. Obviously, functional amyloids may belong to more than one group, because the amyloid structure by itself can have more than one function. Table 1 summarizes a list of functionally annotated amyloids, by group.

Table 1 – Functionally annotated amyloids

Amyloid	Organism	Soluble protein function	Amyloid Function	Refs
Group I – Chemical storage				
Peptide/protein hormones	mammals	Involved in hormone signaling	Sorting, storage and release of hormones	[35]
Major basic protein (MBP) (also group IV – loss-of-function)	mammals	Toxic in eosinophils destabilizes membrane of intruder/host in the oligomer state	Inerte storage of the toxic MBP	[36]
Inclusion body formation of many heterologous proteins when expressed	*Escherichia coli*	Various	Storing proteins inside secretory granules, possibly for detoxification	[37] [38]
Group II – Structure				
Curli (amyloid component: CsgA)	*E. Coli* (homolog in *Salmonella*)	Not known	Component of the extracellular matrix; involved in adhesion, biofilm formation, and invasion	[39]
Biofilm-associated proteins (Baps)	*Staphylococcus, Enterococcus, Salmonella, Pseudomonas, Acinetobacter*	Not known	Involved in primary attachment to surfaces and intracellular adhesion; host invasion; monitoring calcium and pH levels	[40]
Group III – Information				
Sup35 (also group IV – loss-of-function)	S.cerevisiae	Translation termination	Prion form is inactive (has a polyQ sequence alignment)	[41]
Poly-Q-expanded fragment of human huntingtin exon-1	*S.cerevisae*	Not known	Insoluble protein deposit formation	[42]
Group IV – loss-of-function				
Yeast pyruvate kinase Cdc19 (also group I – chemical storage)	S.cerevisiae	Pyruvate kinase	Stored inside stress granules; amyloid form in enzymatically inactive	[43]
Group V – Signaling/Gain-of-function				
HET-s prion	*Podospora anserina*	Not known	Prion form is active (oligomerization) involved in primitive immune system	[44]
Neuronal cytoplasmatic polyadenylation element-binding protein (CPEB)	*Aplysia* (CPEB)*Drosophila*	CPEB regulates messenger RNA (mRNA) translation	Long-term memory (has a polyQ sequence segment)	[44]
Necroptosis-related amyloid system RIP1/RIP3	mammals	Not known	Signaling and cell death of necroptosis (related to the HET-s system)	[45]

3. Materials and Methods

Materials. All reagents were of the highest grade commercially available. Thioflavin T (ThT) was obtained from Sigma. A Chelex resin (Bio-Rad) was used to remove contaminant trace metals from all solutions. S100A9 was expressed in Escherichia coli BL21(DE3) and purified to homogeneity using a previously established protocol[37, 38]. Apo S100A9 was prepared by incubation at 37 ºC for 2h with a 300-fold excess of Dithiothreitol (DTT) and 0.5 mM ethylenediamine tetraacetic acid (EDTA) and eluted in a Superdex S75 (GE Healthcare). S100A9 protein solutions were prepared and stored in 50mM Tris-HCl pH 7.4. Protein concentrations were determined spectrophotometrically using the extinction coefficient 13,980 $cm^{-1}.M^{-1}$ at 280 nm.

Electrophoresis. SDS polyacrylamide gel electrophoresis (PAGE) was carried in 12% Tris-Tricine gel. Protein sample was mixed with loading buffer in 1:1 ratio. The electrophoretic separation was conducted in a Mini protean II Electrophoresis system (BioRad) with two running buffers: cathode buffer (0.1M Tris, 0.1M Tricine, 0.1% SDS with pH 8.25) and anode buffer (0.2M Tris, pH 8.9). The voltage used was 150V. The standard protein marker was purchase from BioRad. Blue Safe solution (Nzytech) was used for staining.

Production of S100A9 multimers. S100A9 solution was incubated at 0.53 and 2.6mg/mL concentration in 50mM Tris-HCl, pH 7.4, 37°C, using a continuous agitation at 250rpm. S100A9 multimers were produced after 48h of incubation. The morphological parameters were studied by AFM imaging.

Analytical Size Exclusion Chromatography (SEC). Analytical SEC was performed at room temperature on a Superdex 75 Tricorn high performance column (GE Healthcare, V_{column} = 24mL) connected to an AKTA Purifier UPC-10 system and run at 1ml/min. The column was calibrated with proteins of known molecular weight: apoprotein (6.5kDa), cytochrome c (11.8kDa), ribonuclease A (13.7kDa), carbonic anhydrase (29kDa), ovalbumine (44kDa) and conalbumine (75kDa). 500µl of S100A9 incubated different times at 0.53mg/mL and 2.6mg/mL, 250rpm, was applied and run at pH 7.4: running buffer was 50mM Tris-HCl (chelex water) pH 7.4.

S100A9 aggregation kinetics Aggregation kinetics was performed by recording the ThT fluorescence intensity as a function of time in a plate reader (Fluostar Optima, BMG Labtech) with a 440 nm excitation filter and a 480 nm emission filter. The fluorescence was recorded using bottom optics in half-area 96-well polyethylene glycol-coated black polystyrene plates with a clear bottom (Corning, 3881). Briefly, different concentrations of S100A9 apo were

diluted in 50mM Tris-HCl, pH 7.4, 5mM TCEP and 0.5mM EDTA or Calcium, and a ratio of ThT: protein of 2:1 was used for each condition. For the Zinc assays, final S100A9 protein concentration was 0.53mg/mL, with a ratio of zinc:protein of 1-12:1. The assays were performed at 37°C, with 86rpm agitation cycles of 20s before each acquisition. Aggregation kinetics of S100A9 in the presence of different zinc ratios was determined spectrophotometrically by measuring the absorbance at 360nm at the endpoint reactions of S100A9: Zinc ThT fluorescence assay.

Circular Dichroism (CD) Spectroscopy CD measurements and kinetics were performed on a JASCO J-1500 spectropolarimeter equipped with a Peltier-controlled thermostatic cell support. Far-UV CD spectra (200-260nm) were acquired using 5nm/min scan speed and 1nm resolution and recorded at 20µM S100A9 with or without 80 µM $CaCl_2$ or $ZnCl_2$ in 50 mM Tris pH7.4. Quartz cells had 1mm optical path.

Dynamic Light Spectroscopy (DLS). DLS measurements were performed on a Zetasizer Nano (Malvem) DLS instrument by scattering light at 630bn and under 173° angle. 20µM S100A9 in 50mM Tris-HCl pH 7.4 was subjected to five repetitive measurements. Hydrodynamic diameter was evaluated from the autocorrelation curves fitted with manufacturer's software and molecular weight was calculated by Protein Utilities program provided by the manufacturer.

Monomer release assay. For monomer release assay, S100A9 multimers were formed upon incubation of 0.53mg/mL in the presence of times calcium, in 50mM Tris-HCl, pH 7.4, 48h at 37°C, using a continuous agitation at 250rpm. After formation, multimers were isolated by SEC. Multimers fraction was introduced into a 50 kDa MWCO dialysis membrane against 20mM Tris-HCl pH 7.4, using stirring 200rpm at 4°C. For 14 days, absorbance was measured at 280nm, Trp fluorescence at 340nm, and dot blot intensity of the inner and outer part at the endpoint. All values were plotted against dialysis time (days). A negative control was used with buffer 20mM Tris-HCl pH 7.4 instead of the multimers. Presented data is a mean between four individual assays.

4. Results and Discussion

4.1. Spontaneous formation of S100A9 polymers and effect of Ca^{2+}-binding

To investigate the spontaneous formation of S100A9 fibrillar aggregates, we incubated purified apo S100A9 at 37°C and pH 7.4 under mild agitation (250 rpm) for up to 48h (Fig 1A). During this period, we observed no concurring precipitation, as denoted by the lack of increased light scattering and no pellet upon end-point centrifugation. To verify oligomer formation, we employed size-exclusion chromatography (SEC) and observed a new band eluting above the column cut-off, corresponding to a high molecular weight species, in addition to that of the S100A9 dimer (Fig. 1B). Bioimaging analysis combining atomic force microscopy (AFM) and transmission electron microscopy (TEM) showed that the species present in the two SEC bands correspond, respectively, to globular S100A9 native dimers and to fibrillar aggregates that we coin as worm-like (Fig. 1C). To unravel the inner structural properties of the fibrillar multimers, we carried out circular dichroism (CD) analysis to investigate the structural features of the filaments. The properties of the S100A9 fibrils were compared to those of the S100A9 dimer, whose far-UV CD spectrum is typical of the α-helical S100 protein fold, with minima at 222 and 208nm (Fig. 1D).

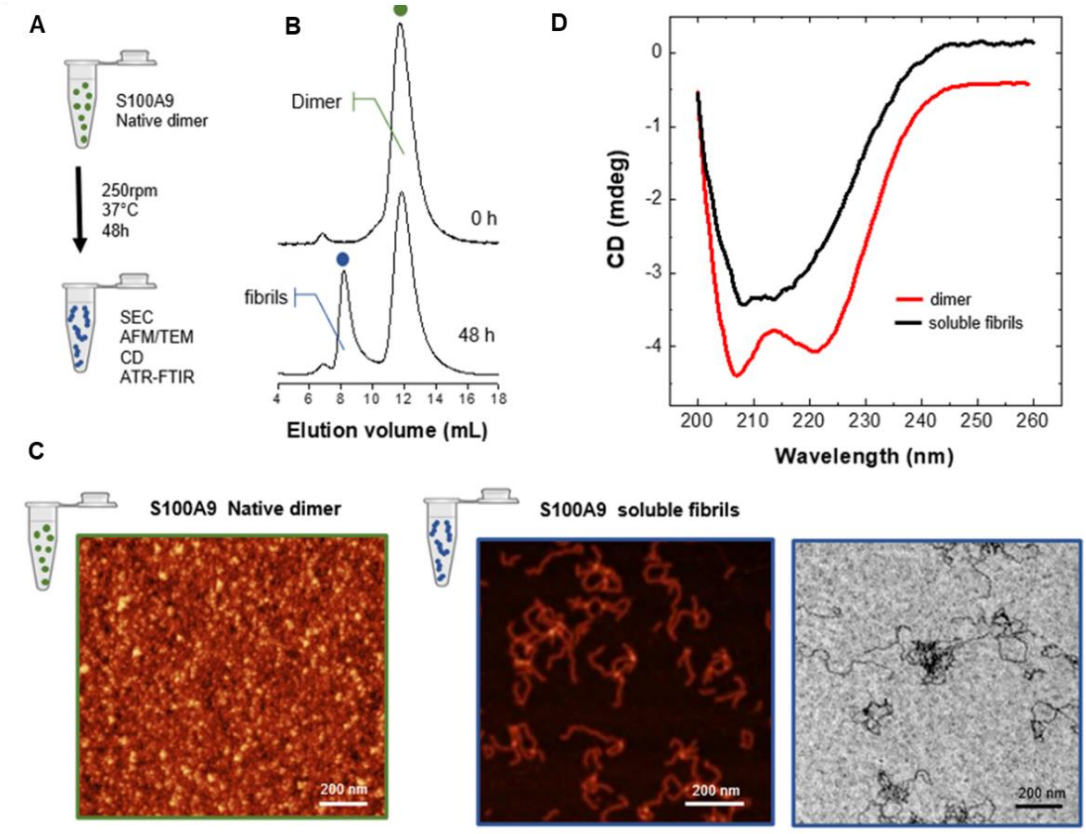

Figure 1 – Structural analysis of S100A9 fibrils formed under physiological conditions. **(A)**S100A9 self-assembly reaction protocol; **(B)** SEC resolution of S100A9 oligomers formed after 48h of reaction; **(C)**

Bioimaging analysis of S100A9 SEC high molecular weight worm-like fibrils (blue frames) and dimers (green frame) by TEM (top panel) and AFM (two bottom panels).

We next set to determine if Ca^{2+} binding to S100A9 influences the formation of fibrillar multimers. For that we monitored the self-assembly reaction of S100A9, in the presence and in the absence of Ca^{2+} in physiological conditions (37 °C, pH 7.6) for up to 144h. Using AFM, we established that, in both cases, fibrils with similar morphologies are formed (Fig. 2A). This observation is compatible with the fact that Ca^{2+}-binding has no destabilizing effect on S100A9, as the protein thermal stability with Ca^{2+}-bound (T_m ~ 85 °C) is even higher than that of the apo form (T_m ~ 73 °C) (Fig. 2B). Therefore, in our experiments and in both conditions, S100A9 fibril formation does not involve any Ca^{2+}-induced destabilization event. We then used SEC to assess the kinetics of the formation of the fibrillar oligomers and, from the obtained SEC profiles, we also noted that Ca^{2+}-binding does not influence the aggregation rate (Fig. 2C, D). Given that soluble higher-order fibrils are promptly formed without noticeable accumulation of intermediary oligomers, we conclude that fibril assembly proceeds through assembly of native S100A9 dimers (Fig. 2C, D). AFM analysis of the species formed at different time points along the fibrillation reaction at 15, 24 and 72h (Fig. 2F) reveals that worm like S100A9 fibrils are rapidly formed and that their morphology gets increasingly complex with no observation of straight fibrils.

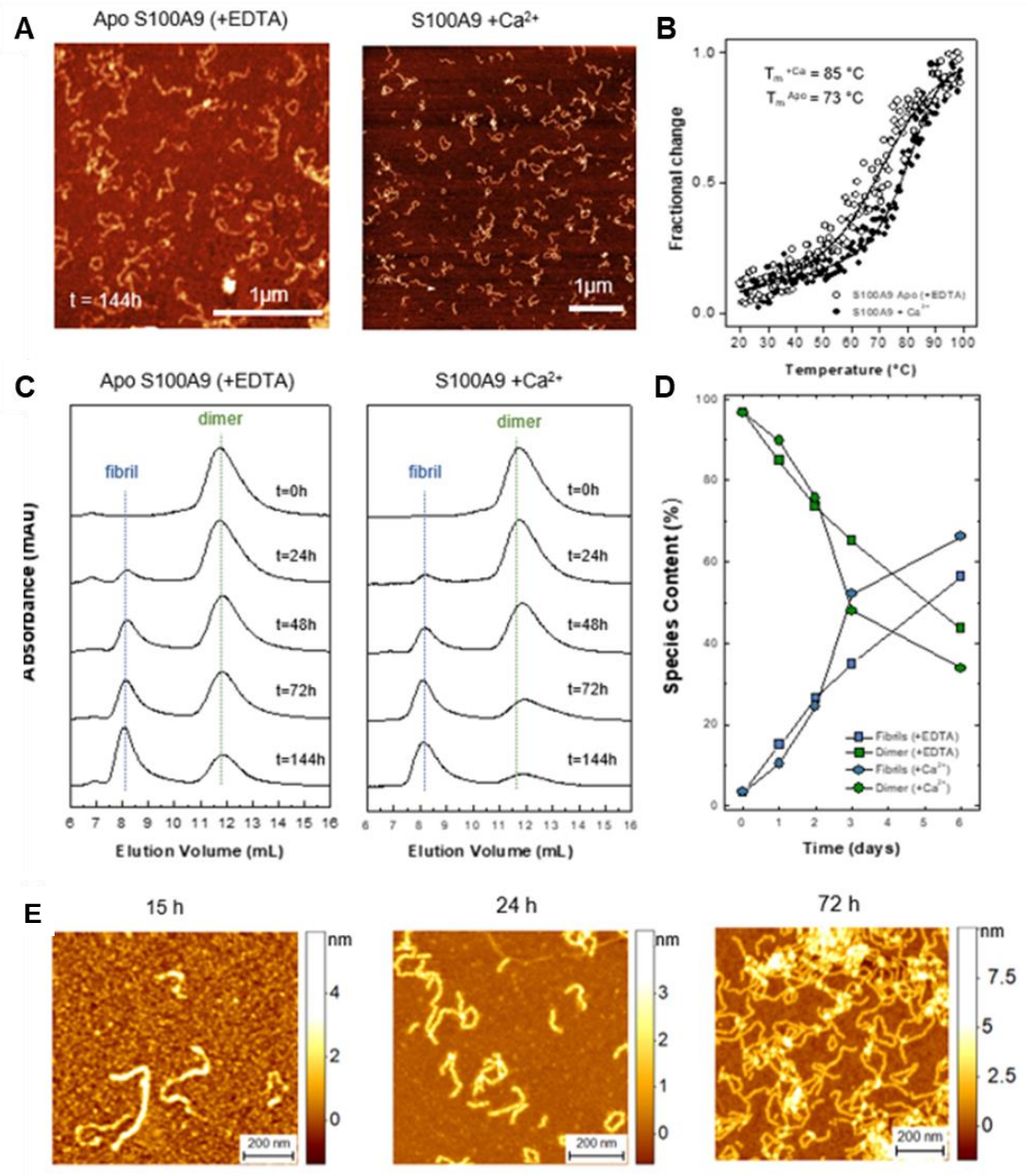

Figure 2 – The morphology of S100A9 worm-like fibrils is marginally influenced by Ca^{2+}-binding. **(A)** AFM topography images of end point filaments formed in both conditions examined after 144h incubation at 37°C pH 7.6; **(B)** Thermal denaturation profiles of apo and Ca^{2+}-S100A9 determined from CD analysis at 222nm; **(C)** SEC chromatogram analysis of oligomer formation by apo and Ca^{2+} bound S100A9 up to 144h; **(D)** Kinetics of formation of S100A9 fibrils and analysis of the relative S100A9 populations showing that a decrease in dimers directly corresponds to an increased in fibrils; **(E)** AFM maps of at different time points illustrating increasing complexity of assembled fibrils

Increased molecular weight of S100A9 assemblies along time is also corroborated by DLS analysis, in Fig. 3. We have measured an average molecular diameter around 4nm for both apo apo and Ca-bound S100A9. This hydrodynamic diameter corresponds to the reported diameter of the dimer S100A9 as in the PDB entry 5I8N. Even thought, it has been previously reported that Ca^{2+} enhances the oligomerization of S100s into high-ordered polymers [24], which increase in size is time-dependent. As we can observe, in the absence and in the presence of calcium the formation of high-ordered species occurs over time. After 5h, apart from dimeric S100A9, we also detect larger species with around 100 nm diameter (Fig. 3A, B) and upon 20h we have a mixture of species ranging from the dimers to species at around 100 nm and even 4000 nm, which can be insoluble aggregates.

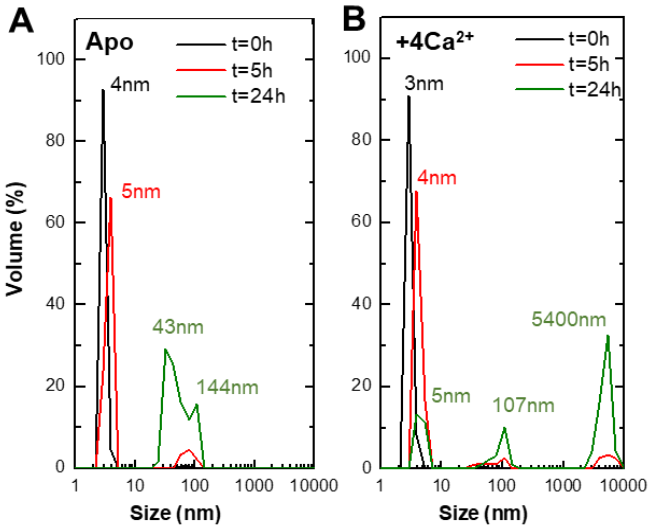

Figure 3 –S100A9 soluble self-assembly structures have high molecular weight. Dynamic Light Scattering (DLS) assay of *in vitro* S100A9 self-assembly structures measurements of S100A9 in apo form (A), in the presence of four-times calcium (B) with 0h, 5h and 20h of incubation times, at pH 7.4. Representative distributions of multiple samples analysed.

4.2. S100A9 polymers are not disulphide crosslinked

To probe the nature of the S100A9 fibrils, we investigated the possible involvement of intermolecular disulfide bonding in the formation of the S100A9 fibrillar multimers, through the single Cys-3 residue present in S100A9, an amino acid which contains a thiol group. For that, we analyzed the S100A9-C3S mutant and determined that the self-assembly reaction also takes places, yielding worm-like fibrillar multimers identical to those obtained for wild type S100A9, thus excluding the involvement of disulfide bonds in these species (Fig. 4).

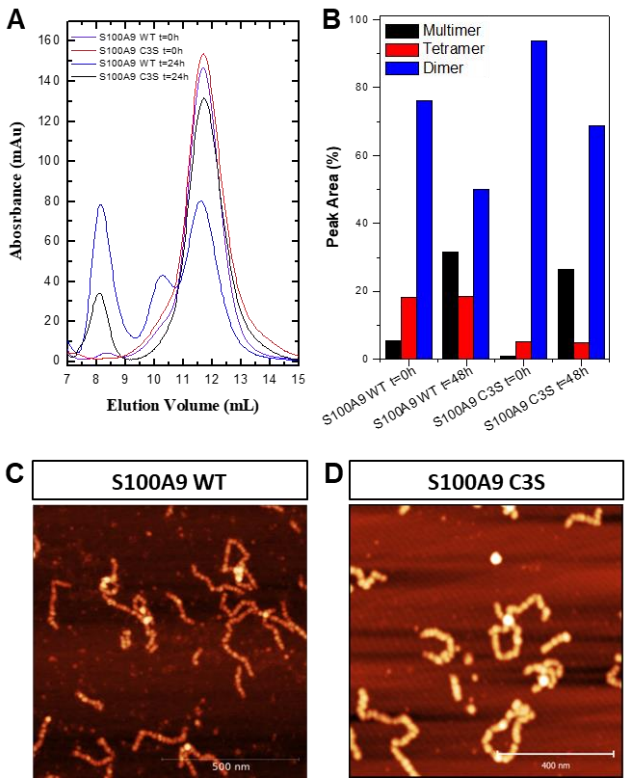

Figure 4 –S100A9 multimers are not disulfide-linked dependent. S100A9 C3S mutant forms multimers upon incubation in physiological conditions as the WT. SEC **(A)** and bars quantification content **(B)** after incubation of 2.5mg/mL of protein for 24h, 37°C and 250rpm. AFM images of the multimers after SEC for S100A9 WT **(C)** and mutant **(D)**.

Altogether, findings in this section show that the spontaneous self-assembly of S100A9 dimers into fibrillar multimers is not dependent of Ca^{2+} binding and does not involve intermolecular disulfide bonding. Multimers also do not depend on electrostatic interactions as high salt concentrations (up to 1 M NaCl) did not abolish their formation (Fig. 5). The observation that S100A9 worm-like polymers are formed reversibly from S100A9 dimers, and that they are protease and SDS sensitive, contrasts with the highly stable and irreversible nature of canonical amyloid fibrils.

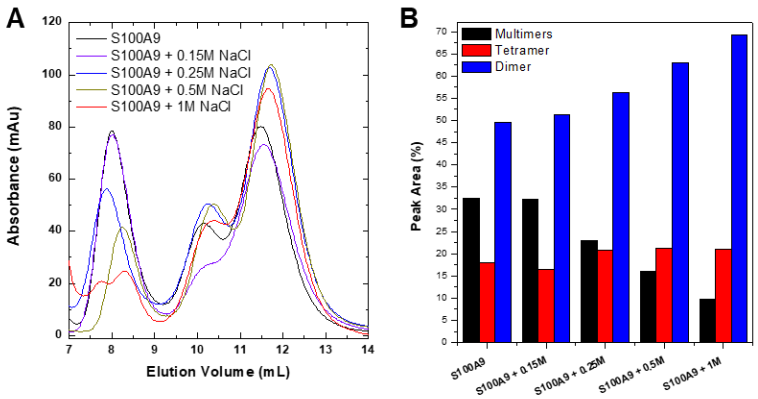

Figure 5 –S100A9 multimeric self-assemblies do not have an electrostatic character. S100A9 protein was incubated with different concentrations of sodium chloride, 0-1M, and incubated in physiological conditions. SEC **(A)** and bars quantification content **(B)** after incubation of 2.5mg/mL of protein for 24h, 37°C and 250rpm.

4.3. S100A9 polymers bind Amyloid-specific fluorophores

To obtain information about the amyloidogenic character of S100A9 multimers (self-assemblies), different fluorescent dyes were used. ThT and ANS are the most used dyes to follow amyloid formation and here, we used other fluorophores such as oligothiophenes (LCOs – Luminescent Conjugated Oligothiophenes – p-FTAA and h-FTAA). LCOs are recent and innovative amyloid specific dyes used to detect non-thioflavinophilic amyloid aggregated species [39].

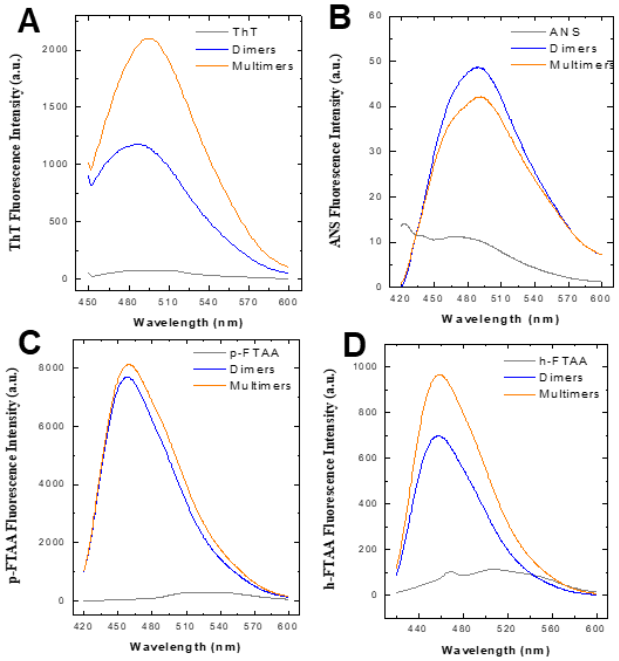

Figure 6 –S100A9 self-assembly structures have a smooth amyloidogenic character. Different fluorescence dyes, Thioflavin-T **(A)**, ANS **(B)**, and oligothiophenes p-FTAA **(C)** and h-FTAA **(D)** were used to characterized S100A9 multimers and dimer. Measurements were performed with 0.04mg/mL of multimers/dimers

of S100A9. Incubation, pre-SEC, were performed at 2.5mg/mL of protein in 50mM Tris-HCl chelex pH 7.4, 37°C, 24h with agitation 250rpm.

The usage of different fluorescent dyes for dimers and multimers of S100A9 shows that there are almost no differences in intensity between the two of them (Fig 6). ThT fluorescence is the one that shows more differences: In one hand, ThT is known to report the formation of β-sheet-rich aggregates which shows intensive fluorescence upon intercalation into stacked β-sheets that form during aggregation [34]. In the other hand, ThT may also bind as excited dimers ("excimers") to large hydrophobic cavities within fibrils, as occurs for S100 proteins [40]. This observed enhancement of ThT bound to multimers means that these assemblies promote the opening of hydrophobic cavities in S100A9 oligomer, allowing the binding of ThT.

S100A9 multimers present some amyloidogenic character by the ThT and h-FTAA binding experiments. In fact, quantitative analysis of the ATR-FTIR spectra of the S100A9 dimers and fibrils shows a noteworthy difference. Spectrum of the fibrils shows a clear and distinct shoulder at ~1620 cm^{-1} in the Amide band I, which is the typical spectral feature characteristic of intermolecular β-sheets and H-bonding in amyloid-like self-assemblies [41-44] (data not shown). This content of intermolecular β-sheet increases from 5 ± 5% in the case of dimers to 30 ± 5% in the case of the flexible fibrillar aggregates, at the expense of an equivalent loss in native α-helix structure. Thus, overall, the nanoscopic and spectroscopic data prove the formation of highly flexible fibrillar (worm-like) aggregates, which are stabilized by a tight network of intermolecular H-bonding and β-sheets.

4.4. Kinetic analysis of S100A9 polymerization and effect of Zn^{2+}-binding

To evaluate the amyloidogenicity of S100A9, we incubate the protein at 5-200µM at 37°C and followed the Thioflavin-T (ThT) kinetics at physiological pH7.4 in the absence and presence of 4xCa^{2+} (Fig. 7A, B). ThT is a fluorescence dye that is frequently used for monitoring the amyloid formation by proteins and peptides [45]. Emission intensity of ThT dye monitored at 480nm (excitation at 450nm) increases when it binds to cross β-sheet structure of amyloids.

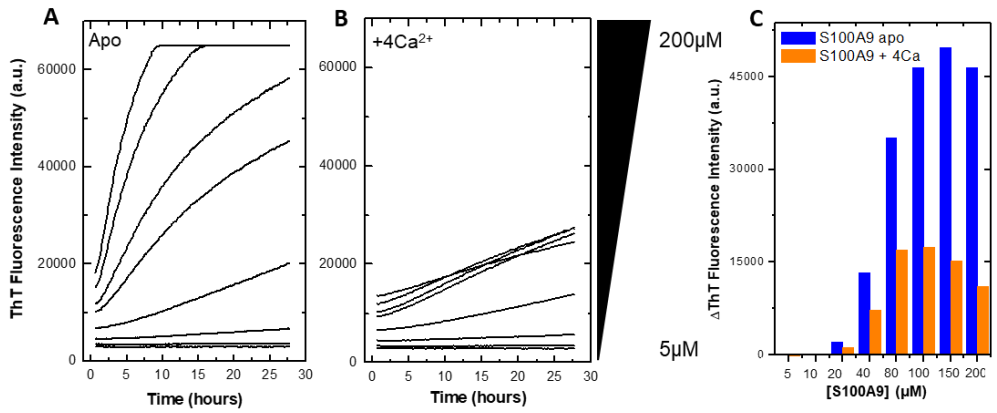

Figure 7 – Amyloidogenic character of S100A9 in a concentration dependent manner. S100A9 in apo form **(A)** and 4 times calcium binding **(B**) in 50mM Tris-HCl chelex pH7.4. Protein used at increasing concentration, between 5μM-200μM, 37°C, 24h with agitation 86rpm, 20sec before cycle. Plots represent averaged intensity curves obtained from three independent replicates for each of the tested conditions. **(C)** Plot of the ThT intensity at the endpoints of the aggregation of S100A9 shown in A and B.

We found that S100A9 in the apo form forms ThT-positive reactive species in a concentration-dependent manner but no lag phase was observed, which reflects an instantaneous nucleation process and may suggest that S100A9 are able to form nuclei directly from their soluble dimer conformation [46]. On the other hand, in the presence of 4xCa^{2+}, ThT reactive species have much lower intensity, suggesting some molecular rearrangement differences between the formed multimers during oligomerization process. Fig. 7C plotted the ThT intensity of the end-point reaction for both incubations.

Protein misfolding conformational changes are a mainstay of neurodegenerative diseases involving formation and deposition of toxic protein oligomers, which can be favored by dysregulations of labile metal ions within the cellular environment. Metal ions such as calcium, zinc and copper are key players in brain neurobiology, their homeostasis is altered in most neurodegenerative conditions, and they are found within proteinaceous inclusions from patients [47]. Considering that S100A9 is a calcium-binding protein and the fact that metal ions play essential roles in the brain and there is evidence about their homeostatic dysfunction across different neurodegenerative disorders [47], we first postulated that metal-ions may interfere with S100A9 aggregation processes. Calcium, as well as zinc binding, have been shown to induce conformational changes within S100 proteins leading to the exposure of hydrophobic surfaces, that may allow interaction with the target protein [48].

Circular dichroism (CD) spectra showed an α-helical conformation of S100A9 with no incubation, in the absence or presence of calcium, Fig. 8A. In the presence of Zinc, S100A9 immediately starts to lose its native conformation, accompanied by spectral band broadening and a slight shift of the minimum to 210nm. Right upon incubation, zinc destabilizes the native

structure causing S100A9 to precipitate into insoluble aggregates (Fig. 8), and effect which is also noted monitoring CD changes at 222nm (Fig. 8B). In contrast, incubation for 48h at 37°C maintained apo S100A9 in the native form with soluble oligomers being formed as confirmed by SEC of the endpoint incubation product (Fig. 8C) where different components can be separated. The same was observed for Ca-bound S100A9, with no changes in CD signal at 222 nm.

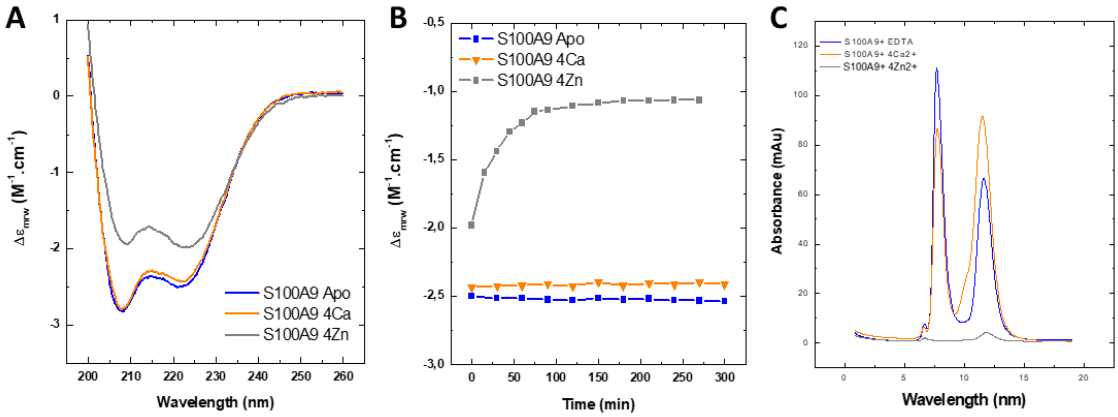

Figure 8 – S100A9 protein forms oligomeric species maintaining its α-helical conformation upon incubation. (A) CD spectra of S100A9 in the absence (blue) and presence of calcium (orange) and zinc (grey) with no incubation; **(B)** CD kinetics during incubation, plotted the 222nm wavelength with time at 37°C and in absence (blue) and presence of metal-ions, S100A9+4Ca^{2+} (orange), and S100A9+4Zn^{2+} (grey and purple) and **(C)** SEC analysis after S100A9 homodimer the incubation 24h with the metal-ions, 37°C. Spectrum obtained from 0.25mg/mL protein samples dissolved in 50mM Tris-HCl buffer pH 7.4.

Focusing our attention on Zinc, and knowing that S100B protein acts as a zinc metallochaperone by suppressing $A\beta_{42}$ oligomerization [49], we investigated how S100A9 behaves in the presence of zinc. Although in the presence of calcium S100A9 does not change its conformation and is not amyloidogenic upon incubation, in the presence of zinc, an inverse scenario in observed. Upon addition of Zn^{2+}, S100A9 immediately precipitates producing a concentration-dependent decrease in α-helix content, once there are only two Zn^{2+}-binding sites, coordinated by residues from two homodimers. Zn^{2+} is also reported to influence the degree of oligomerization associated with a decrease in secondary structure content [50], Fig. 8A. Binding of Zn^{2+} occurs invariably at the dimer interface, involving coordination residues formed by HEXXH motives from both subunits that are close to the dimer interface, being able to bound two Zn^{2+} ions per homodimer [38].

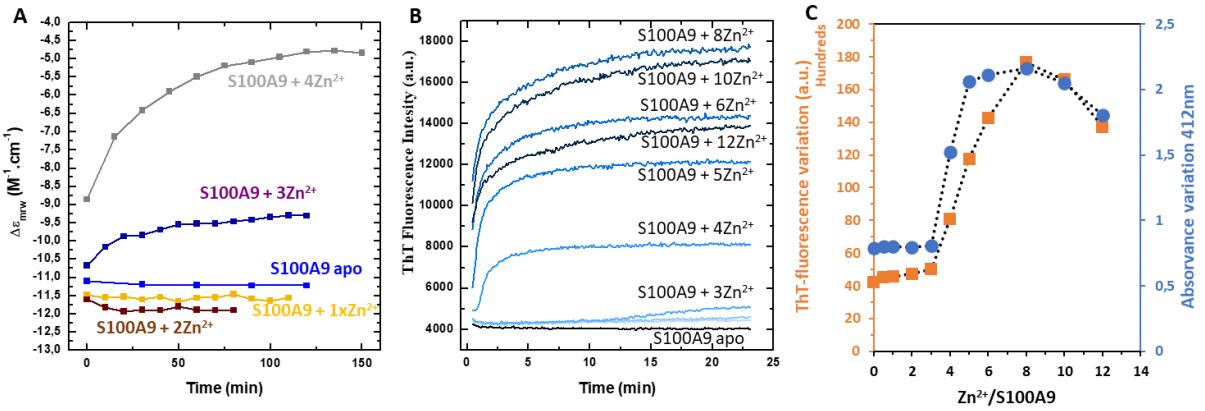

Figure 9 – Zinc induces conformational changes in S100A9 and forms ThT-reactive species. Zinc binding kinetic curves for S100A9 in increasing Zinc molarity. **(A)** CD kinetics during incubation, plotted the 222nm wavelength with time at 37°C in the presence of 1-4 times zinc equimolar to S100A9. **(B)** S100A9 zinc-dependent (0-14 equimolar) ThT fluorescence kinetics and **(C)** ThT intensity (orang squares) and turbidity kinetics (blue circles) at the endpoint of the reaction plotted with the equimolar of zincs. Turbidimetry measured at absorbance of 412nm at 20h in function of zinc molecules per S100A9 dimer. Protein used at 0.5mg/mL, pH 7.4, 37°C with agitation 86rpm, 20sec before cycle.

Generally, dimeric S100A9 protein binds four Ca^{2+} ions per dimer while there are just two putative sites for Zn^{2+} [24]. In contrast with calcium (Fig.9), the presence of Zn^{2+} enhances ThT intensity meaning that there are ThT-positive species formed with time. ThT is known to report the formation of β-sheet-rich aggregates which shows intensive fluorescence upon intercalation into stacked β-sheets that form during aggregation [40]. A zinc-dependent kinetic was performed to study the impact of zinc at different stoichiometries, Fig. 9C. These experiments show that above $4xZn^{2+}$:S100A9 there is a concentration-dependent enhancement of ThT fluorescence intensity and turbidity, meaning that are being formed ThT-reacting and insoluble aggregates (macroscopically appeared as a white precipitate). For ratios up to $4xZn^{2+}$/S100A9, there are no significant variations neither of ThT intensity or turbidity, which may be due to the Zn^{2+} nonspecific binding to the four coordinated Ca^{2+}-specific binding sites of the S100A9 homodimer. Zn^{2+}- ions might bind not exclusively to specific zinc-binding sites but may interact also with other sites [38].

4.5. S100A9 fibrillar polymers disassemble into dimeric S100A9

To probe the nature of the S100A9 fibrils, we subsequently assessed their resistance to degradation, which is a hallmark of canonical amyloid fibrils. Unlike amyloids, we determined that S100A9 fibrils are sensitive to proteinase K digestion and migrate as monomers in SDS-PAGE (data not shown), with no noticeable evidence for high molecular weight species. Also,

we performed dilution/dialysis experiments (Fig. 10) and observed that the S100A9 worm-like fibrils revert to soluble S100A9 dimers, indicating that their assembly is reversible.

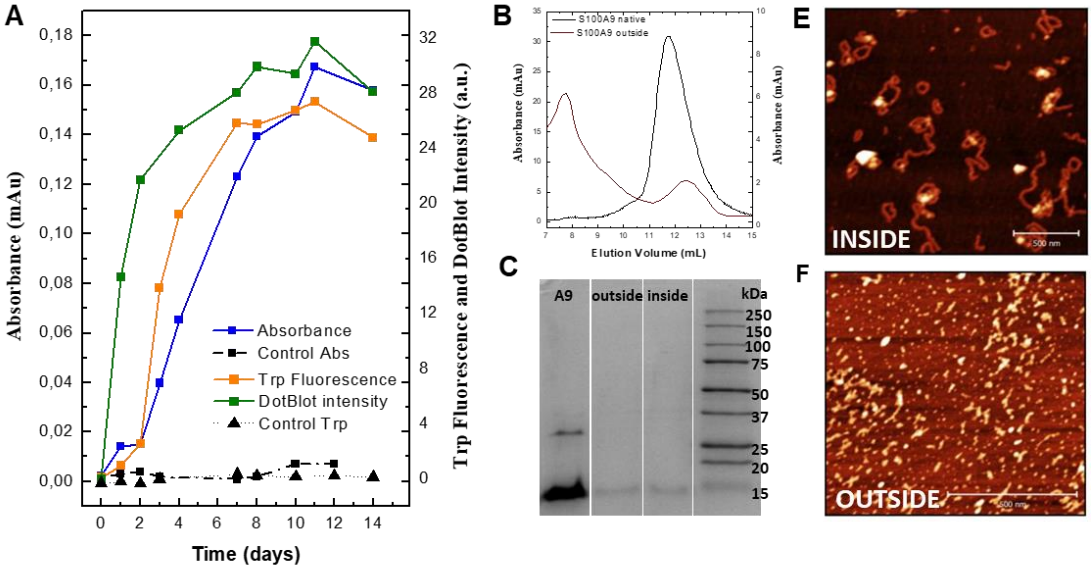

Figure 10 – **S100A9 dimers are released from S100A9 fibrils along time. (A)** Increment in absorbance at 280nm(blue), Trp fluorescence in 340nm (orange) and in dot blot intensity (green) of solution outside de dialysis membrane denoting releasing of building-blocks of S100A9 (n=4) and the respective negative controls (black). **(B)** SEC of the solution outside the membrane at the endpoint of the assay. **(C)** SDS-PAGE of the solutions inside and outside the membrane at the endpoint of the assay, as well as the native S100A9 as a control. AFM topography images of end point of dialysis inside **(E)** and outside **(F)** of the membrane.

Immediately on the first day we can observe an enhancement in absorbance and Trp fluorescence in the outer part of the membrane, and the values increased until the day eleven, meaning that S100A9 protein are being released from the multimers, over time. To make sure that the enhancement is due to the release of the S100A9, we performed a dot blot assay using S100A9-antibody, Fig. 11, and we can observe that the signal is specific for S100A9 and is in accordance with the obtained results. The behavior of the three curves is similar, and we can conclude that S100A9 building blocks are being released from the multimers with time. To confirm the presence of S100A9 in both compartments we performed SDS-PAGE gel and to check the molecular weight and the morphology of the species that were present in the outer part we ran a SEC and we did AFM, respectively (Fig. 10E, F). SEC chromatogram from the outer part suggests that we are in the presence of dimers with approx. 33 kDa, which is very close to the reported molecular weight 26 kDa [38].

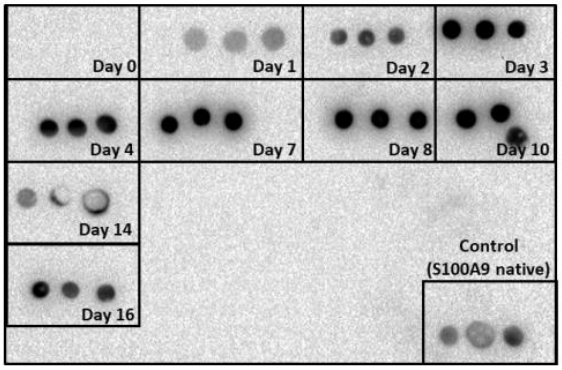

Figure 11 – **S100A9 multimers release assay**. Dot blot assay using S100A9-antibody. Sample were deposited day-by-day and then incubated with specific antibody.

4.6. S100A9 C-terminus mediates polymer assembly

Interestingly, the formation of this type of filament seems to be limited to S100A9 and not to other members of the S100 protein family. The premise derived from our observations is that this is due to unique structural characteristics of S100A9, namely disordered C-terminal (with IDP character) extension of ~20 residues which is absent in other proteins from this family and a less stable fold, that altogether favor permissive conformational excursions of the native state that populate assembly-competent conformers. As a proof of concept, we expressed and purified the truncated S100A9 C3S, with deletion of ca. 90 base pairs at C-terminal, Fig. 11A. The mutation at the cysteine was maintained to exclude eventual self-assembly through disulphide bounds.

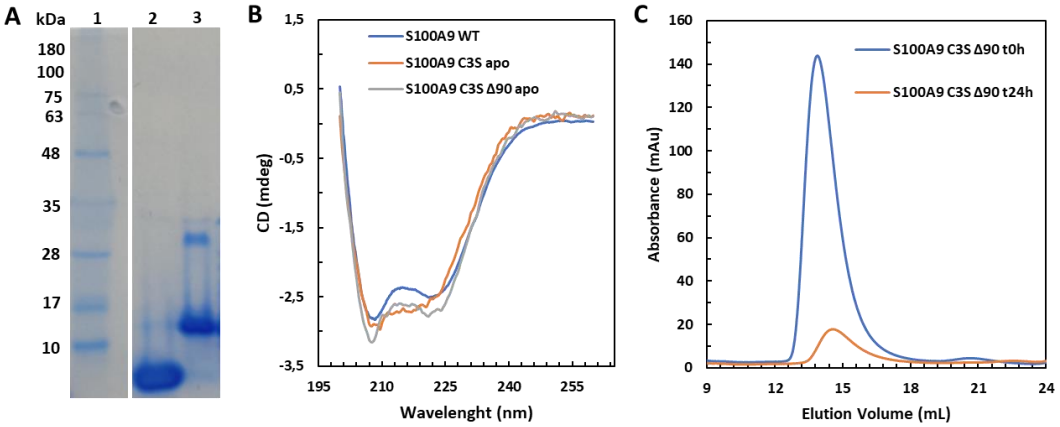

Figure 11 – **Truncated S100A9 C3S does not form self-assemblies upon incubation.** Purified truncated mutated S100A9 C3S (S100A9 C3S Δ90) **(A)** has a CD spectrum like the native S100A9 and the mutated S100A9 C3S (B) with composed by the characteristic α-helical content. **(C)** SEC analysis after S100A9 C3S Δ90 homodimer 24h incubation with no metal ions, at 37°C. Samples were dissolved in 50mM Tris-HCl buffer pH 7.4.

Truncated mutated S100A9 – S100A9-C3S-Δ90 – has the same fold as native S100A9, as observed by CD spectra in Fig. 11B. C-terminal amino acids are not required to reach the

α-helical fold characteristic of S100A9. In order to study the importance of the C-terminus in the formation of self-assemblies, S100A9 C3S Δ90 was incubated in the same conditions used for the WT, Fig. 1A, B. SEC analysis, Fig. 11C, revealed that C-terminal is essential for the formation the polymers. Upon incubation, most of the protein precipitates, and there is no formation of larger oligomers. Thus, our data suggests that the C-terminal may be a mediator of dimeric S100A9 polymerization. Once S100A9 is the only member of the family that have this longer C-tail, it gives to S100A9 a unique characteristic that can result in this unique structural feature.

5. Conclusion

S100A9 is a protein implicated in neurodegeneration. It is highly present in AD brains and has been shown to be a relevant AD biomarker. In this work, we have shown that S100A9 forms fibrillar self-assemblies which maintain a native-like conformation. We demonstrated the spontaneous formation of S100A9 polymers and that Ca^{2+}-binding has no effect on the process. Kinetic analysis of S100A9 polymerization shows that Zn^{2+}-binding enhances aggregation but S100A9 immediately precipitates producing a concentration-dependent decrease in α-helix content. Interestingly, S100A9 polymers bind amyloid-specific fluorophores but these properties do not necessarily reflect the formation of canonical type amyloids. The fact that the S100A9 fibrillar polymers disassemble into dimeric S100A9 upon dialysis shows that these polymers are not truly amyloid but rather likely result from stacking of native-like S100A9 proteins. One aspect that may be relevant to elucidate this self-assembly process is the C-terminus extension of 20 amino acid residues, that is exclusive to S100A9 among members of the S100 protein family. Indeed, we generated a truncated deletion variant without the C-terminus extension and found that, although S100A9 is still expressed and folded, once purified it does not polymerize but forms amorphous aggregations. Future research will uncover the molecular and structural underpinnings of this process, which may be an important mechanism for storage of S100A9 in tissues.

6. References

1. Wang, C., et al., *S100A9-Driven Amyloid-Neuroinflammatory Cascade in Traumatic Brain Injury as a Precursor State for Alzheimer's Disease.* Sci Rep, 2018. **8**(1): p. 12836.
2. Horvath, I., et al., *Co-aggregation of pro-inflammatory S100A9 with alpha-synuclein in Parkinson's disease: ex vivo and in vitro studies.* J Neuroinflammation, 2018. **15**(1): p. 172.
3. Yanamandra, K., et al., *Amyloid formation by the pro-inflammatory S100A8/A9 proteins in the ageing prostate.* PLoS One, 2009. **4**(5): p. e5562.
4. Wang, C., et al., *Proinflammatory and amyloidogenic S100A9 induced by traumatic brain injury in mouse model.* Neurosci Lett, 2019. **699**: p. 199-205.
5. McPartland, L., et al., *Atomic insights into the genesis of cellular filaments by globular proteins.* Nature Structural & Molecular Biology, 2018. **25**(8): p. 705-714.
6. Makin, O.S. and L.C. Serpell, *Structures for amyloid fibrils.* The FEBS Journal, 2005. **272**(23): p. 5950-5961.
7. Knowles, T.P.J. and M.J. Buehler, *Nanomechanics of functional and pathological amyloid materials.* Nature Nanotechnology, 2011. **6**(8): p. 469-479.
8. Wishner, B.C., et al., *Crystal structure of sickle-cell deoxyhemoglobin at 5 Å resolution.* Journal of Molecular Biology, 1975. **98**(1): p. 179-194.
9. Pauling, L., et al., *Sickle Cell Anemia, a Molecular Disease.* Science, 1949. **110**(2865): p. 543.
10. Otzen, D. and R. Riek, *Functional Amyloids.* Cold Spring Harb Perspect Biol, 2019. **11**(12).
11. Ulamec, S.M., D.J. Brockwell, and S.E. Radford, *Looking Beyond the Core: The Role of Flanking Regions in the Aggregation of Amyloidogenic Peptides and Proteins.* Frontiers in Neuroscience, 2020. **14**(1216).
12. Beerten, J., J. Schymkowitz, and F. Rousseau, *Aggregation prone regions and gatekeeping residues in protein sequences.* Curr Top Med Chem, 2012. **12**(22): p. 2470-8.
13. D'Alessio, G., *The evolutionary transition from monomeric to oligomeric proteins: tools, the environment, hypotheses.* Progress in Biophysics and Molecular Biology, 1999. **72**(3): p. 271-298.
14. Maji, S.K., et al., *Functional Amyloids As Natural Storage of Peptide Hormones in Pituitary Secretory Granules.* Science, 2009. **325**(5938): p. 328.
15. Afroz, T., et al., *Functional and dynamic polymerization of the ALS-linked protein TDP-43 antagonizes its pathologic aggregation.* Nature Communications, 2017. **8**(1): p. 45.
16. Raskatov, J.A. and D.B. Teplow, *Using chirality to probe the conformational dynamics and assembly of intrinsically disordered amyloid proteins.* Sci Rep, 2017. **7**(1): p. 12433.
17. Ostendorp, T., et al., *Structural and functional insights into RAGE activation by multimeric S100B.* Embo Journal, 2007. **26**(16): p. 3868-3878.
18. Heizmann, C.W., *The multifunctional S100 protein family.* Methods Mol Biol, 2002. **172**: p. 69-80.
19. Donato, R., et al., *Functions of S100 proteins.* Curr Mol Med, 2013. **13**(1): p. 24-57.
20. Bresnick, A.R., D.J. Weber, and D.B. Zimmer, *S100 proteins in cancer.* Nature Reviews Cancer, 2015. **15**(2): p. 96-109.
21. Austermann, J., C. Spiekermann, and J. Roth, *S100 proteins in rheumatic diseases.* Nature Reviews Rheumatology, 2018. **14**(9): p. 528-541.
22. Cristóvão, J.S. and C.M. Gomes, *S100 Proteins in Alzheimer's Disease.* Frontiers in Neuroscience, 2019. **13**(463).
23. Gonzalez, L.L., K. Garrie, and M.D. Turner, *Role of S100 proteins in health and disease.* Biochimica et Biophysica Acta (BBA) - Molecular Cell Research, 2020. **1867**(6): p. 118677.
24. Fritz, G., et al., *Natural and amyloid self-assembly of S100 proteins: structural basis of functional diversity.* FEBS J, 2010. **277**(22): p. 4578-90.
25. Cristóvão, J.S., et al., *Cu2+-binding to S100B triggers polymerization of disulfide cross-linked tetramers with enhanced chaperone activity against amyloid-β aggregation.* Chemical Communications, 2020.
26. Carvalho, S.B., et al., *Intrinsically disordered and aggregation prone regions underlie beta-aggregation in S100 proteins.* PLoS One, 2013. **8**(10): p. e76629.
27. Carvalho, S.B.C., I.; Botelho, H. M.; Yanamandra, K.; Fritz, G.; Gomes, C. M.; Morozova-Roche, L. A., *Structural Heterogeneity and Bioimaging of S100 Amyloid Assemblies*, in *Bionanoimaging: Protein Misfolding and Aggregation*. 2013.
28. Wang, C., et al., *The role of pro-inflammatory S100A9 in Alzheimer's disease amyloid-neuroinflammatory cascade.* Acta Neuropathol, 2014. **127**(4): p. 507-22.

29. Gruden, M.A., et al., *The misfolded pro-inflammatory protein S100A9 disrupts memory via neurochemical remodelling instigating an Alzheimer's disease-like cognitive deficit.* Behav Brain Res, 2016. **306**: p. 106-16.
30. Horvath, I., et al., *Pro-inflammatory S100A9 Protein as a Robust Biomarker Differentiating Early Stages of Cognitive Impairment in Alzheimer's Disease.* ACS Chem Neurosci, 2016. **7**(1): p. 34-9.
31. Iashchishyn, I.A., et al., *Finke-Watzky Two-Step Nucleation-Autocatalysis Model of S100A9 Amyloid Formation: Protein Misfolding as "Nucleation" Event.* ACS Chem Neurosci, 2017. **8**(10): p. 2152-2158.
32. Pansieri, J., et al., *Templating S100A9 amyloids on Aβ fibrillar surfaces revealed by charge detection mass spectrometry, microscopy, kinetic and microfluidic analyses.* Chemical Science, 2020. **11**(27): p. 7031-7039.
33. Gruden, M.A., et al., *S100A9 Protein Aggregates Boost Hippocampal Glutamate Modifying Monoaminergic Neurochemistry: A Glutamate Antibody Sensitive Outcome on Alzheimer-like Memory Decline.* ACS Chem Neurosci, 2018. **9**(3): p. 568-577.
34. Tayeb-Fligelman, E., et al., *The cytotoxic Staphylococcus aureus PSMalpha3 reveals a cross-alpha amyloid-like fibril.* Science, 2017. **355**(6327): p. 831-833.
35. Salinas, N., et al., *Extreme amyloid polymorphism in Staphylococcus aureus virulent PSMalpha peptides.* Nat Commun, 2018. **9**(1): p. 3512.
36. Taglialegna, A., et al., *The biofilm-associated surface protein Esp of Enterococcus faecalis forms amyloid-like fibers.* NPJ Biofilms Microbiomes, 2020. **6**(1): p. 15.
37. Ehrchen, J.M., et al., *The endogenous Toll-like receptor 4 agonist S100A8/S100A9 (calprotectin) as innate amplifier of infection, autoimmunity, and cancer.* J Leukoc Biol, 2009. **86**(3): p. 557-66.
38. Vogl, T., et al., *Biophysical characterization of S100A8 and S100A9 in the absence and presence of bivalent cations.* Biochim Biophys Acta, 2006. **1763**(11): p. 1298-306.
39. Klingstedt, T., et al., *Synthesis of a library of oligothiophenes and their utilization as fluorescent ligands for spectral assignment of protein aggregates.* Org Biomol Chem, 2011. **9**(24): p. 8356-70.
40. Groenning, M., et al., *Study on the binding of Thioflavin T to beta-sheet-rich and non-beta-sheet cavities.* J Struct Biol, 2007. **158**(3): p. 358-69.
41. Shivu, B., et al., *Distinct β-Sheet Structure in Protein Aggregates Determined by ATR–FTIR Spectroscopy.* Biochemistry, 2013. **52**(31): p. 5176-5183.
42. Ruggeri, F.S., et al., *Infrared nanospectroscopy reveals the molecular interaction fingerprint of an aggregation inhibitor with single Aβ42 oligomers.* Nature Communications, 2021. **12**(1): p. 688.
43. Otzen, D.E., et al., *In situ Sub-Cellular Identification of Functional Amyloids in Bacteria and Archaea by Infrared Nanospectroscopy.* Small Methods, 2021. **5**(6): p. 2001002.
44. Ruggeri, F.S., et al., *Infrared nanospectroscopy characterization of oligomeric and fibrillar aggregates during amyloid formation.* Nature Communications, 2015. **6**(1): p. 7831.
45. LeVine, H., 3rd, *Thioflavine T interaction with synthetic Alzheimer's disease beta-amyloid peptides: detection of amyloid aggregation in solution.* Protein Sci, 1993. **2**(3): p. 404-10.
46. Cohen, S.I., et al., *From macroscopic measurements to microscopic mechanisms of protein aggregation.* J Mol Biol, 2012. **421**(2-3): p. 160-71.
47. Leal, S.S., H.M. Botelho, and C.M. Gomes, *Metal ions as modulators of protein conformation and misfolding in neurodegeneration.* Coordination Chemistry Reviews, 2012. **256**(19-20): p. 2253-2270.
48. Kerkhoff, C., et al., *Zinc binding reverses the calcium-induced arachidonic acid-binding capacity of the S100A8/A9 protein complex.* FEBS Lett, 1999. **460**(1): p. 134-8.
49. Cristóvão, J.S.F., A.J.; Carapeto, A.; Rodrigues, M.S.; Cardoso, I.; Gomes, C.M., *The S100B alarmin is a dual-function chaperone suppressing Aβ oligomerization through combined zinc chelation and inhibition of protein aggregation.* ACS Chem. Neurosci., 2020. **11**: p. 2753-2760.
50. Korndorfer, I.P., F. Brueckner, and A. Skerra, *The crystal structure of the human (S100A8/S100A9)2 heterotetramer, calprotectin, illustrates how conformational changes of interacting alpha-helices can determine specific association of two EF-hand proteins.* J Mol Biol, 2007. **370**(5): p. 887-98.
51. Ruggeri, F.S., et al., *Atomic force microscopy for single molecule characterisation of protein aggregation.* Archives of Biochemistry and Biophysics, 2019. **664**: p. 134-148.
52. Ruggeri, F.S., et al., *The Influence of Pathogenic Mutations in α-Synuclein on Biophysical and Structural Characteristics of Amyloid Fibrils.* ACS Nano, 2020. **14**(5): p. 5213-5222.

Chapter VI: General Conclusions - A systems perspective on S100 proteins as novel players in proteostasis

---

1. Systems approaches to understand biological processes

Systems biology has been responsible for some of the most important developments in human health. In general terms, it consists of a global approach in biomedical research to understand the larger picture - from the level of the organism, tissue or cell form the combination of different elements. It seeks to decipher the complexity of biological systems that starts from the understanding that the networks that form the whole are more than the sum of the parts. Systems biology is collaborative, since it integrates many specific areas – biology, computer science, engineering, bioinformatics, physics, and others - to predict how these systems change over time and under varying conditions, and to develop solutions. For that, its focus is on the study of biological constituents including genes, proteins, and cellular and

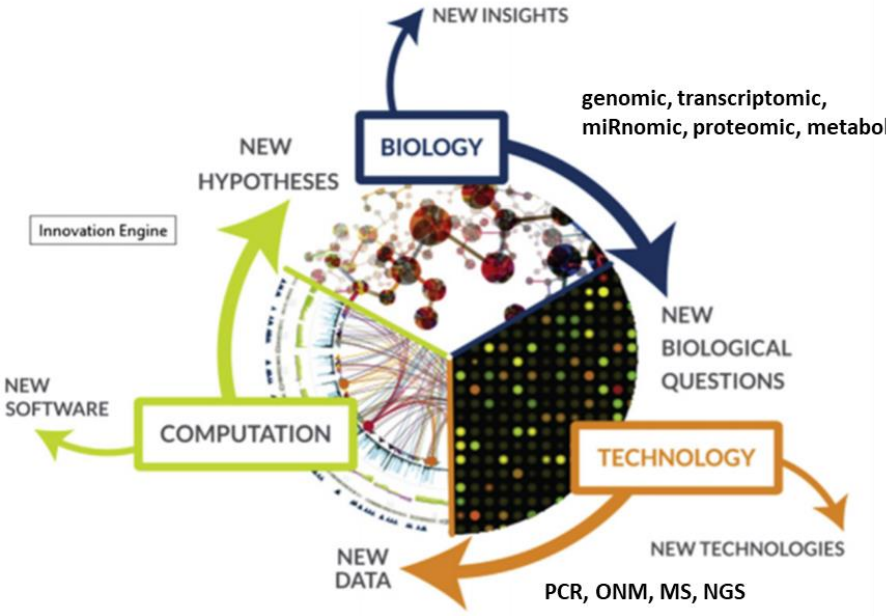

metabolic components using mathematical and computational systems with a multidisciplinary and integrative approach (Fig. 1)

Figure 1 – **Illustration scheme of a possible integrative and multidisciplinary approach of systems biology.** First, is needed to define the biological components that participate in a cellular mechanism, then form a genome-scale maps in a stepwise manner and a conversion of reconstructed gene networks into a mathematical model and, finally use the models in a prospective and predictive manner. Adapted from [41]

Over the past two decades, clinicians and scientists learnt how to familiarize with genomic, transcriptomic, miRnomic, proteomic, and metabolomic data which are obtained from technologies including quantitative polymerase chain reaction, oligonucleotide microarrays, mass spectrometry, and next-generation sequencing [41]. Through sophisticated computational models and simulations, information is extracted and interpreted with an

interdisciplinary approach. Systems biology offers an opportunity to study how the phenotype is generated from the genotype. The ability to design predictive, multiscale models enable to discover new biomarkers for disease, stratify patients based on unique genetic profiles, and target drugs and other treatments. Systems biology creates the potential for entirely new kinds of exploration and drives constant innovation in biology-based technology and computation.

This work did not follow a classical systems biology approach but resorted to multiple disciplines – biophysics, cellular biology, biochemistry, and techniques to build the larger picture underlying the role of a family of proteins in the one important biological process. Our studies on S100 proteins, spanning from studies in animal models to investigations on protein structure attempted to leverage a broader understanding of their role in proteostasis. Thanks to this comprehensive, systems-inspired approach, we have gained insights on the distributions of S100 proteins in the brains of AD mice models along disease progression and on how S100 proteins can modulate Aβ aggregation, uncovering new potential roles for these proteins in health and disease states.

2. S100 proteins as novel players in proteostasis and AD

Alzheimer's disease is the most common progressive neurodegenerative disease and the most prevalent age-related dementia which affects millions of people in the world [1]. The imbalance on proteostasis, metallostasis (metals ion levels) and many other cellular processes promotes dysfunction in nervous cells that cause neurodegeneration and lead to declining brain functions. Along this continuum there is a progressive self-assembly and accumulation of the Aβ peptide into toxic aggregates and amyloid fibrils that form extracellular plaques. The deposition of Aβ in the brain then prompts dissociation and hyperphosphorylation of the tau microtubule associated protein, that self assembles into oligomers with proteotoxic spreading potential and amyloids forming neurofibrillary tangles.

Protein aggregation in AD is accompanied by neuroinflammation [2] and microglia and innate immune cells of the central nervous system play key roles in mediating neuroinflammatory responses [3]. Neuroinflammation is mediated by the production of cytokines, chemokines, reactive oxygen species (ROS), which are produced by glia (astrocytes and microglia), endothelial cells and immune cells. Most of the times neuroinflammation is referred to as a deleterious and negative process that aggravates cell death, and most of ongoing research is focused on these pathological aspects. However, some

neuroinflammatory responses are positive. In fact, the degree of neuroinflammation depends on the context, duration, and course of the primary stimulus or insult [3], Fig. 2.

In many circumstances, there is a balance between inflammatory and intrinsic repair processes that influences functional recovery. Moreover, communication between the brain and immune system involves neuroinflammatory processes that are beneficial and adaptive. Therefore, to discuss whenever neuroinflammation is positive or detrimental, it is important to establish which pathways and players represent positive and negative aspects, and which are the transition threshold between the two situations.

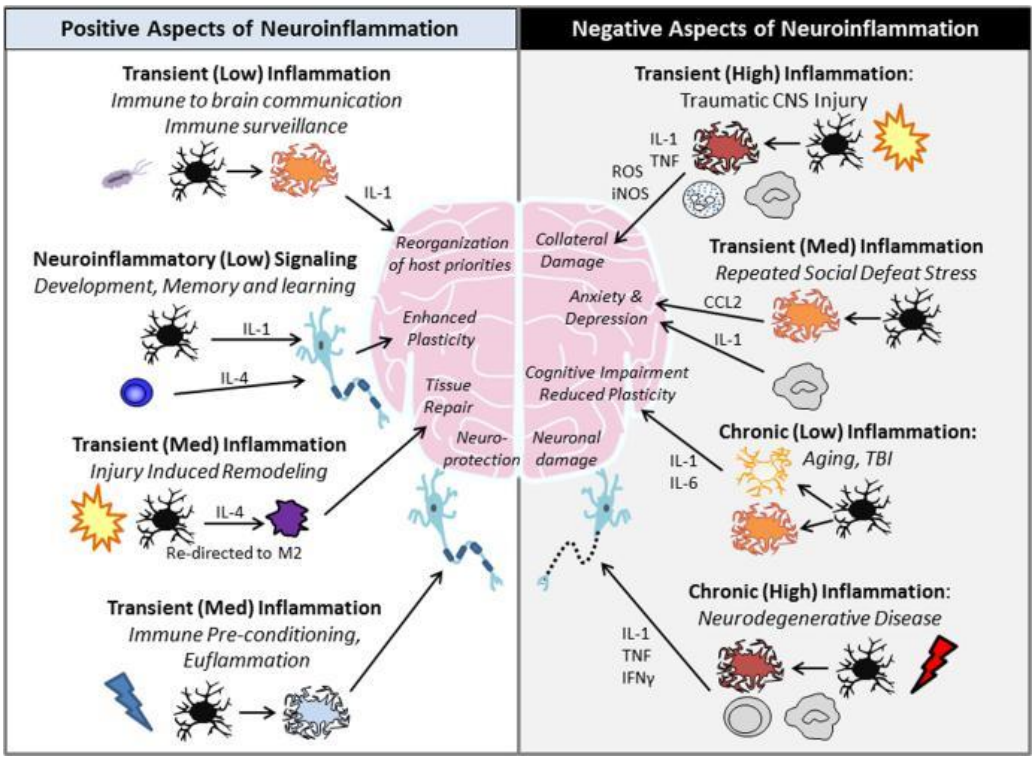

Figure 2 - Positive and Negative Aspects of Neuroinflammation. Degrees of neuroinflammation influences supportive or destructive immune signals to the central nervous systems, depending on the intensity and duration. Positive and negative aspects of neuroinflammation are shown on the left and right, respectively. Insults leads to induction of sickness behaviors by the production of interleukins (group of cytokines). From [3]

As described in this thesis, S100 proteins are mostly presented as pro-inflammatory cytokines with disease aggravating roles. For instance, S100B is secreted from astrocytes; S100A9 is expressed by mononuclear cells (as lymphocytes and monocytes); and S100A8/A9 is constitutively expressed in neutrophils and monocytes as a calcium sensor. S100s are introduced as key players in AD neuroinflammatory responses and S100B, S100A9, S100A8, and S100A6 are among the most prominent brain expressed S100 proteins, which are all upregulated by aging and neuronal damage. In this work, we put together multiple complementary approaches and techniques to investigate if and how S100 protein modulates

and/or influence cellular proteostasis. S100 proteins are multifunctional and are involved in several processes within cells, including regulation of proliferation, calcium homeostasis and inflammation, and some S100 proteins are secreted or released to regulate cell functions via activation of surface receptors. Also, extracellular S100 proteins regulate the biological activity of other cells and participate in innate and adaptive immune responses. Here, we sought to study new protective functions and structural characteristics of members of this protein family that may be relevant to understand the plethora of S100 protein functions. One of the goals was to uncover mechanistic details of the cross talk between S100 proteins during pathological states, under different physiological concentrations. In addition, in the context of AD, we were interested in study their effect on Aβ aggregation, once they co-localized around Aβ plaques during disease state.

To reach the goal it was very important to use a combined approach: Cellular studies in neurodegeneration models and protein analysis, in Chapter III, where S100 localization in healthy and diseased brains of APP23 mice models were identified. Using fluorescent dyes, we showed that several S100 proteins (S100B, S100A6, and S100A8) are co-localized with Aβ plaques. As reported in literature and as confirmed by our results, at early stages of AD, S100 proteins are located surrounding Aβ plaques, in mice brains. Once co-localized, S100s might be able to interact with the Aβ peptide, preventing or delaying its aggregation; to confirm this we established a putative interaction between neuronal S100A6, S100A8, S100A9, S100A8/A9 and the Aβ peptide, based on their effect on Aβ aggregation, monitored using ThT fluorescence, studied in chapter IV. It had been previously shown in [4] that S100B delays $A\beta_{42}$ aggregation and now, in this work, we were able to demonstrate that other S100 proteins also inhibit $A\beta_{42}$ aggregation. Our results suggest that these proteins may act on different stages of the aggregation reaction (primary nucleation, secondary nucleation), without however changing the dominant $A\beta_{42}$ aggregation mechanism. Therefore, it is possible that S100 proteins contribute to the maintenance of proteostasis, as long as possible. At early AD stages, S100 proteins may have beneficial effects delaying Aβ aggregation, but, at late stages, as the accumulation of aggregated protein increases, their pro-inflammatory activities over and their action becomes disease aggravating. Eventually, co-aggregation phenomena between S100 proteins and Aβ42 may even occur, which might be indicative of a mechanism of chaperone inactivation by deposition. The apparently contradictory protective versus deleterious functions of S100 proteins in neurodegeneration is explained by the realization that these are multi-functional proteins that exert different functions depending on disease stages and expression levels. Presumably, the protective chaperone-type functions prevail at early stages, at the onset of proteotoxic insults and involve dynamic interactions with monomeric and proto-filament forms of aggregation-prone peptides, that mitigate their aggregation and toxicity. The

pro-inflammatory functions take over at later disease stages, activating RAGE mediated inflammation and increasing accumulation of protein inclusions that promote misfit interactions with mature fibrillar materials promoting co-aggregation processes. These findings suggest that S100 proteins might constitute potential therapeutic targets e.g. resorting to function-blocking antibodies, as proposed in [5].

In chapter V, we focused on the characterization of the S100A9 filamentous assemblies, which are unique among the S100 family. S100A9 protein is abundant in the brain and has been found in diseased and aged tissues as punctiform inclusions in correlation with classical amyloid pathological hallmarks, which has led to the suggestion of co-aggregation phenomena [11]. Also, this protein is known to be secreted by astrocytes at high levels into the vicinity of amyloid plaques, where it has been indicated to play protective anti-aggregation properties. Using different spectroscopic and imaging techniques, we found that under physiological conditions, S100A9 forms string-like polymeric structures, very stable which are not truly amyloid, as it has been proposed in other studies, that can reversibly dissociate and are composed by assembly units comprising native-like dimeric S100A9 protomers. Such structures illustrate the diversity of protein oligomerization mechanisms. We describe these filaments as pseudo-amyloid, as they are explicitly distinct from the *bona fide* straight and relatively rigid amyloid fibrils, highly enriched in tightly stacked cross-β motifs. While these filaments share some features like those described for shorter semi-flexible worm-like amyloid polymorphs usually generated at low pH, namely lower β-sheet content and inferior nanomechanical properties [6-9], they have characteristics that better match those of filaments formed by stacking of globular proteins, namely lack of major conformational changes associated to filament formation, end-to-end stacking hydrophobic interactions rather than cross-β packing, susceptibility to proteolysis and effective de-polymerization into functional protomers.

Other S100 proteins such as S100B that are even more abundant in the brain, do not form filaments such as those of S100A9. We argue that, in the context of its increased expression and extracellular secretion to high level, as during the neuroinflammatory process in Alzheimer's neurodegeneration, S100A9 has evolved the capacity to self-assemble into filamentous structures composed by interacting pairs of S100A9 dimers, as a possible mechanism for extracellular storage or enhancement of signaling activity, among many possible. This unique S100A9 filament might be due to the C-terminal extension, exclusively found in this protein. S100A9 protein may adopt these conformations as protective roles, promoting its availability in cells whenever is necessary, or may be a form of protein stabilization to maximize the lifetime of the protein in extracellular environments.

3. References

1. Masters, C.L., et al., *Alzheimer's disease.* Nat Rev Dis Primers, 2015. **1**: p. 15056.
2. Iqbal, K., F. Liu, and C.X. Gong, *Alzheimer disease therapeutics: focus on the disease and not just plaques and tangles.* Biochem Pharmacol, 2014. **88**(4): p. 631-9.
3. DiSabato, D.J., N. Quan, and J.P. Godbout, *Neuroinflammation: the devil is in the details.* J Neurochem, 2016. **139 Suppl 2**: p. 136-153.
4. Cristóvão, J.S., Morris, V. K., Cardoso, I., Leal, S. S., Martinez, J., Botelho, H. M., et al. , *The neuronal S100B protein is a calcium-tuned suppressor of amyloid-beta aggregation. .* Sci. Adv. , 2018. **4:eaaq1702.**
5. Gonzalez, L.L., K. Garrie, and M.D. Turner, *Role of S100 proteins in health and disease.* Biochim Biophys Acta Mol Cell Res, 2020. **1867**(6): p. 118677.
6. Jain, S. and J.B. Udgaonkar, *Defining the Pathway of Worm-like Amyloid Fibril Formation by the Mouse Prion Protein by Delineation of the Productive and Unproductive Oligomerization Reactions.* Biochemistry, 2011. **50**(7): p. 1153-1161.
7. Gosal, W.S., et al., *Competing Pathways Determine Fibril Morphology in the Self-assembly of β2-Microglobulin into Amyloid.* Journal of Molecular Biology, 2005. **351**(4): p. 850-864.
8. vandenAkker, C.C., et al., *Morphology and Persistence Length of Amyloid Fibrils Are Correlated to Peptide Molecular Structure.* Journal of the American Chemical Society, 2011. **133**(45): p. 18030-18033.
9. Hatters, D.M., et al., *The circularization of amyloid fibrils formed by apolipoprotein C-II.* Biophys J, 2003. **85**(6): p. 3979-90.
10. Castillo, V. and S. Ventura, *Amyloidogenic regions and interaction surfaces overlap in globular proteins related to conformational diseases.* PLoS Comput Biol, 2009. **5**(8): p. e1000476.
11. Horvath, I., et al., *Co-aggregation of pro-inflammatory S100A9 with alpha-synuclein in Parkinson's disease: ex vivo and in vitro studies.* J Neuroinflammation, 2018. **15**(1): p. 172.